NTNU
Norwegian University of
Science and Technology

Rheology and Flow Properties of Water-in-Oil Emulsions

Comparing Measured Flow Rates to
Predicted Flow Rates Based on the
Rheological Results From the Laboratory

Marthe Bodahl Lunde

Petroleum Geoscience and Engineering
Submission date: June 2017
Supervisor: Harald Arne Asheim, IGP

Norwegian University of Science and Technology
Department of Geoscience and Petroleum

Abstract

Emulsions of oil and water can be formed throughout all processes during the production of petroleum. The properties of these may be very different from those of oil and water alone and knowledge about how different factors affect emulsions are therefore crucial. There are several rheological models which may describe such mixtures, but analyzing the precision of such models are rare in the literature. If the rheology models provide precise results they could be enabled when designing transport and separation systems.

In this thesis, engine oil emulsions have been made and measured to investigate the applicability of such models. Emulsions were made with varying water content, and several properties were measured; their temperature dependency, interfacial tension, droplet size and the concept of aging. A simple test facility was constructed to compare measured flow rates to flow rates estimated based on the rheological results from the laboratory. The average deviation between measured and estimated flow rates was 17.2% and the maximum 41.9%.

Sammendrag

Emulsjoner av olje og vann kan dannes i alle prosesser når olje produseres. Egenskapene til disse emulsjonene kan være svært forskjellig fra hvordan olje og vann oppfører seg på egen hånd og kunnskap om hvordan de ulike faktorene påvirker emulsjonene er derfor svært viktig. Det finnes mange ulike reologiske modeller som kan brukes til å beskrive egenskapene til slike blandinger, men forskning som fokuserer på presisjonen til disse modellene er vanskelig å finne. Hvis disse modellene kan bidra til å gi tilnærmet nøyaktige resultater i forhold til hva som skjer i virkeligheten, kan de bli tatt i bruk når transport- og separasjonssystemer skal designes.

I denne oppgaven blir emulsjoner av motorolje brukt for å undersøke nøyaktigheten av slike modeller. Emulsjonene ble laget med varierende vanninnhold, og forskjellige egenskaper ble målt; temperaturavhengighet, grenseflatespenning, dråpestørrelse og aldring. Et enkelt rørstrømningsoppsett ble konstruert for å sammenligne strømningsratene med raten estimert ut ifra resultatene i laboratoriet. Gjennomsnittsavviket mellom målt og estimert strømningsrate var 17.2% med et maksimum på 41.9%.

Acknowledgment

This thesis has been carried out at the Department of Geoscience and Petroleum, Norwegian University of Science and Technology (NTNU). It is the final product of the 5 years Master's Degree Programme within Petroleum Production.

First, I would like to thank Harald Arne Asheim, my supervisor, for always keeping his door open and being supportive. I would also like to thank my co-student, Ann-Othilie Helgesen Væhle, for an irreproachable cooperation in the laboratory, as well as George Voss and Håkon Myhren for their practical contributions. And last, thanks to Katherine Rose Aurand and Roger Overå for teaching me everything I know about laboratory work.

Parts of Chapter 2 and 3 are taken directly from the project assignment last semester (fall 2016), since this thesis is a continuation of last year's work.

M.B.L

Content

List of Figures

List of Tables

1. Introduction

Oil and water together often mix to form emulsions with flow properties (rheology) very different from those of water and oil alone. As these properties may be difficult to predict, the design of pipelines for emulsion transport carries its challenges. If the apparent viscosity of emulsions becomes really high, large pressure drops may become a problem. Maintaining the desired flow rate may also be challenging. When emulsions are produced, it may be necessary to use expensive demulsifiers to meet crude oil quality criteria. There are also strict rules concerning the water being injected back into the reservoir or released in the ocean.

Emulsions are not only causing problems, but may be helpful when producing heavy crude oil. The International Energy Agency says that heavy crude oil (below 20°API) and extra heavy crude oil (below 10°API) accounts for at least half of the recoverable oil resources in the world, which means that heavy crude oil production will only be more and more common (Martínez-Palou et al., 2011, pp. 1 - 2). The viscosity can be drastically reduced by emulsifying heavy crude oil, hence ease the transport.

The rheology of oil and water emulsions has been studied for over a hundred years, the first publications being traced back to the beginning of the 20th century. But even though there are an enormous amount of research done on the rheology, finding any studies investigating the applicability of rheology models has been a great challenge. In this thesis, the rheology of water-in-oil emulsions was investigated, and a simple pipeline facility was constructed to compare the measured flow rate with the predicted flow rate based on the rheology behavior observed in the laboratory. The apparent viscosity of the emulsions at different shear rates was used to find the appropriate rheology models and estimate the parameters of the model.

The emulsions were made using engine oil with varying water content. They were analyzed at different temperatures over a extended period of time to observe how the temperature affected the separation. It was observed that even though the emulsions contained as much as 60% water, oil was the only fluid being secreted from the mixture during the three weeks the emulsions were monitored. The apparent viscosity of the emulsions was also measured at different temperatures, and some diverging results were observed. Emulsions are known to break more easily when exposed to high temperatures, which is why heat is a well-used method for separating emulsions. However, in this study, the emulsions experienced breaking at lower shear rates at cold temperatures.

2. Theory

2.1 Emulsions

Emulsion simply means a colloid of two or more immiscible liquids where one liquid contains a dispersion of the other liquids.

Emulsions can be divided into two different groups based on their size. In macroemulsions, the droplet diameters exceed 0.1 μm. Microemulsions have droplet sizes that are usually smaller than the wavelength of visible light (< 0.1 μm), hence these types of emulsions are transparent or, at least, translucent. Another difference between macro- and microemulsions is that the macroemulsions are considered thermodynamically unstable, while microemulsions are considered stable (Becher, 2001, pp. 5-6).

2.1.1 Emulsions in Everyday Life

Emulsions are commonly encountered in everyday life; butter, ice cream, mayonnaise, and milk are all emulsions widely known and used. Emulsion science is also used to make beauty products like facial cream and lotion. The texture of an emulsion often reflects the continuous phase, which is why milk feels watery, but body lotion feels greasy. While water is the continuous phase in milk, oil is the continuous phase in lotion and creams (Schramm, 2005, p. 41).

2.1.2 Emulsions in the Petroleum Industry

Emulsions are formed throughout almost all processes in petroleum production. Some are desirable, while others form naturally and only contribute to increased costs, delays and excess treating of the produced fluids. The water content in natural water-in-oil emulsions can sometimes be as high as 60%, which it not very economical, both regarding the amount of crude oil produced and the fact that both the oil and water needs to be processed to meet industry criteria (Oliveira and Gonçalves, 2005, p. 1). The water might either come from the reservoir itself, or it may have been injected into the reservoir to contribute to excess pressure to produce more oil.

For instance, by emulsifying heavy crude oil, dramatic decreases in apparent viscosity can be achieved which will ease the transportation. This method has been utilized many places around the world, but for this to be economical, the oil concentration must be kept as high as possible, while still maintaining the low viscosity (Pal, 1996, p. 1). For emulsions to form there must be an excessive form of energy, for example when flowing through valves or pumps. To ensure

the stability of the emulsion, it may be necessary to add surfactants (Chapter 2.1.4) to reduce the interfacial tension of the oil (Martínez-Palou et al., 2011, p. 4).

In the case of crude oil spill in the ocean, the formation of emulsions may be a solution. When crude oil is spilled, oil-in-water emulsions may be formed if there is sufficient energy available. This can prevent the oil from spreading away from the source and keeps it away from sensitive shorelines (Schramm, 2005, p. 226).

Emulsions are also convenient in drilling fluids. They can, for instance, solve gumbo related problems (swelling of soft and sticky shale formations) by drying the formation. The droplets in the emulsion have a thin, semi-permeable membrane, which only water can get through because of the size of the water molecules. When the drilling fluid is present in the borehole, there are a lot of droplets close to the formation, and if the salt content in the droplets is lower than in the formation, water will travel from the formation through the membrane and into the emulsion droplets. This transport process is called osmosis since it is the content of salt (NaCl) which decides which direction the transport will go. When the water travels from the formation into the droplets in the drilling fluid, the formation gets dried out and can prevent problems like stuck pipe due to swelling of shale (Skalle, 2017).

In addition, emulsions can be used as fracturing fluid, which is used to increase flow capacity in the reservoir by being injected at high pressure and velocity through a wellbore and into the formation in order to enlarge the fractures. By using emulsions instead of water, water damages to the formation are minimized (Schramm, 2005, pp. 263-265).

In heavy oil reservoirs, water-in-oil (from now on indicated as W/O) emulsions can be formed in the reservoir during water and steam flooding. For lighter oils, more energy (mixing) is needed to form emulsions. This kind of mixing is naturally present in several parts of the oil production process; hence emulsions can develop in pumps, in the flow through tubing and flowlines, in valves and other surface equipment. These kinds of emulsions can be challenging to treat and can result in more trips with equipment and an increased use of demulsifiers (Denney, 2000, p. 1).

In addition to W/O emulsions, oil-in-water emulsions (indicated as O/W emulsions) and multiple/complex emulsions can occur as well. An example of a multiple emulsion is water-in-oil-in-water (W/O/W). This is a double emulsion, containing water droplets dispersed in oil droplets that are dispersed in a continuous water phase (**Fig. 2-1**). There are even more complex types, for example water-in-oil-in-water-in-oil (W/O/W/O) (Schramm, 2005, p. 5).

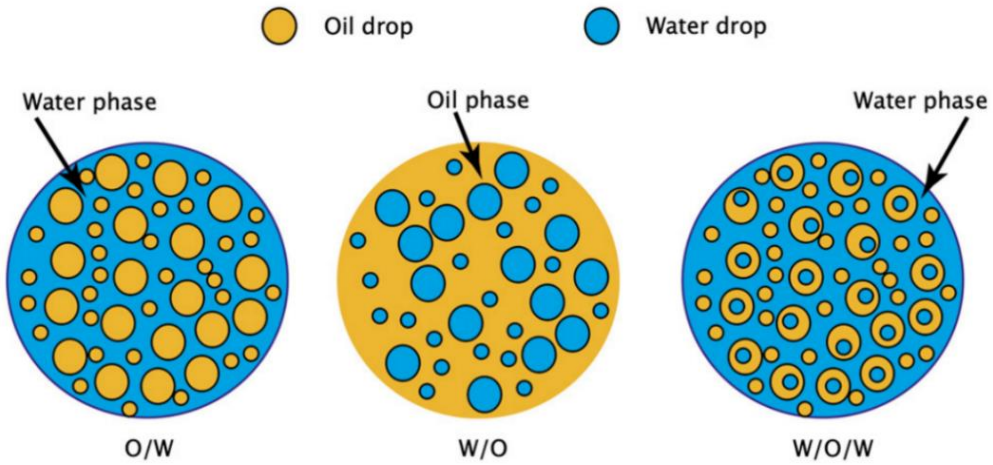

Fig. 2-1: Emulsions typically found in oil production and transport (Martínez-Palou et al., 2011, p. 3)

2.1.3 Emulsion Characteristics

As mentioned, W/O emulsions are often formed intentionally to reduce the apparent viscosity of heavy crude oils and then ease the transportation in pipelines. But knowledge about how different emulsions will behave is necessary before implementing emulsions in oil production and transport, since pipeline transportation of highly viscous crude oils and off-shore crude oil production can be extremely challenging, especially during cold weather.

There are several thermal methods which have shown to be important in the production of heavy crude oil due to how it behaves when exposed to hot temperatures. **Fig. 2-2** illustrates how the viscosity of four different (unknown) crude oils decreases when the temperature rises. This decrease in viscosity is why thermal methods are useful when producing very heavy crude oil. Heated–water injection is one of the methods used. Either steam or hot water is injected through an injection well and drives oil towards the production wells. Hot water flooding is less efficient than steam flooding because hot water carries less heat than steam. In-situ combustion is another method, in which there is a fire either near an injection well which moves towards the production wells, or the fire is started near a production well and moves away from it. In either case, the viscosity of the oil is reduced. SAGD, or Steam – Assisted Gravity Drainage, is another method used for heavy oils. It consists of two horizontal wells, where steam is being injected into the reservoir from both wells for approximately 2 – 4 months, before the steam injection from the production well, or the lower well, is stopped. The heavy oil/water mixture is then moved down to the lower production well by the help of gravity (Armstrong, 2016, pp. 7 - 35).

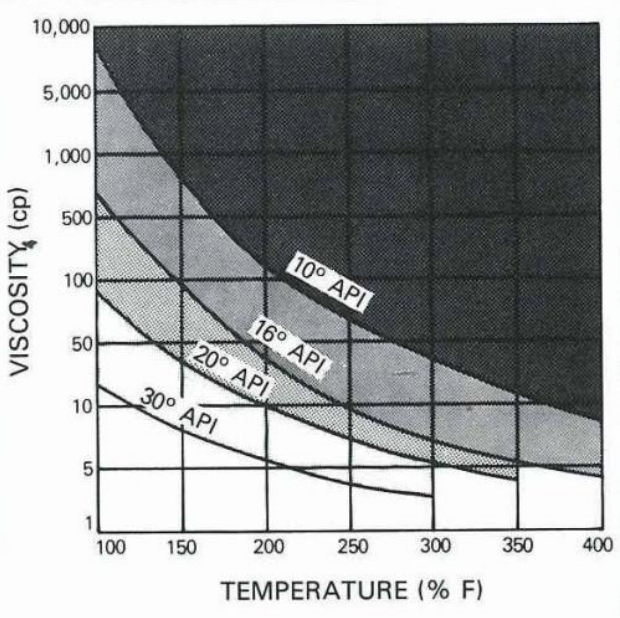

Fig. 2-2 Viscosity of four oils at various temperatures (Armstrong, 2016, p. 6)

When it comes to ease the transport of emulsions, it comes back to the basic concept behind thermal methods. As the temperature goes down, the apparent viscosity increases. This can affect the transport of emulsions over long distances in cold conditions. One example is in Campos Basin, where most of the Brazilian heavy crude oil gets produced. The temperature of the oil decreases from typically 80°C in the reservoir 3000 meters below the seabed, to about 60°C at the top of the wellbore. Then the oil has to be transported hundreds of meters through a pipeline surrounded by sea water with a temperature of 4°C to 10°C. This lap has a major influence on the oil's temperature, and the crude oil has often arrived with a temperature below 30°C (Oliveira and Gonçalves, 2005, p. 1).

There have been several studies carried out to find a cohesion between apparent viscosity and water content. This has turned out to be a great challenge due to all the other factors affecting the viscosity of emulsions. Higher aqueous phase volume fractions are known to give increased shear stress and viscosity, while an increase in temperature is known to decrease the apparent viscosity of the emulsion. The problem is that there are so many other factors affecting the rheology. Chemical components in the oil, emulsifier agents, polydispersity, and degree of mixing are examples of factors affecting the viscosity and shear stress behavior, and it is therefore extremely difficult to predict the behavior of a new emulsion produced from a new reservoir under different conditions.

Keleşoğlu et al. (2012) conducted several rheological and pipeline flow experiments on water-in-crude oil emulsions. The emulsions were studied at different temperatures (from 20°C to 50°C), different water fractions (from 0% to 70%) while shear rates varied from 0.1 s^{-1} to 1000 s^{-1}. The synthetic emulsions were made using North Sea heavy crude oil and brine containing 3.5% weight/volume (w/v) of NaCl. Some of the results are shown in **Fig. 2-3**.

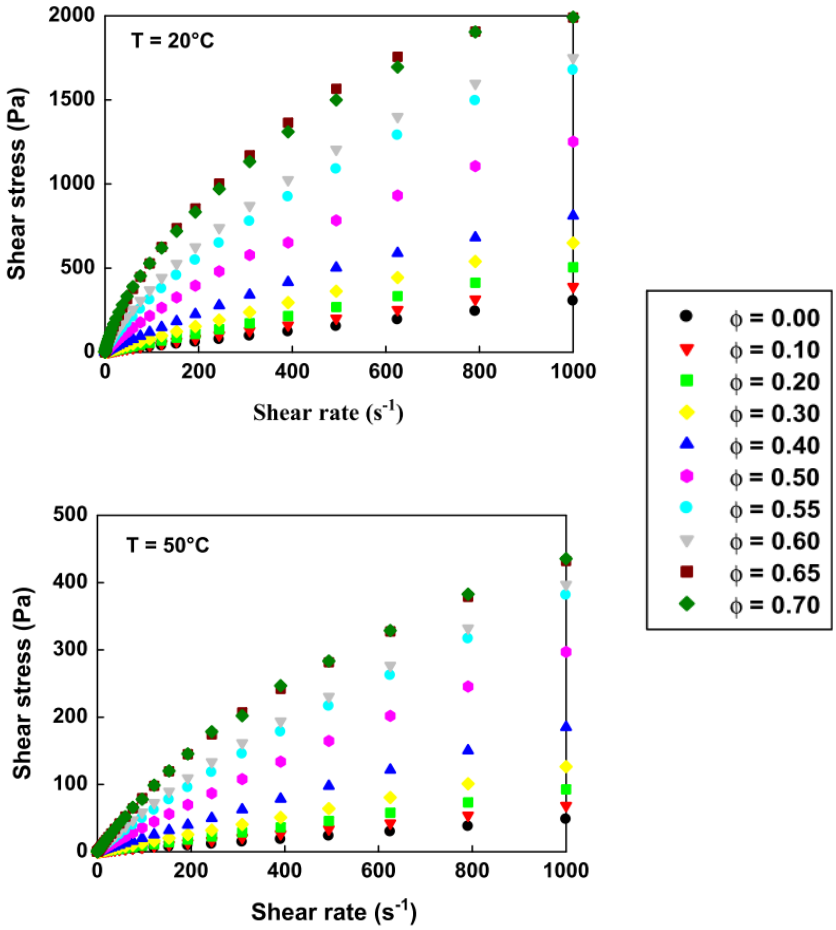

Fig. 2-3: Results of water-in-North Sea crude oil emulsions obtained using Anton Paar Physica MCR 301 Rheometer (ϕ indicates water volume fraction) (Keleşoğlu et al., 2012, p. 5)

These results are in accordance with most results from experiments done with emulsions. First, the emulsions experience more stress with increasing shear. Second, higher aqueous phase fraction results in higher shear stress. And third, increasing the temperature will result in less stress.

O/W emulsions give similar results. Pilehvari et al. (1988) did experiments on O/W emulsions. Their results indicated the same as previous work have before; higher temperature lowers the apparent viscosity and an increase in dispersed phase concentration results in higher viscosity

and shear stress with increasing shear rate. So, by increasing the dispersed fluid concentration, higher shear stress and viscosity are achieved. **Table 1** shows how the rheology of different emulsions change when either the water or oil content increases.

Table 1: Results of increasing water or oil concentration in emulsions

Emulsion type	↑ **Water**	↑ **Oil**
Oil-in-water	↓ Viscosity ↓ Shear Stress	↑ Viscosity ↑ Shear Stress
Water-in-oil	↑ Viscosity ↑ Shear Stress	↓ Viscosity ↓ Shear Stress

Pilehvari et al. (1988) also included oil droplet size and the influence of mixing intensity and duration in their work. They concluded that the rheological behavior of emulsions is highly dependent on oil droplet size in O/W emulsions and by reducing the droplet size, the behavior of the emulsion could change from Newtonian to highly shear thinning. The duration of mixing is important, as longer mixing times will give a smaller mean particle diameter. This means that the degree of mixing (intensity and duration) is important for the rheology of the emulsion. The intensity of mixing can be explained using energy dissipation per volume unit, ε [J/kg·s].

Another researcher who focused on the rheological properties of emulsions was Rajinder Pal in his AIChE Journal "Effect of Droplet Size on the Rheology of Emulsions" from 1996. He used both O/W and W/O emulsions in his research and concluded that fine emulsions have much higher viscosities and have stronger shear thinning effects than coarse emulsions. He also noticed that the fine emulsions have a greater tendency to flocculate because the amount of emulsifier that may not be able to cover the increased surface area. Pal (1996) also discussed polydispersity (wider range of droplet sizes) as a reason to why a coarse emulsion would give lower viscosity. If the emulsion is more polydispersed (coarser), the small particles will isolate or lubricate the large ones, hence decrease the viscosity. The corresponding monodispersed emulsions consist of small droplets which have smaller average distance between them, which leads to more interactions, hence increased viscosity for finer emulsions. In addition, Pal (1996) tested the rheological properties of the emulsions five times during a ten-day period and concluded that the viscosity and the shear thinning effects decreased with aging. The mean droplet size and the degree of polydispersion increased during this period.

2.1.4 Emulsifiers

For a stable emulsion of oil and water to form there must be an emulsifying agent or emulsifier present. This may be a macromolecule, finely and divided solids or a surfactant. Such a surfactant can be seen in **Fig. 2-4 (A)**. The figures (A-D) are retrieved from an online video, which explains the concept of emulsification (Education, 2013).

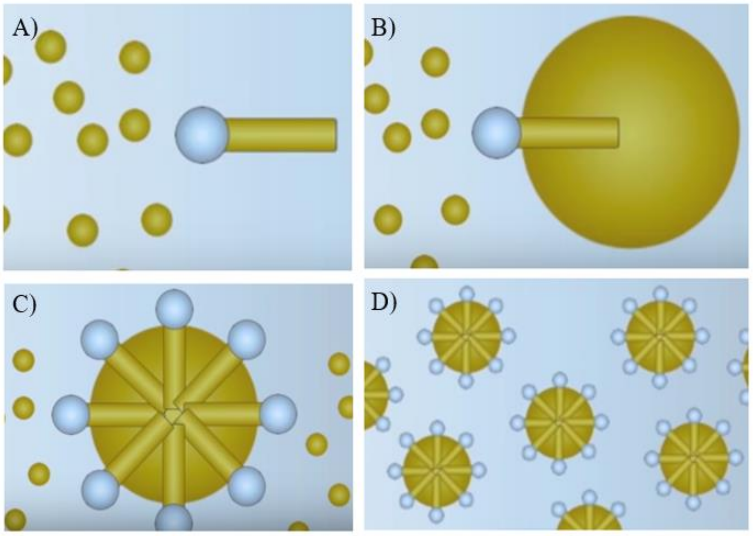

Fig. 2-4: Emulsifiers, surfactants, with hydrophilic heads and hydrophobic tails (Education, 2013)

To prevent that oil and water will separate after being mixed together, emulsifiers are added. The emulsifiers used to make the products mentioned previously consists of a hydrophilic (water-loving) head and a hydrophobic (water-fearing) tail, and these components prevent the two phases from separating, hence stabilizes the emulsion. In Fig. 2-4 (A) an emulsifier with a hydrophilic head and hydrophobic tail is shown in an O/W emulsion. The water-loving head wants to stay in the water phase and the water-fearing tail wants to stay in the oil phase **(B)**. Multiple emulsifiers will surround the oil drops **(C)**, and make an interfacial film between the two phases **(D)**. The interfacial tension between the oil drops will not be large enough for them to break out of the emulsion and thus prevents that a distinct layer of oil forms on top of the water phase (Kokal, 2005, p. 1). In W/O emulsions, the hydrophilic heads turn inwards towards the water drops and form so-called inverse micelles. **Fig. 2-5** shows how the surfactants will behave differently in O/W emulsions compared to in W/O emulsions.

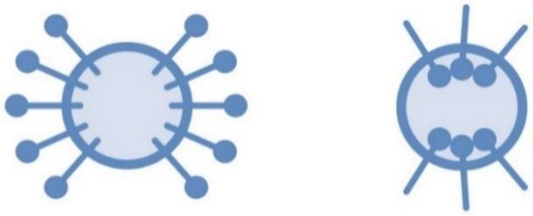

Fig. 2-5: Oil-in-water (left) and water-in-oil (CES, 2016)

During drilling operations and other processes affecting the fluids in the reservoir, the oil and water can be introduced to new chemicals which can act as surfactants and make stable emulsions. But there are some components that will work as natural emulsifiers in the crude oil as well. Heavy components, with higher boiling point fractions, like resins, waxes, and asphaltenes in crude oil play important roles in emulsion stabilization. In an oilfield emulsion, these components form the interfacial film surrounding the dispersed water droplets in the oil phase (Zhang et al., 2016, p. 2).

2.1.5 Emulsion Stability and Separation

Most emulsions are unstable by nature, and it will not take long before the emulsion starts to separate. They are classified based on their kinetic stability, and the separation of the emulsion can take a few minutes up to hours or days. Even though most emulsions related to the oil industry are unstable, quite stable emulsions can occur that can resist destabilization treatments and stay stable for weeks, months or even years (Schramm, 2005, p. 5).

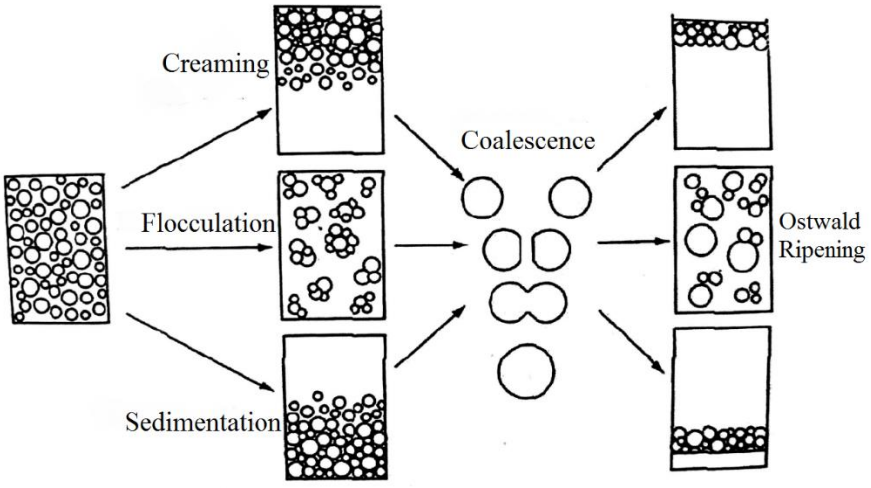

Fig. 2-6: Illustration of emulsion breakdown (Chen, 2006, p. 11)

The breakdown mechanism of emulsions involves four different processes; creaming or sedimentation, flocculation, and coalescence, but there are other processes too. These situations are often related (**Fig. 2-6**), but up to a point, these forms of emulsion instability can be explained separately. The different scenarios are as followed:

- **Creaming and sedimentation**: The name creaming comes from the process taking place in the separation of the cream of unhomogenized milk. Creaming does not represent a breaking of the emulsion, but can be part of a process that will lead to separation (Becher, 2001, p. 201). Whether a drop in a viscous fluid floats to the surface (creaming) or sinks to the bottom (sedimentation), depends on the relative values of the densities. Stoke's Law (Eq. 1) is an equation for the slip velocity of a droplet in a viscous liquid.

$$v_s = \frac{1}{18}\frac{d_d^2}{\mu}(\rho_d - \rho_f)g \qquad \mathbf{1}$$

Where

v_s is the rate of sedimentation

g is the acceleration of gravity

d_d the droplet diameter

ρ_d and ρ_f are the densities of the droplet and surrounding liquid

μ the viscosity of the surrounding liquid

The sign of v_s indicates in which direction the droplet will move. Since the oil density is usually smaller than the water density, an O/W emulsion is expected to give a negative v_s, hence upward sedimentation, or creaming, will occur. In a W/O emulsion downward sedimentation is expected (**Fig. 2-7**) (Becher, 2001, p. 201).

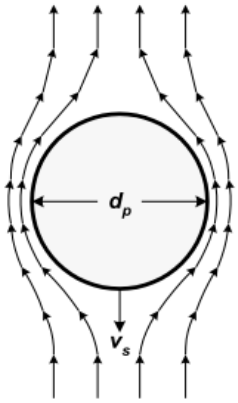

Fig. 2-7: Particle settling
(Chen, 2016, p. 39)

- **Flocculation**: While gravity and density differences are driving mechanisms in sedimentation and creaming, particle attraction is the main force in flocculation. Flocs are clusters with two or more droplets which behave as one unit. The droplets in this unit are still in the shape of droplets, with virtually no change in the total surface area. Formation of flocculates will increase the rate of sedimentation/creaming, due to greater influence by gravity. Flocculation, along with creaming and sedimentation, are reversible processes that can obtain its initial form if exposed to high shear rates (Becher, 2001, p. 244).
- **Coalescence**: In this process, droplets collide with each other and immediately coalesce into larger droplets. Coalescence is an irreversible phenomenon, and the merged droplets will not separate and retrieve the original emulsion (Becher, 2001, p. 244).
- **Ostwald ripening**: Material is drawn from smaller to bigger particles, causing small drops to lose material and disappear, while the bigger drops increase in size (Zang, 2016, p. 1). The process is displayed in **Fig. 2-8**.
- **Phase inversion**: This can occur if the emulsion undergoes too much mixing or if the dispersed phase becomes too large compared to the continuous phase. The emulsion may suddenly change from an O/W emulsion to a W/O emulsion.

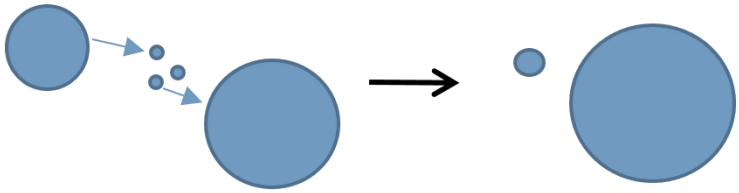

Fig. 2-8: Mechanism of Ostwald ripening

The processes mentioned often occur in combination. Creaming/sedimentation and flocculation usually happen before coalescence, but other compositions of the breakdown process occur as well. The dispersed phase in an emulsion can start to flocculate, and these flocs can coalescence into bigger droplets. These droplets can create creaming behavior which again can lead to coalescence and the remaining product is a totally separated emulsion with two phases. Another scenario is that the initial emulsion undergoes flocculation, which can lead to creaming and then coalescence. These two scenarios are characteristic for O/W emulsions, since oil is a lighter fluid than water and the oil droplets will rise to the surface. W/O emulsions often experience sedimentation, since the dispersed water is often heavier than oil and will therefore sink to the bottom of the container. Flocs can be established, and these floc units can sink to the bottom, hence the sedimentation, or they can coalescence and then settle, before the big droplets coalesce and the emulsion is totally separated.

Flocculation of droplets may not only affect the separation process of the emulsion, it can also affect the apparent viscosity and rheological properties. At low shear rates, the flocs may act as bigger droplets with a fixed size, but as the shear rate increases, the forces between the droplets are not big enough to keep them together, and they get separated into smaller droplets. The flocs can be stretched and align with the shear field which will result in viscosity reduction, and give the emulsion shear thinning behavior (**Fig. 2-9**)(Floury et al., 2000, p. 132). Pal (1996) found in his research that droplets in fine emulsions will flocculate easier than in more coarse emulsions. Two different versions (fine and coarse) were made of three emulsions with different water content. Both the viscosities were higher and shear thinning effects were stronger for the emulsions with fine droplets.

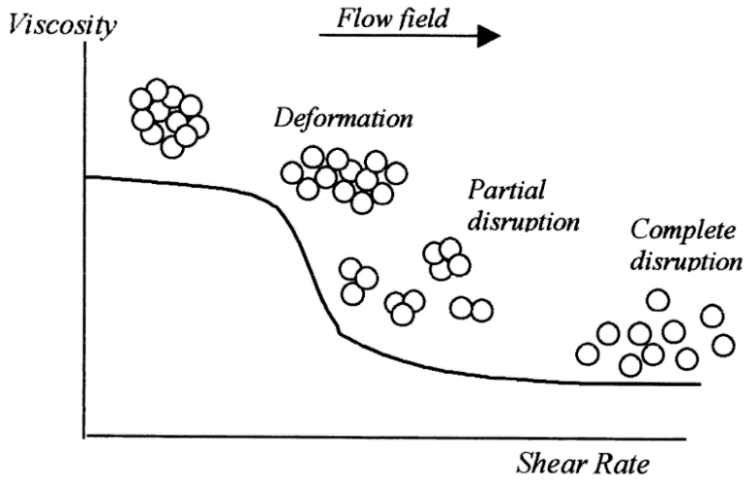

Fig. 2-9: Illustration of how flocs may change the viscosity (Floury et al., 2000, p. 132)

When oil is produced as either W/O or O/W emulsions, demulsifying treatment is necessary. Even though some of the water may come out of the emulsions naturally, other physical methods designed to accelerate coalescence are used. These methods may include setting, heating, electrical dehydration, chemical treatment, centrifugation and filtration (Schramm, 2005, p. 278). Chemical treatment often consists of adding high-molecular-weight compounds which are adsorbed on the oil-water interface, and results in a change in the hydrophile-lipophile balance, which decreases the stability of the system (DowChemical, n.d). The hydrophile-lipophile balance is called HLB, and expresses the relationship between the water-loving and water-fearing parts of a surfactant. A W/O emulsion requires low HLB surfactants, but an O/W emulsion requires higher HLB surfactants. The HLB concept is mostly used to describe the balance of the strength and size of the lipophilic/hydrophilic groups of an emulsifier (Schramm, 2005, p. 90).

2.1.6 Interfacial and surface tension

The difference between interfacial tension and surface tension is where is occurs. While interfacial tension is the force on the interface between two immiscible liquids, surface tension is the force on the surface when a liquid is exposed to a gas.

Since the adhesive forces between liquid-gas are much weaker than the cohesive forces between liquid-liquid, the surface molecules will get attracted towards the center of the liquid and create a thin surface layer. This layer is strong enough to hold some small animals, a metal paper clip or certain flowers. When two immiscible liquids are present, there is an interfacial tension present, which wants to minimize the interfacial free energy. The fluids are miscible if the force

on the surface molecules from one of the liquids is equal to the corresponding opposite force (Schramm, 2005, p. 54).

2.2 Fluid Flow Properties

2.2.1 Fluid Flow in Pipelines

When a flow is transported in a pipeline, it is classified as internal flow. In petroleum production, most fluids are transported in circular pipes which are completely filled with fluid and primarily driven by pressure difference. The pipes are circular because they are better at handling the pressure difference that occurs between the inside and outside of the pipe. The roughness of the pipes is also important since it affects the friction in the pipes, which is directly related to pressure drop and head loss (Çengel and Cimbala, 2014, pp. 321 - 322).

The Reynolds number (Eq. 2) is used to identify the flow regime in pipes. Laminar flow ($N_{Re} < 2300$) is characterized by smooth streamlines and ordered motion, while turbulent flow ($N_{Re} > 4000$) is characterized by velocity fluctuations and highly disordered motion. Transitional flow ($2300 < N_{Re} < 4000$) is the transition from laminar to turbulent flow (Çengel and Cimbala, 2014, p. 324). The Reynold number equation for an internal flow in a circular pipe is given below.

$$N_{Re} = \frac{\rho D V_{avg}}{\mu_d} \qquad \mathbf{2}$$

Where ρ is the density of the fluid

μ is the dynamic viscosity of the fluid

D is the hydraulic diameter of the pipe (the inside diameter if the pipe is circular)

V_{avg} is the mean velocity of the fluid

Fully developed laminar flow is one of a few simple cases that can be obtained using theoretical solutions, and occurs when highly viscous fluids (oils etc.) flow in small pipelines. Hence, turbulent and transitional flow problems are dependent on experimental results and empirical solutions (Çengel and Cimbala, 2014, p. 322).

To obtain a fully developed laminar flow, the pipe needs to be longer than the entrance region. The entrance region is the length of pipeline needed before a fully developed velocity profile is achieved. **Fig. 2-10** illustrates this process for a laminar flow. In a turbulent flow, the parabolic seen in this figure are somewhat flatter and fuller. The fluid velocity is zero at the pipe wall due

to the no-slip condition, and reaches its maximum in the center of the pipe. Due to the no-slip condition the fluid in the adjacent layers is slowed down. The velocity in the middle of the pipe must increase in order to maintain the mass flow rate.

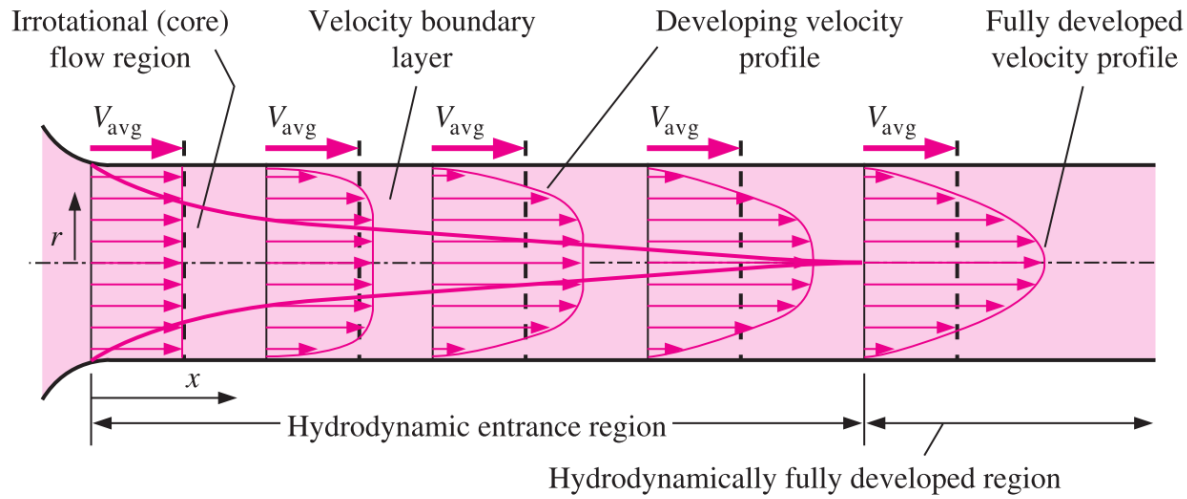

Fig. 2-10: The development of the velocity boundary layer in a pipe(Çengel and Cimbala, 2014, p. 325)

2.2.2 Viscosity

The two – plates model (**Fig. 2-11**) is a common way of explaining viscosity, and can also be used to explain the concept of shear rate and stress. It consists of two parallel plates of area A with a distance r between them. The upper plate moves in one direction due to a force F, and the liquid closest to this plate, fluid layer 1, will move in the same direction as the plate. Due to the internal friction in the fluid, layer 2 will also move, but at a lower velocity than layer 1, and fluid layer 3 will then have a lower velocity than fluid layer 2 (Chen, 2016, pp. 4-5).

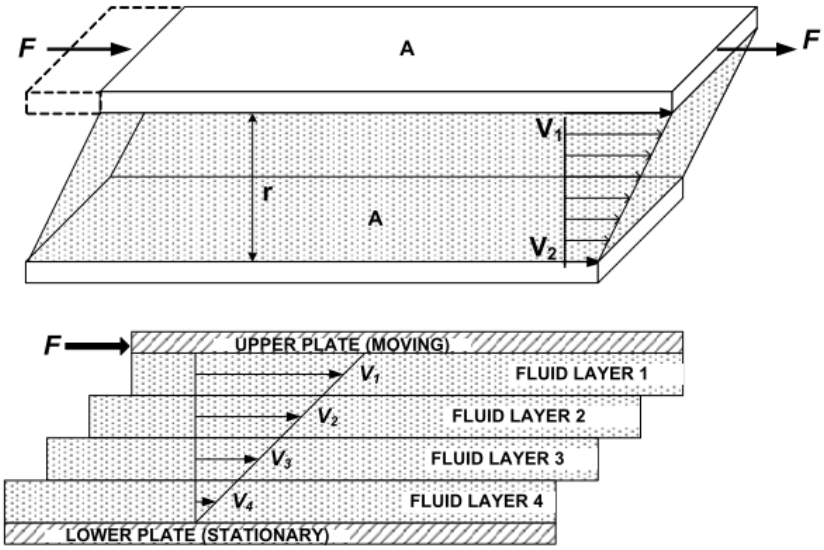

Fig. 2-11: Two-plates model (Chen, 2016, p. 4)

Shear stress is defined as the force applied to the upper plate divided by the upper plate's area (Eq. 3), and shear rate is given by the velocity of the upper plate divided by the distance between the two plates (Eq. 4), and is defined as "the rate of change of velocity at which one layer of fluid passes over an adjacent layer" (Garrett, 2016b).

$$\tau = \frac{F}{A} \quad \textbf{3}$$

$$\dot{\gamma} = \frac{v}{r} \quad \textbf{4}$$

The ratio shear stress/shear rate describes the fluid's resistance to flow; the fluid's apparent viscosity (Eq. 5).

$$\mu = \frac{\tau}{\dot{\gamma}} \quad \textbf{5}$$

2.2.3 Rheology Models

For **Newtonian fluids**, the shear stress/shear rate ratio is constant in laminar flow. Thus, viscosity can be considered a fluid property and shear stress is proportional to shear rate (Eq. 6). Newtonian flow behavior is mostly exhibited by low-molecular-weight substances, such as organic and inorganic liquids, molten metals and salts and gases (Krishnan et al., 2010, p. 13).

$$\tau = \mu \cdot \dot{\gamma} \quad \textbf{6}$$

In **Fig. 2-12**, five types of flow that may be exhibited by fluids are shown, where each type has a different relation between shear stress and rate.

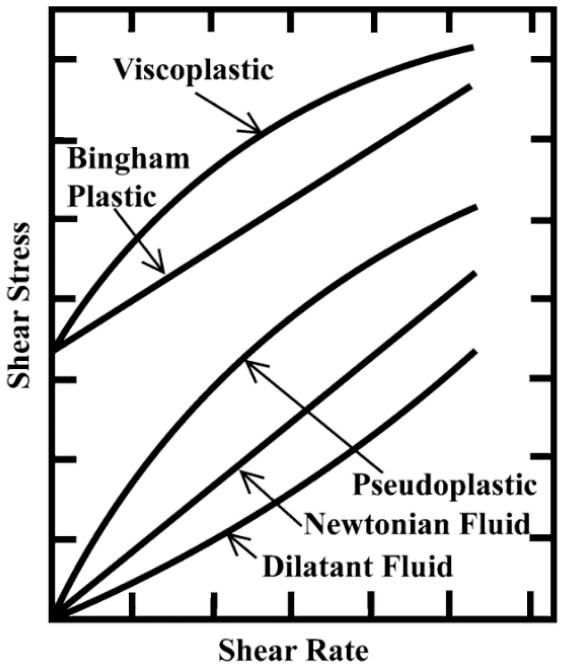

Fig. 2-12: Rheology Models(Krishnan et al., 2010, p. 9)

Bingham Plastic fluids (Eq. 7) have a structure which resists shearing until the yield strength, τ_y, is reached. When this yield strength is reached, the structure breaks down and the fluid acts Newtonian. This type of fluid is common for drilling muds, which is a kind of emulsion with water or oil as the continuous phase (Becher, 2001, p. 77).

$$\tau = \tau_y + \mu_p \cdot \dot{\gamma} \qquad \textbf{7}$$

Power-Law fluids (Eq. 8) describes shear thinning when n < 1 (pseudoplastic fluid). This implies decreasing the apparent viscosity under shear strain. Examples are ketchup and nail polish, in which the bottles need to be shaken to get the liquid more easily out. When n > 1 it describes shear thickening, which means that the apparent viscosity will increase under shear strain (dilatant fluid). Corn starch suspended in water is a shear thickening fluid. When pressure is applied or it is being stirred, it becomes more viscous.

$$\tau = \kappa \cdot \dot{\gamma}^n \qquad \textbf{8}$$

If the Power-Law fluids were plotted in a log-log plot, they would show a straight line, where κ (the consistency index) would be the point at which the straight line intersects the shear stress axis and n (the flow behavior index) would be the slope of the straight line.

A **Herschel-Bulkley fluid** (Eq. 9), or viscoplastic fluid, is described using three parameters, and can therefore provide a more accurate model of the rheological behavior (Garrett, 2016a). Similar to Bingham fluids, a H-B fluid requires a finite stress in order to deform. Once this yield is exceeded, the material can either flow as a shear thickening - or as a shear thinning fluid.

$$\tau = \tau_y + \kappa \cdot \dot{\gamma}^n \qquad \textbf{9}$$

The rheology models on page 18 will all experience a constant shear stress at a given shear rate, but this is not always the case. In **thixotropic and rheopectic** systems, flow properties depend not only on the shear rate, but also on the length of time the shearing stress is applied. Thixotropic is the case of time dependent pseudoplastic flow, while rheopectic flow is time-dependent dilatant flow (Schramm, 2005, pp. 176-177).

When thixotropic fluids are sheared at a constant rate, it experiences a decrease in apparent viscosity ($\mu = \tau/\dot{\gamma}$) with the duration of shearing. If the shear rate is increased at a constant rate from zero to a given maximum, then decreased at the same rate, the hysteresis loop shown in **Fig. 2-13** will appear. The fluid has larger time-dependent behavior the larger the enclosed area in the hysteresis loop, hence the area would be zero for the rheology models introduced previously (Krishnan et al., 2010, pp. 16-17).

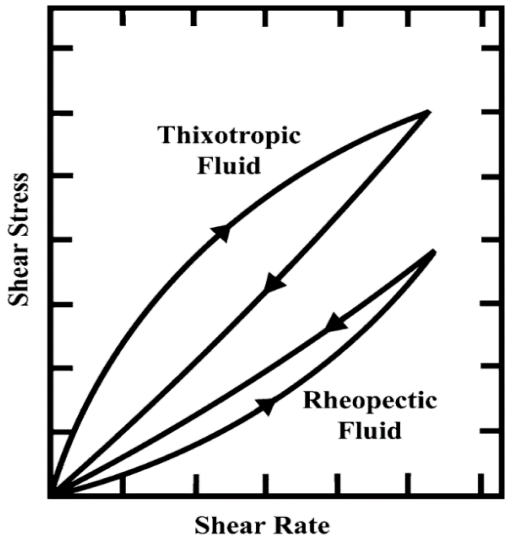

Fig. 2-13: Thixotropic and rheopectic fluid flow behavior (Krishnan et al., 2010)

Rheopectic fluid behavior is rather rare, since the external shear promotes the build-up of the internal structure, rather than tearing it down as in thixotropic fluids. If the same experiment is conducted for a rheopectic fluid, that is increasing the shear rate at a constant rate before decreasing it, an opposite hysteresis loop is obtained (Krishnan et al., 2010, p. 19).

2.2.4 Heavy Crude Oil Transportation

The production of heavy crude oil is increasing all over the world, and this results in an increase in transport of heavy crude oil. While the conventional pipelines are designed for light and medium crude oils, transport of heavy crude oil can be challenging due to their high viscosities (>10^3 cP at 25°C). They also contain asphaltene, paraffin deposition, salt and more formation water that lighter oils, which makes them heavier, more viscous and can contribute to more corrosion on the pipes (Martínez-Palou et al., 2011, p. 1).

Transportation of heavy crude oil can result in multiphase flow, clogged pipes, high pressure drops and the production may need to be stopped. The high viscosity can cause problems which will take time and money to solve.

Fig. 2-14 illustrates how the chemical composition of oil affects the viscosity. The light North Sea oil has a lot of light hydrocarbons, while the very heavy crude oil has almost exclusively long and heavy hydrocarbons.

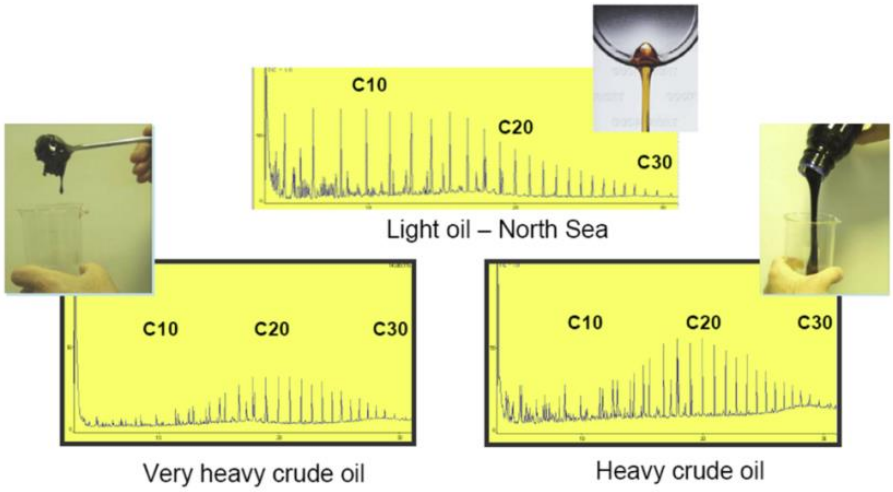

Fig. 2-14: Viscosity reflects oil composition (Armstrong, 2016, p. 5)

According to Martínez-Palou et al. (2011) there are three methods for transporting heavy and extra heavy crude oil; viscosity reduction, drag minimization and in-situ oil upgrading.

Reduction of viscosity can be done by either dilution of the oil, where lighter liquid hydrocarbons (condensates from natural gas production) or lighter crude oils are added to the heavy oil, by heating of the oil or pipelines, by utilizing PPD (Pour Point Depressant) or by creating emulsions. Water-in-oil and oil-in-water-in-oil emulsions occur naturally in the production process, but oil-in-water emulsions may be a suitable alternative when transporting heavy or extra heavy crude oil because of the viscosity reduction taking place. PPD are chemical additives that affect nucleation, adsorption or solubility of waxes, which may help to decrease the oil's viscosity and yield stress. The friction can be reduced by adding drag reducing additives, which will restrain the growth of eddies in turbulent flow. Since heavy and extra heavy crude oil often creates laminar flow, these additives may only be useful after the oil is heated or diluted. Another way of minimizing the drag is to create a different type of flow (annular), by lubricating the inner wall of the pipe with a thin film of water. In – situ oil upgrading implies producing a synthetic fuel or synthetic crude with a higher API gravity and lower viscosity.

3. Experiments

The complex properties of emulsions may be investigated by different measurements. Many publications consider this. However, researchers often use crude oil in their analysis, even though crude oils are varying in composition which will influence the rheology.

The goal of these measurements is to provide input parameters to rheology models to predict flow capacity. However, different rheology models exist and none can be expected to cover all aspects.

The object of the experiment is to compare the results found in the laboratory with the measurements conducted in a vertical pipeline. The purpose is to examine if the predicted flow rate is more precisely when the appropriate rheology model is used, compared to when another rheology model is employed.

3.1 Preparation of Water-in-Oil Emulsion

3.1.1 Fluids

Emulsion rheology is a complicated topic since the rheological properties vary between the different emulsions. Two crude oils with similar viscosity, density and rheology, can show different rheological behavior when used in emulsions (Pilehvari et al., 1988, p. 3). Since the focus of this thesis is the rheological and physical properties of the emulsions, a lubricating oil is used, instead of the intentional crude oil. If a crude oil was employed, it would be natural to focus on the chemical composition of that specific oil. Some lubricating oils contain natural emulsifiers or suitable emulsifiers are added to make stable W/O emulsions.

The oil used is a classic 15w-40 engine oil. The oil is used in engines to keep engine components clean and prevent the formation of black sludge and the build-up of particles. When this oil is mixed with water, in this case a 3% (w/v) NaCl brine, adding emulsifiers is not necessary. There are natural emulsifiers present in the mineral oil, and the oil and brine are therefore capable of making a stable emulsion without additional emulsifiers.

To make sure the right amount of water and oil were used when making the emulsions, their densities were determined using a simple pycnometer. By operating with weight instead of volume, it is easier to control the ratio between water and oil. The densities of water and oil were found to be 1.02 g/cm^3 and 0.8755 g/cm^3 respectively (**Table 2**).

Table 2: Densities of 3% (w/v) NaCl brine and engine oil

	3% (w/v) NaCl brine	Engine oil
Density [g/cm^3]	1.0200	0.8755

3.1.2 Mixing

The samples were prepared in batches of 400 ml. When the emulsions were made, a regular axial laboratory blender was used (**Fig. 3-1**). It consists of 4 small blades, with a total diameter of 3.176 cm. The diameter of the beaker is 9.53 cm. The 400 Watt blender has a rpm of 18000, so the emulsions experience high shear rates during mixing. The fluids were mixed for one and a half minute to apply the same emulsification condition for all emulsions. The emulsions were mixed at a temperature of 21 ± 1°C, which is the ambient temperature in the laboratory.

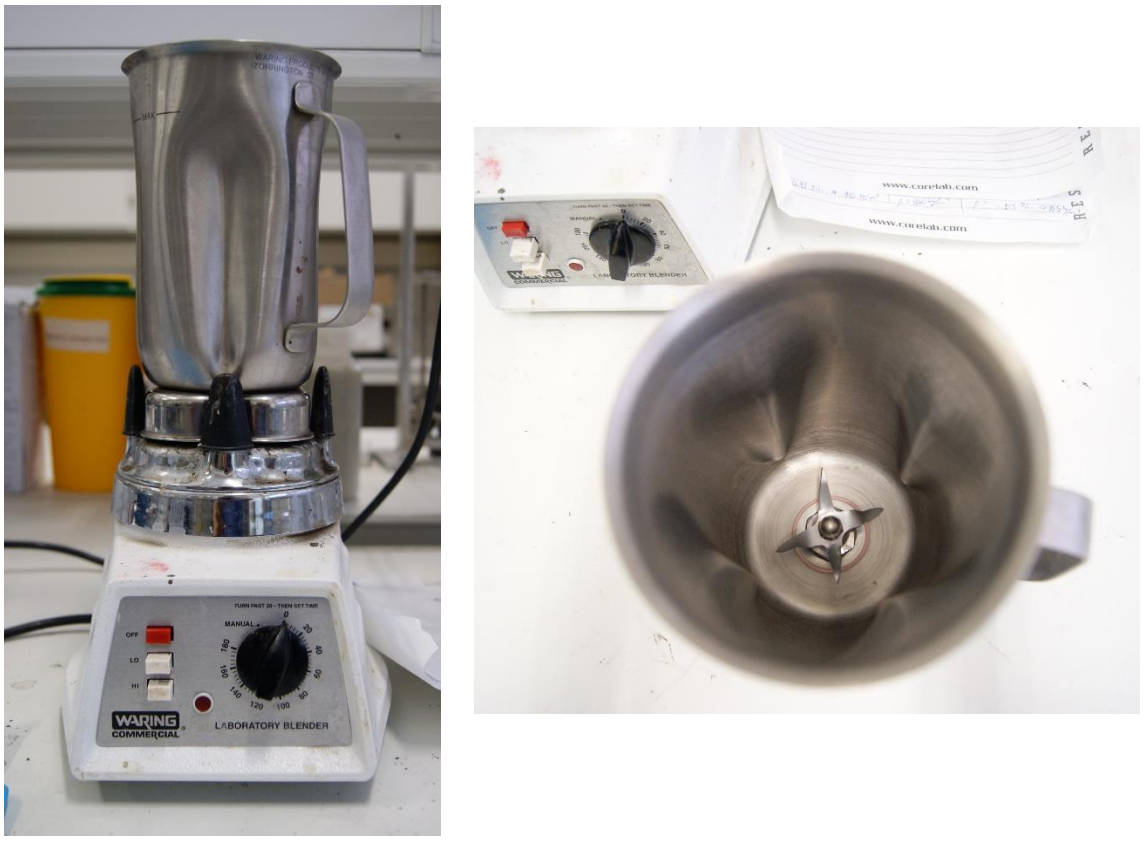

Fig. 3-1: Laboratory blender used to mix emulsions

To make sure that the emulsions made were in fact W/O emulsions, a simple drop test was conducted. By pouring water into a container with a small amount of emulsion, the continuous phase could be determined. While emulsions with water as the continuous phase would get totally diffused when getting in contact with water, an emulsion droplet with oil as the

continuous phase would stay together. **Fig. 3-2** illustrates this test. The emulsion droplets on the left show obvious signs of staying together and not spreading out in the water phase, hence the emulsion is confirmed to be a W/O emulsion. While the emulsion on the right side is more spread out than the other, this is also a confirmed W/O emulsion since the emulsion is not blending in with the water.

Fig. 3-2: Determination of continuous phase

Five different emulsions with varying water concentration were prepared. The water content varied from 30% to 70%. Fig. **3-3** shows the emulsion with 70% water content straight after making, and due to the early separation, the emulsion containing 70% water were not included later in the experiments. The other water-in-engine oil emulsions made consisted of 60%, 50%, 40% and 30% water.

Fig. 3-3: 70/30 W/O emulsion. Straight after making (left) and 22 hours later (right)

Since there are different rheology models available for emulsions, it is of interest to consider emulsions with different rheological characteristics. Experiments from last year showed that water-in-soybean oil exhibit Herschel-Bulkley behavior when tested at different shear rates. This emulsion is therefore concluded in this project as well.

The water-in-soybean oil emulsions were made using a regular soybean oil bought at the grocery store. Palsgaard AS located in Denmark delivered two different kinds of emulsifiers which together should be able to make W/O emulsions. The two types of emulsifiers are called Palsgaard DMG 0298 and Palsgaard PGPR 4175. DMG 0298 is distilled monoglycerides of vegetable fatty acids and can be used as an emulsifier for low fat and very low-fat margarine. The PGPR 4175 is a polyglycerol polyricinoleate (PGPR), and used as W/O emulsifier for the production of e.g. low fat spread emulsions and tin greasing emulsions (low viscosity types for spray equipment).

When making the emulsions, a recipe provided by Knut Gåseidnes was used (Appendix G). A 3% (w/v) NaCl brine were used together with soybean oil and the emulsifiers from Palsgaard AS. Since this emulsion is only used to illustrate Herschel-Bulkley behavior, a single 60/40 W/O emulsion were made.

In the recipe, the amount of emulsifiers needed are calculated based on volume, but since the emulsifiers are so thick and viscous it can be a big challenge to measure the exact volume. To solve this problem the density of the emulsifiers was found using a pycnometer (**Table 3**). The DMG 0298 emulsifier is initially very hard and impossible to pour into a pycnometer, but got into a liquid state by heating it up to about 40 degrees Celsius.

Table 3: Densities of emulsifiers and soybean oil

	PGPR 4175	**DMG 0298**	**Soybean oil**
Density [g/cm^3]	0.9829	0.9575	0.918

To separate the emulsions the letter E (for engine oil) or S (for soybean) is given, followed by the water/oil ratio. For example, a water-in-engine oil emulsion containing 40% water is indicated as E40/60.

The energy dissipation per volume unit, ε [J/kg·s], can give an idea of how much energy the different emulsions have been exposed to during mixing. It was calculated using Eq. 10. A 400-watt blender was used to make 400 ml emulsion. The results are shown in **Table 4**.

$$\varepsilon = \frac{Watt_{blender}}{Density_{emulsion} \cdot Volume_{emulsion}} \qquad \textbf{10}$$

$$\varepsilon = \frac{400\ W}{Density_{emulsion} \cdot 0.0004\ \mathrm{m}^3}$$

Table 4: Calculated Energy dissipation

Emulsion	Energy Dissipation [J/kg·s]
E60/40	1063.83
E50/50	1098.90
E40/60	1149.43
E30/70	1226.99
S60/40	1052.63

3.2 Parameter Measurements

3.2.1 Density

The densities of the prepared emulsions were found using a Baroid Mud Balance (**Fig. 3-4** and **Fig. 3-5**). The procedure is to fill the cup with emulsion, put on the lid and remove the fluid that gets squeezed through the little hole in the lid. When the air bubble in the small glass chamber is stabilized in the middle, the density can be easily read of the side of the rider (Caenn et al., 2011, p. 96)

Fig. 3-4: Mud Balance for finding density of fluids

Fig. 3-5: Air bubble stabilized in the middle of glass chamber

The densities found using the Baroid Mud Balance are shown in **Table 5** and presented graphically in **Fig. 3-6**.

Table 5: Measured densities for the different emulsions

Emulsion	Density [kg/m^3]
E60/40	940
E50/50	910
E40/60	870
E30/70	815
S60/40	950

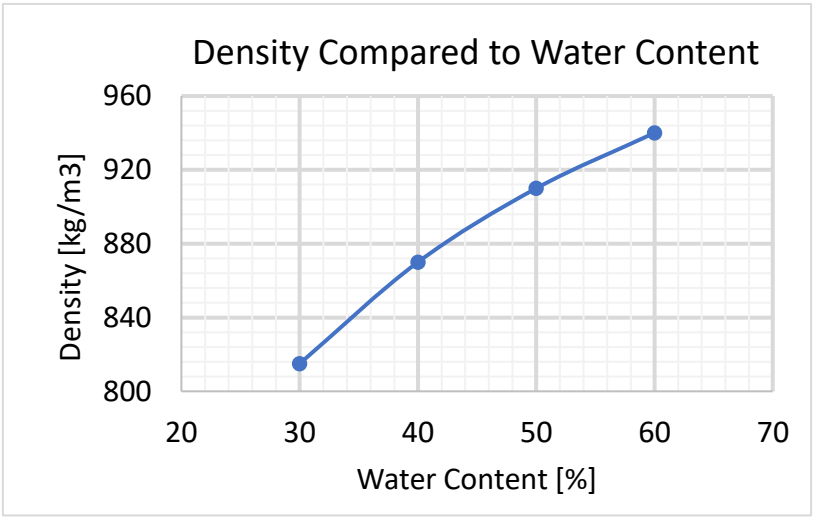

Fig. 3-6: Density compared to water content for the water-in-engine oil emulsions

3.2.2 Viscosity and Shear Stress

An Anton Paar Modular Compact Rheometer 302 (**Fig. 3-7**) were used to find the rheological properties of the emulsions. These rheometers can measure the shear stress and apparent viscosity while increasing the shear rate, and these results can be used to determine the parameters of the rheology model. The measurements were conducted using a concentric/coaxial cylinder geometry (CC27) with 28.92 mm cup and 26.66 mm bob diameter.

Fig. 3-7: Anton Paar Rheometer used to measure the apparent viscosity and rheology of the emulsions

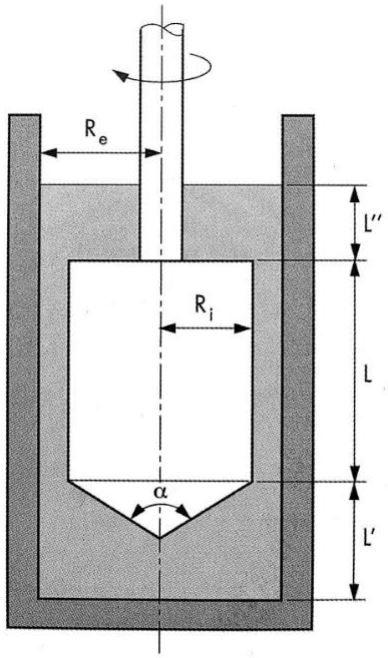

Fig. 3-8: Concentric or coaxial cylinder measuring system (Mezger, 2014, p. 233)

The rheological properties of the emulsions were examined using the following procedure: The emulsion was poured in the cup and the temperature was set. During these experiments, the temperature ranged from 4 degrees C to 60 degrees C. The spindle was connected to the apparatus and lowered down into the cup, and the system then attained the experiment temperature. The initial shear rate was set to 1 s^{-1}, and the final value to 1200 s^{-1}. Some experiments were aborted before the final shear rate was reached due to early breaking. **Fig. 3-8** illustrates how the cylinder measuring system consists of an inner cylinder (bob) and an outer cylinder (cup). In this case, the cylinder is the moving part, and the cup is stationary. The disadvantage when using this method is that turbulent flow conditions can occur when low-viscosity liquids are measured at high rotational speeds (Mezger, 2014, pp. 233-234).

Five different emulsions with varying water content were used when the concept of aging was examined using the Anton Paar Rheometer. The emulsions were tested when they were fresh, 4 hours, 24 hours, 5 days, and 12 days old, and apparent viscosity, shear stress and droplet size were examined. The rheometer gave results like the ones given below (**Fig. 3-9** and **Fig. 3-10**). However, only one of the graphs will be shown later in this thesis, as they represent the same results. Higher apparent viscosity implies higher shear stress. The results for the remaining emulsions can be found in Appendix B.

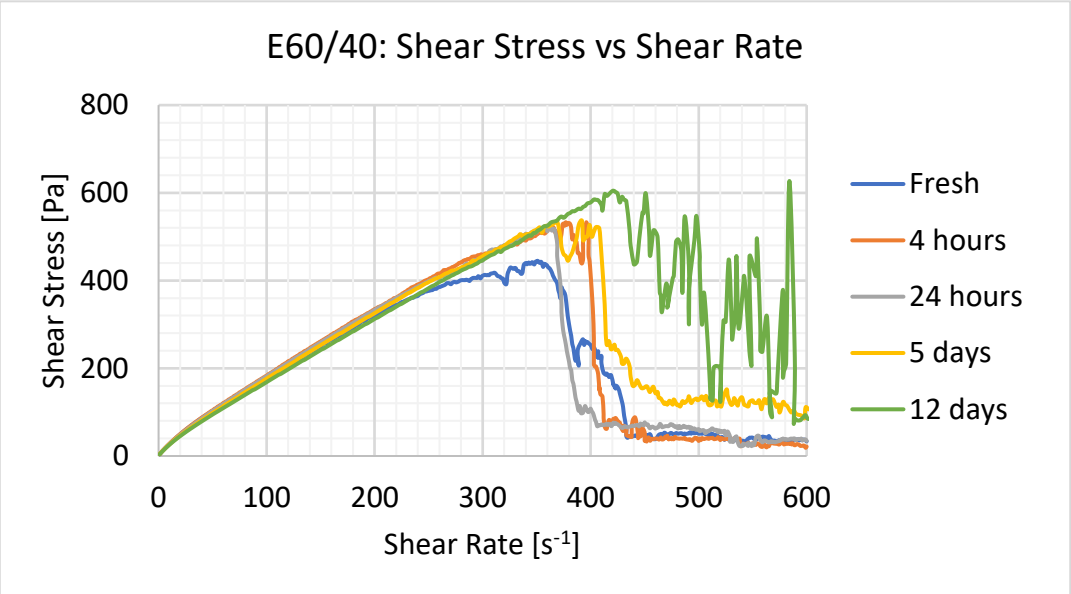

Fig. 3-9: E60/40 - Shear Stress vs Shear Rate

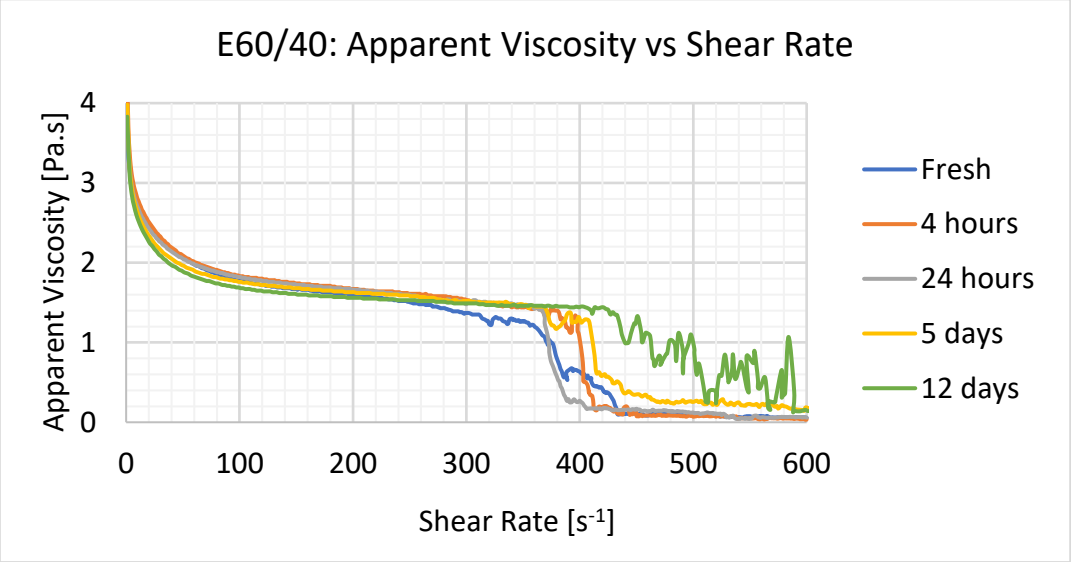

Fig. 3-10: E60/40 - Apparent Viscosity vs Shear Rate

3.2.3 Interfacial Tension

The interfacial tension (IFT) of oil and brine was measured using a Drop Shape Analyzer from Krüss (**Fig. 3-11**). When measuring the IFT, the pendant drop method was used.

Fig. 3-11: Drop Shape Analyzer (KRÜSS, 2017)

The Drop Shape Analyzer measures the IFT of the oil drop as it is released from a small needle submerged in brine. **Fig. 3-12** shows how the droplet moved upwards due to density differences between the oil and brine.

Fig. 3-12: Pendent Drop Method

Table 6 shows the IFT measurements done using the drop Shape Analyzer and the pendant drop method. The IFT was measured at 4°C, 20°C, and 60°C.

Table 6: Results from Drop Shape Analyzer

Temperature	**4°C**	**20°C**	**60°C**
Droplet Volume [µL]	32.791 ± 8.243	17.811 ± 4.439	16.183 ± 3.085
IFT [mN/m]	17.255 ± 0.567	10.103 ± 0.497	8.454± 0.618

3.3 Droplet Size Analysis

In addition to analyzing the rheology of the emulsions, the droplet sizes where found in order to see how the droplets changed due to aging.

3.3.1 Microscope Pictures

In this experiment, an Optical Microscope like seen in **Fig. 3-13** was used to take pictures of the emulsions. On top of the microscope, a CCD (charged coupled device) color camera is installed which can deliver pictures with 4000x4000 pixels (16 megapixels).

Fig. 3-13: Optical Microscope with CCD color camera

The microscope is used to take pictures of the emulsions at different stages during the aging process. Two thin glass plates were used to take pictures of the emulsion. First, 0.5 ml of Exxsol D60 oil were placed in a small container and a single drop of emulsion was added. This mixture was blended, then one drop of this mix was placed on one plate, and the other plate was positioned on top of it. The pictures taken in this microscope has a small white bar in the bottom right corner which illustrates a given length which is used as calibration when the pictures are processed further.

3.3.2 ImageJ

The pictures taken using the microscope were then processed using ImageJ. ImageJ is widely used all over the world and is a user-friendly tool when analyzing scientific pictures. It is mostly used in medical research and biological microscopy. The goal output when using ImageJ in this experiment is an Excel document with the number of droplets, droplet diameter, Feret's diameter and minimum Feret's diameter. Feret's diameter is defined as "the maximum distance between the two parallel tangents touching the particle outline in all directions," whereas the minimum Feret's diameter is the minimum distance between two parallel tangents (Wagner, 2015).

The procedure for analyzing pictures are presented in Appendix E. A picture processed using this procedure is shown in **Fig. 3-14**. In ImageJ, the background is subtracted, the pictures are converted to black and white, and then made binary which means they only consist of two colors. The challenging part of the processing is to remove the noise and make sure that all droplets are visible. When the image is done, the particles are analyzed and the data needed for further processing is available.

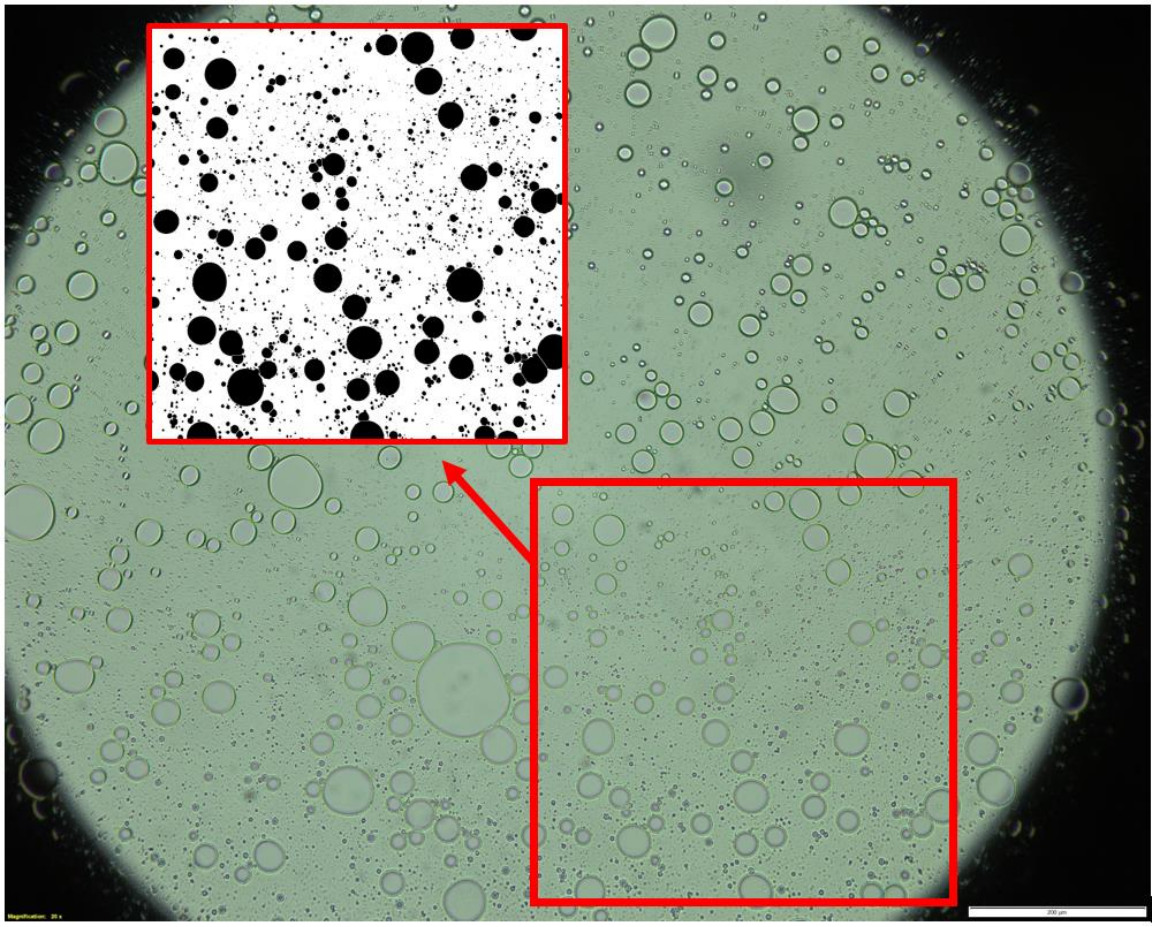

Fig. 3-14: Original microscope picture and duplicate processed in ImageJ

3.3.3 Droplet Size Distribution

The droplet sizes were found using the MATLAB code in Appendix F - 1. The code is made and presented by Harald Arne Asheim, and used to make a graphical representation of the droplets. It includes two different graphs (**Fig. 3-15**), whereas the first graph is a cumulative distribution function, which shows the log-normal droplet distribution along with an optimized distribution. The optimized distribution uses the least square method to minimize the distance between the actual measured data and the cumulative distribution graph. The second graph is a distribution density graph, which shows the variance of the measured data. This graph only represents the gradient of the first graph, but is an indication of where most of the droplets are located regarding volume. The code uses the results represented by ImageJ; number of droplets, droplet diameter, Feret's diameter and minimum Feret's diameter.

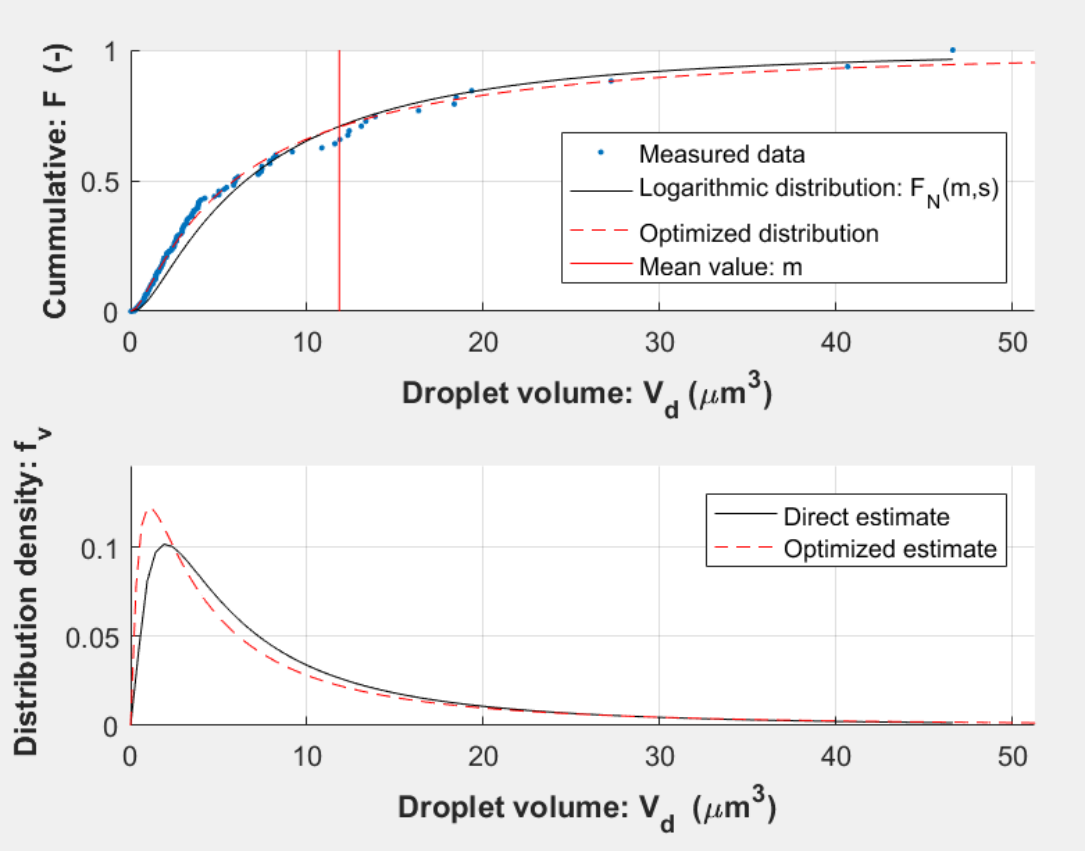

Fig. 3-15: Outcome when analyzing the droplets using the MATLAB codein Appendix F-1

To compare the droplet sizes due to aging or water content, the measured data were extracted, that is the blue points in the upper graph.

Fig. 3-16 through Fig. 3-19 shows the results obtained using the procedure explained above.

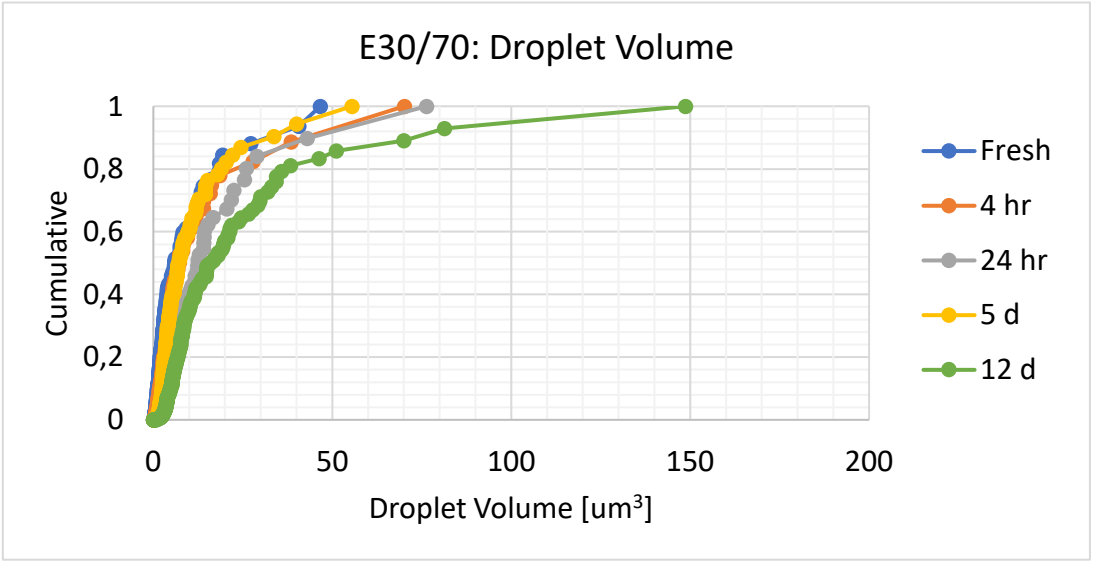

Fig. 3-16: E30/70 - Change in Droplet Volume

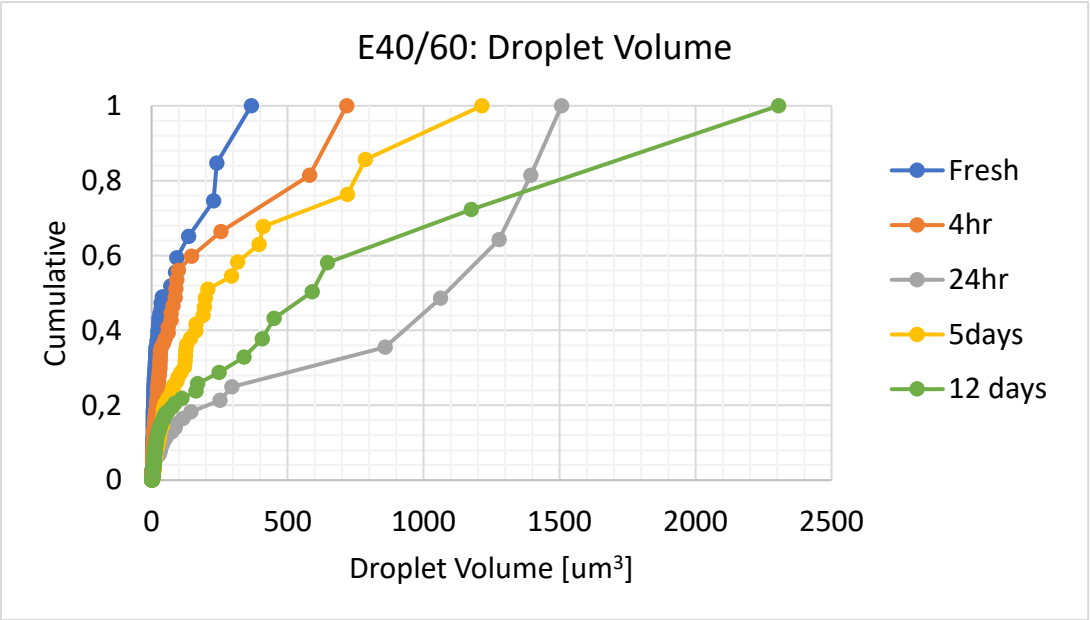

Fig. 3-17: E40/60 - Change in Droplet Volume

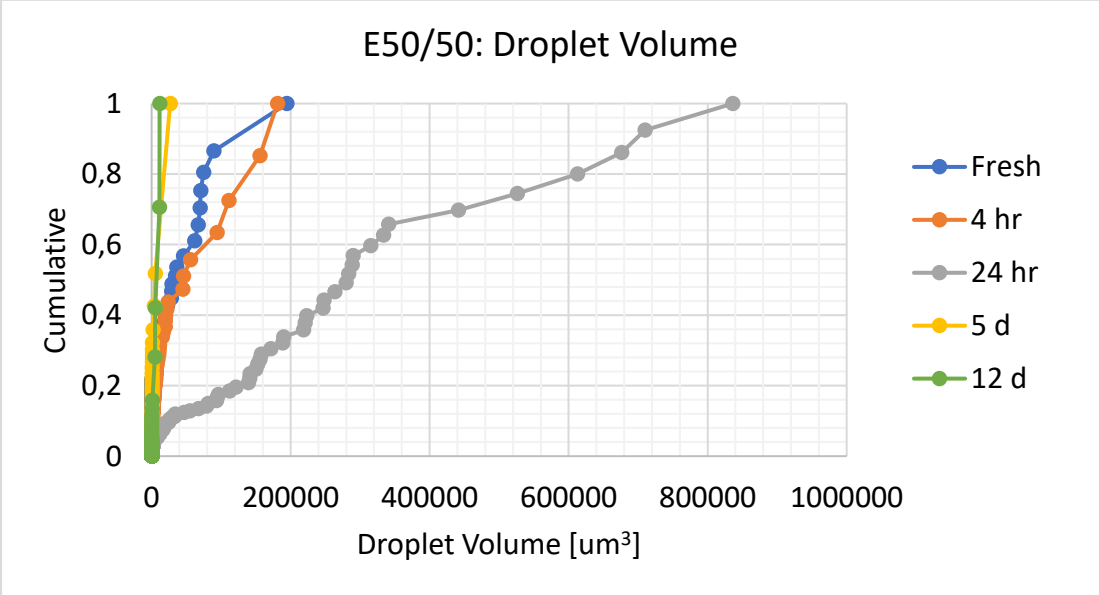

Fig. 3-18: E50/50 - Change in Droplet Volume

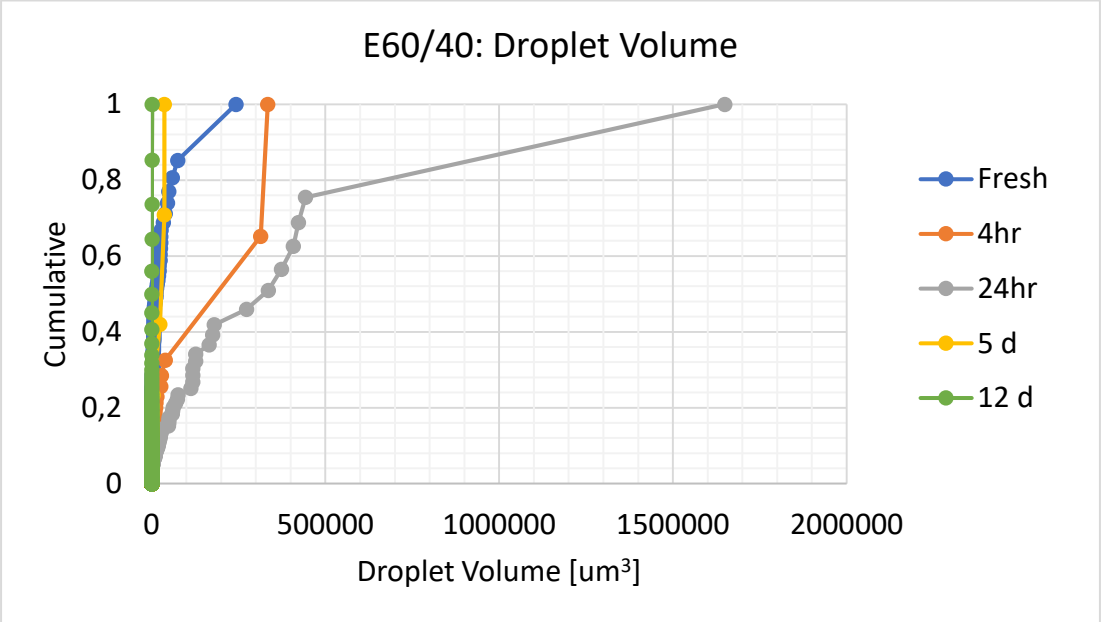

Fig. 3-19: E60/40 - Change in Droplet Volume

3.4 Flow Measurements

3.4.1 Pipeline Facility

A pipeline with two containers is used to measure the flow rate of the different emulsions. One container is placed at the top of the pipeline and one at the bottom to collect the emulsion after the pipeline transportation. A valve is placed at the bottom of the pipeline so that the pipe can be filled with emulsion before starting the experiment. That way the results will not be affected by air bubbles in the pipe.

To determine suitable dimensions for the pipeline, a small portion of emulsion were made and tested using the Anton Paar Rheometer to give an indication of what values that could be expected. An emulsion containing 60% water were used and the results from the rheometer were processed using the MATLAB codes given in Appendix F.

It was decided that a pipe length of 1.5 m and diameter of 2 cm was appropriate. These values would theoretically give a laminar flow with a flow rate of 15 cm^3/s. Since this setup is handmade in the workshop, some divagation is tolerated, and the exact values are therefore measured and these are the values used in the MATLAB codes when the theoretical values are calculated. The variation in fluid height are taken into account by employing the average of the fluid height before the valve is opened (h_{top}), and after the emulsion has flooded through the pipe (h_{bottom}) (**Fig. 3-20**).

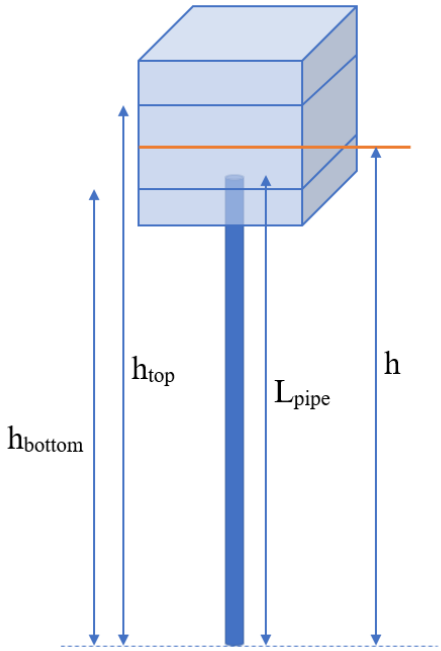

Fig. 3-20: Pipeline Set-Up

After construction, the pipe turned out 1.79 m long with an inner diameter of 2.5 cm.

$$L_{pipe} = 1.79\ m$$

$$h = 1.8636\ m$$

Fig. 3-21 through Fig. 3-23 shows how the pipeline facility was installed.

Fig. 3-21: The valve used at the bottom of the pipeline

Fig. 3-22: The container on top of the pipeline

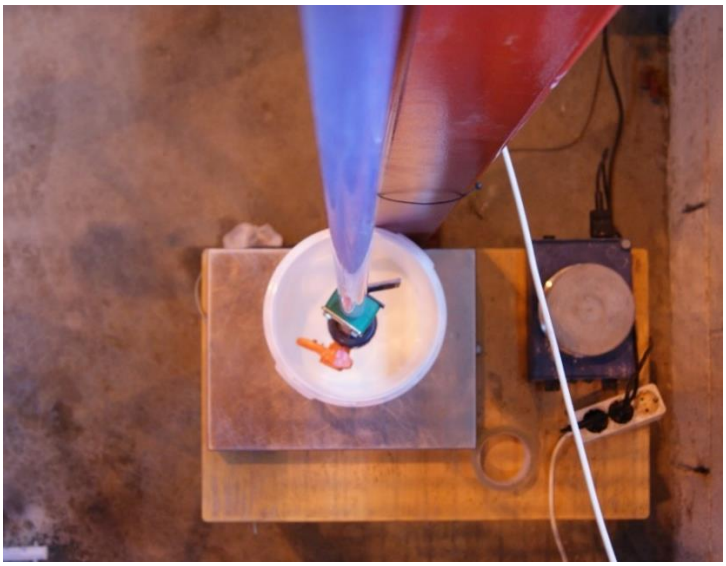

Fig. 3-23: The pipe and bucket used for collecting fluid seen from above

3.4.2 Parameterization

The theoretical flow rates were found using the results of the fresh emulsions from the Anton Paar Rheometer. The derivations of the rheology models are presented in Appendix C and D, and the final equations for the flow rates can be seen below.

$$Q = \frac{\pi R^3}{\frac{1}{n}+3}\left(\frac{\Delta P R}{2CL}\right)^{\frac{1}{n}} \quad \textbf{11}$$

$$Q = v_0\pi\left(r_0^2 + \frac{2n+2}{2n+1}r_0(r_w - r_0) + \frac{n+1}{3n+1}(r_w - r_0)^2\right) \quad \textbf{12}$$

Where $r_0 = \tau_0\frac{2L}{\Delta p}$ and $v_0 = -\left(\frac{\Delta p}{2CL}\right)^{\frac{1}{n}}\frac{n}{n+1}(r_w - r_0)^{\frac{n+1}{n}}$

Eq. 11 represents the flow rate obtained when using the Power-Law rheology model, while a Herschel-Bulkley fluid is given by Eq. 12.

The MATLAB codes in Appendix F-2 and F-4 are used to find the parameters needed to calculate the flow rate using the different rheology models and the codes in Appendix F-3 and F-5 are used to find the flow rates using the equations above. The estimated flow rates are shown in **Table 7**.

Fig. 3-24 illustrates the difference between utilizing the Herschel-Bulkley model and the Power-Law model on the soybean oil emulsion which exhibits Herschel-Bulkley rheology behavior.

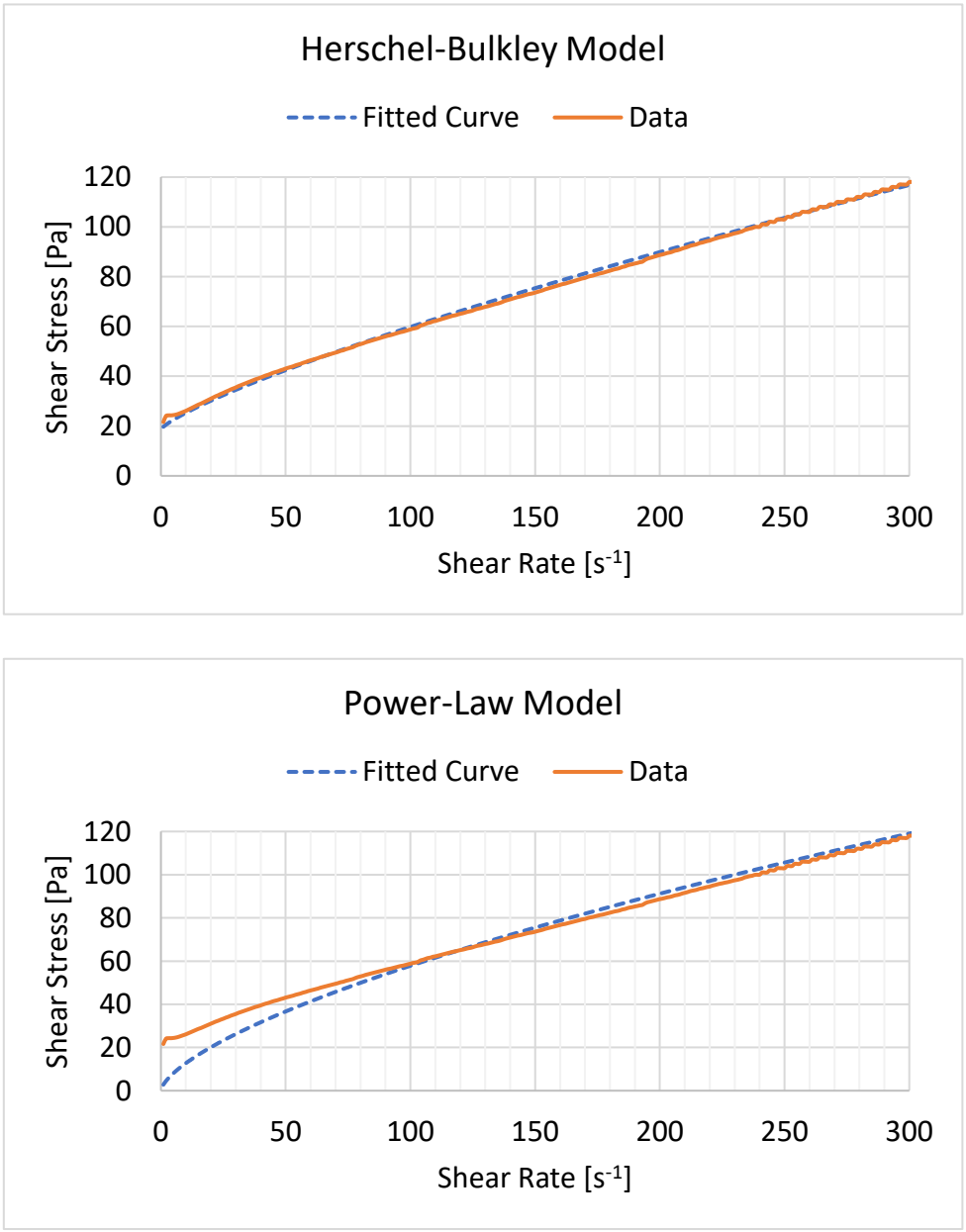

Fig. 3-24: HB (upper) and PL model presented in MATLAB with a soybean oil emulsion with HB behavior

3.4.3 Flow Experiment

Three liters of emulsion were made to conduct the pipeline experiment. It was poured into the container on top of the pipeline while the valve on the bottom was closed. The pipe was filled, and the valve was opened. The container under the pipe was standing on a scale so that the weight can be recorded and the flow rate can be determined.

The pipe was drained before a new emulsion was flooded through the pipe, but completely wiped clean before the soybean oil emulsion was poured into the pipe, since this emulsion has different rheological characteristics than the others.

Every emulsion was flooded through the pipe twice. Since the pipe was filled with fluid before the pipe was opened, local differences on the pipe wall can be neglected and both tests are included. **Fig. 3-25** shows the cumulative weight measured on the scale with time.

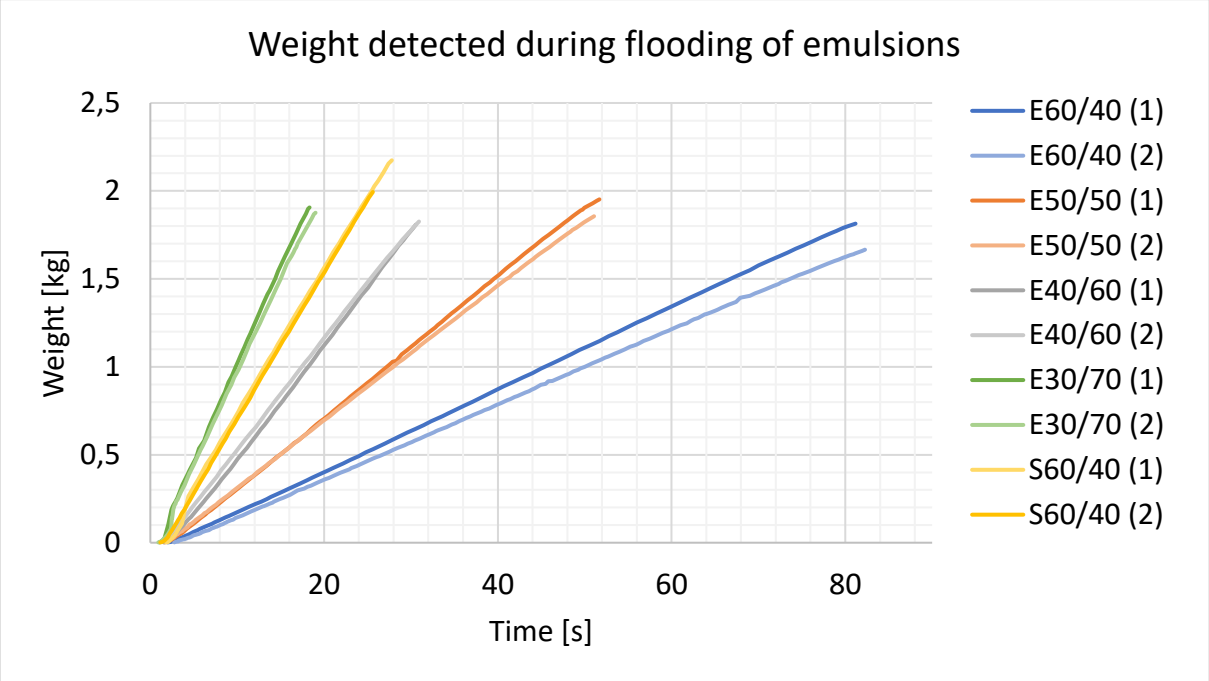

Fig. 3-25: Weight vs time for the different emulsions when being flooded through the pipeline

Table 7 shows the theoretical flow rates found using the MATLAB codes (Appendix F) and the measured flow rates when the emulsions were flooded through the pipeline.

Table 7: Flow rate results from MATLAB codes and pipeline experiments

Emulsion	Q [L/s]: MATLAB Power-Law	Q [L/s]: MATLAB Herschel-Bulkley	Q [L/s]: Pipeline Experiment	
			Run 1	Run 2
E60/40	0.0345	0.0384	0.0237	0.0223
E50/50	0.0438	0.0567	0.0428	0.0412
E40/60	0.0818	0.0823	0.0716	0.0703
E30/70	0.1153	0.1157	0.1353	0.1272
S60/40	0.1447	0.1226	0.0880	0.858

Green color indicates that the appropriate rheology model was used in MATLAB when calculating the theoretical flow rate, and red indicated that the other rheology model was used. The engine oil emulsions were observed to behave as Power-Law fluids and are therefore marked green in the first column and red in the second. The soybean oil emulsion, which behaves as a Herschel-Bulkley fluid, is marked green in the second column.

4. Results and Discussion

4.1 Water Content

Fig. 4-1 shows that higher water content results in higher apparent viscosity. An emulsion containing 55% water were made to show what happened in-between the E60/40 and E50/50.

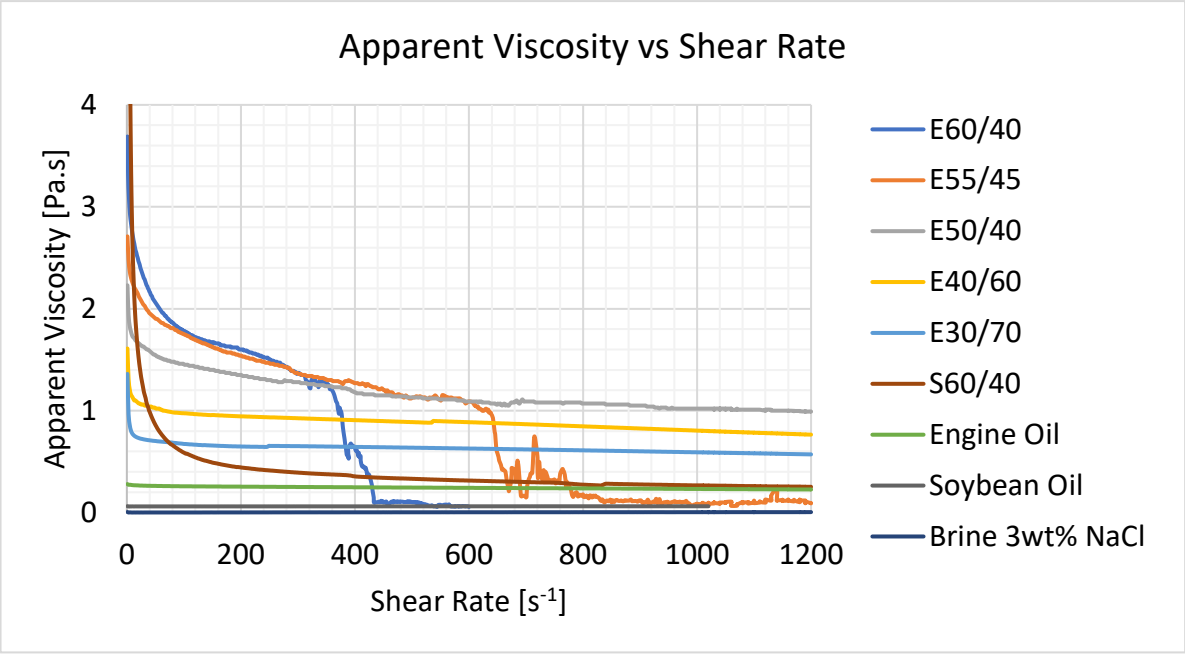

Fig. 4-1: Comparing Apparent Viscosity vs Shear Rate of engine oil emulsions with different water contents, S60/40, pure engine oil, soybean oil, and brine

Similar results were obtained for water-in-soybean oil emulsions using a Fann Viscometer during last year's specialization project (**Fig. 4-2**). The emulsions were made using a homogenizer with a mixing speed of 140 rpm for 20 minutes.

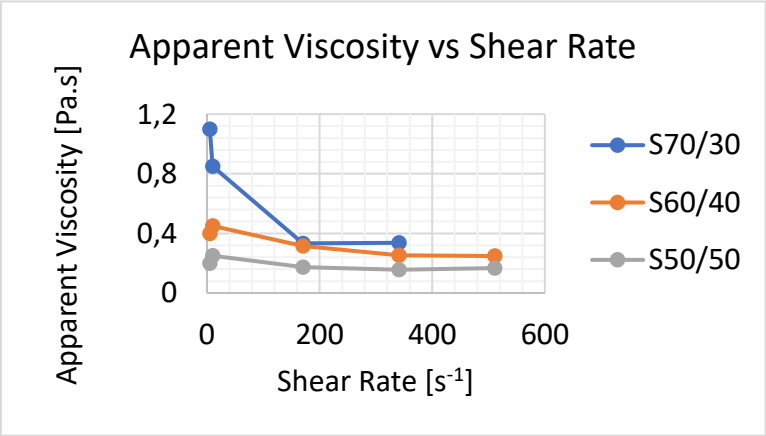

Fig. 4-2: Apparent Viscosity vs Shear Rate for water-in-soybean oil emulsions

Keleşoğlu et al. (2012) analyzed the rheological behavior of W/O emulsions with heavy North Sea crude oil as the continuous phase. The apparent viscosity of this emulsion was overall higher than the viscosity of the engine oil emulsions made in this study. Comparing the viscosity of the crude oil, the engine oil and the soybean oil, shows that more viscous oils create more viscous emulsions. In this study, the apparent viscosity of the emulsion is significantly higher than oil and water alone. Depending on the chemical components in the oil, the emulsion can give lower or higher rheological values than the initial oil. An example is heavy crude oil being emulsified to ease the pipe transport.

The results indicate that higher water content in the emulsions leads to breaking at lower shear rates. This phenomenon is most likely a result of either water or oil coming out of the emulsion and creates a thin film around the bob of the rheometer, hence reducing the drag and decreases the apparent viscosity and shear stress. After breaking, the apparent viscosity decreases down to a level between the brine and engine oil. The one containing 60% water breaks first, followed by the one with 55% water. The graph representing the emulsion with 50% water has a rough and uneven appearance, which makes it reasonable to believe that it is about to break. The shear rate in the rheometer increased steadily from 1 s^{-1} to 1200 s^{-1} during the tests, but 1200 s^{-1} was only sufficient enough to break the two emulsions with most water. It is expected that all the emulsions would experience breaking if the experiments included higher shear rates.

Fig. 4-3 clearly shows that while the engine oil, soybean oil, and brine acts like Newtonian fluids, the emulsions exhibit Bingham Plastic behavior.

- E60/40: Exhibits shear thinning behavior until it breaks at about 320 s^{-1}.
- E55/45: Displays shear thinning effects, slightly weaker than E60/40, all the way until it breaks at 640 s^{-1}.
- E50/50: Clear shear thinning effects below 10 s^{-1}, but Bingham Plastic behavior can be seen until the final shear rate of 1200 s^{-1}.
- E40/60: Clear shear thinning effects below 10 s^{-1}, but the emulsion behaves slightly as a Bingham Plastic until a shear rate of 1200 s^{-1}.
- E30/70: Definite shear thinning effects below 5 s^{-1}, and slight Bingham Plastic behavior beyond.
- S60/40: Strong shear thinning effects below 150 s^{-1}.
- Engine oil, soybean oil, and brine: Exhibits clear Newtonian behavior for all shear rates.

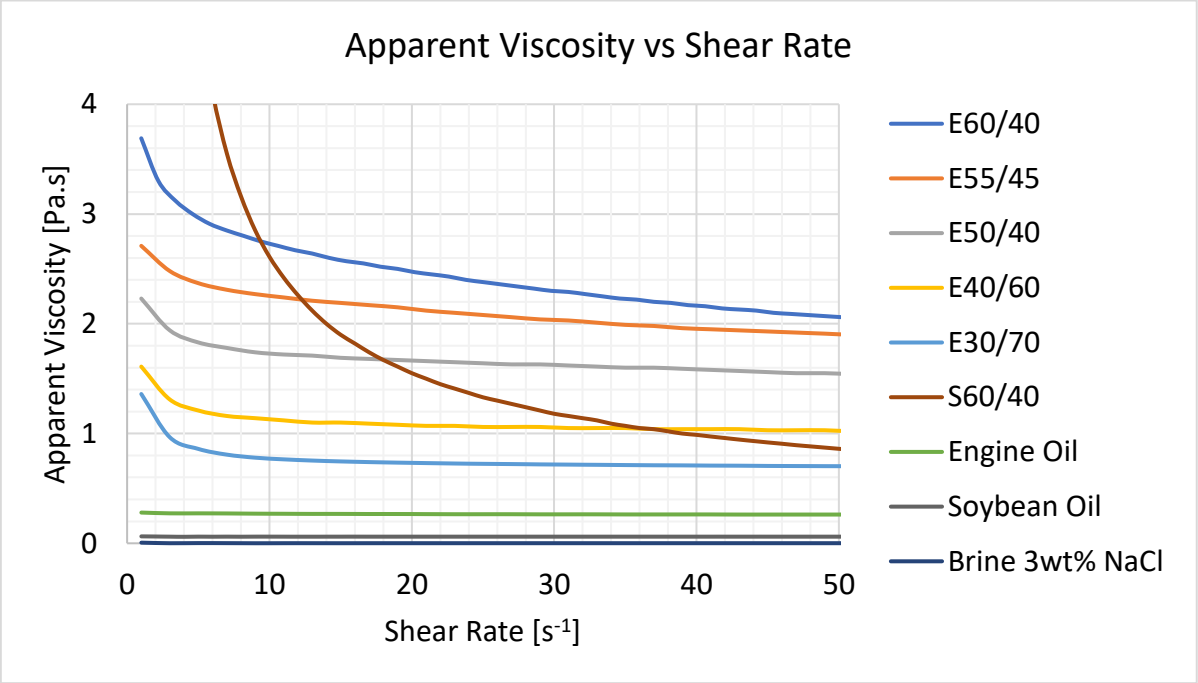

Fig. 4-3: Apparent Viscosity vs Shear Rate (low shear rates)

While the soybean oil emulsion shows a strong shear thinning behavior over a wide range of shear rates, the engine oil emulsions exhibit clear shear thinning effects below 10 s^{-1}. When the water content is low, the influence of shear rate becomes nearly insignificant. Even though Bingham Plastic behavior was observed for all the engine oil emulsions, the emulsions with low water contents (E40/60 and E30/70) behaved almost as Newtonian fluids at high shear rates.

From the shear rate/shear stress graph (**Fig. 4-4**), it is easy to see that the soybean oil emulsion must overcome a yield before being able to flow. This yield indicates Bingham Plastic or Herschel-Bulkley fluid.

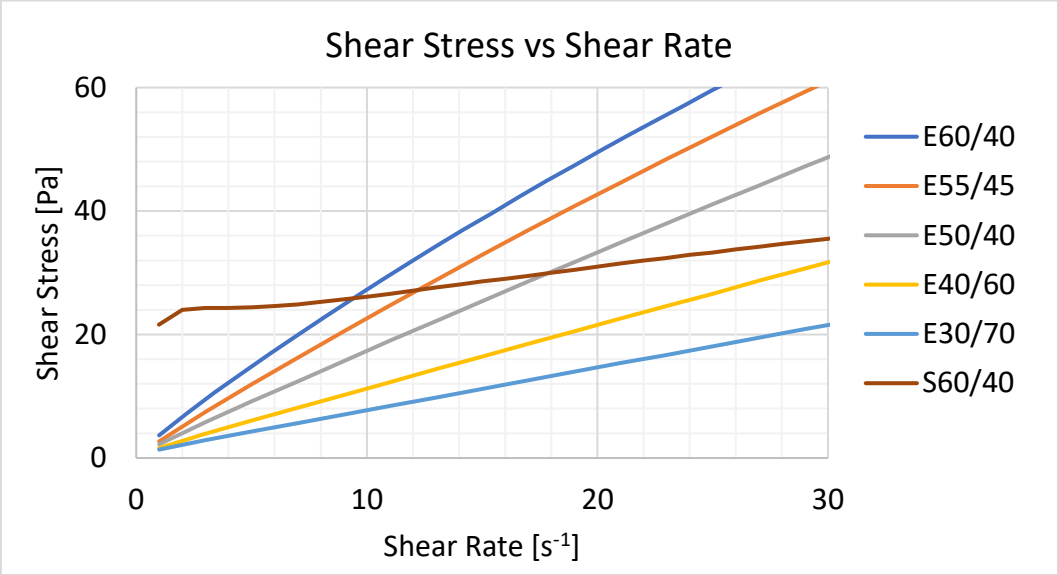

Fig. 4-4: Shear Stress vs Shear Rate (low shear rates)

Fig. 4-5 shows the shear rate/shear stress graph for the S60/40 emulsion. A linear trendline is placed on top to illustrate that the emulsion does not follow the Bingham Plastic rheology model, but rather the Herschel-Bulkley model.

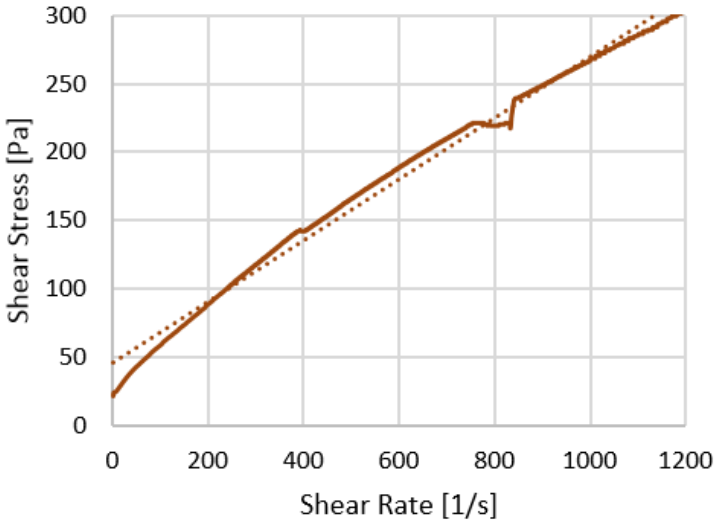

Fig. 4-5: S60/40 - Determination of Bingham Plastic or Herschel-Bulkley fluid

Fig. 4-6 shows how the droplet sizes changed due to water content. The graph is made logarithmical since the droplets are so much bigger in the emulsions containing 60% and 50% water, compared to the ones with less water.

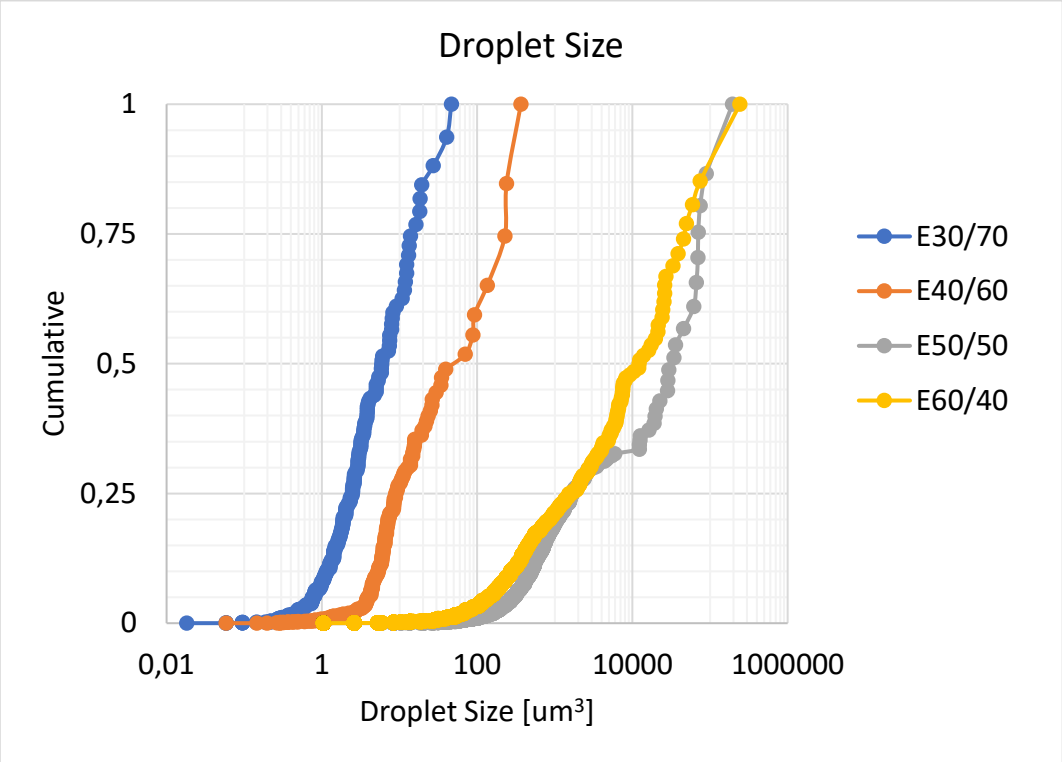

Fig. 4-6: Droplet size for fresh emulsions

4.2 Aging

Emulsions containing 60%, 50%, 40% and 30% water were tested in Anton Paar Rheometer over a 12-day period. The emulsions were kept at room temperature (20°C). The shear stress and apparent viscosity graphs are presented in Appendix B.

- E60/40: The fresh emulsion is the one reaching the breaking point first. The 5-day and 12-day emulsions are the last to break, the latter reaching a shear rate of 420 s^{-1} before breaking.
- E50/50: The emulsion containing 50% water shows no signs of breaking within the investigated shear rate interval from 1 s^{-1} to 1200 s^{-1}. The graphs show no distinct behavior differences between the youngest emulsions, but 5-days and 12-days have lower shear stress and apparent viscosity.
- E40/60: The shear stress and apparent viscosity decrease with time.

- E30/70: Even though the fresh and 4-hour old emulsions are almost identical in behavior, the others show the same trend as the E40/60. It should be noted that the values on the y-axis cover a very small interval, so the apparent viscosity barely changes, and the fluid behaves almost like a Newtonian fluid.

When the W/O emulsions are made, there may be some free water in the mixture. However, some emulsions get more stable with time, due to a more even spread of emulsifying agents. The emulsifiers may need some time to surround all the dispersed droplets, which is why the 12-day old emulsion containing 60% water can reach higher shear rates before breaking. This is only the case if there is enough emulsifying agent present in the emulsion to surround all the dispersed droplets, otherwise it would become unstable and the separation process would begin.

For the emulsions not experiencing breaking before a shear rate of 1200 s^{-1} is reached, there are clear trends that show that the shear stress and apparent viscosity decrease with time. Hence, it is reasonable to expect even older emulsions to be more viscous.

The microscope was used to take pictures of the emulsions at the different stages of this 12-day period. Some of the emulsion show clear signs of flocculation with aging. **Fig. 4-7 through Fig. 4-10** shows how droplets of varied sizes have flocculated due to the forces between them. The pictures are presented at the same scale, so the droplets are comparable.

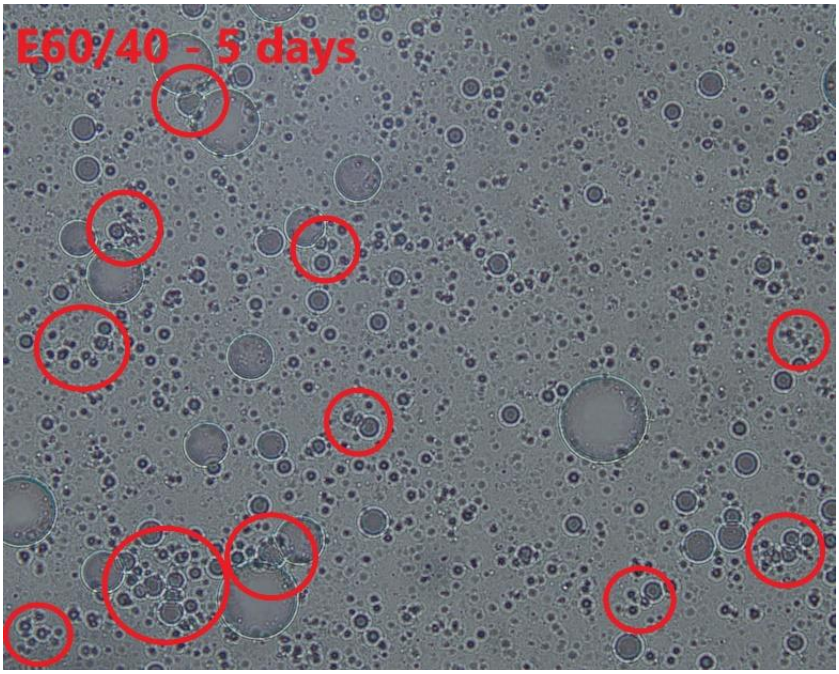

Fig. 4-7: Flocculation in E60/40 after 5 days

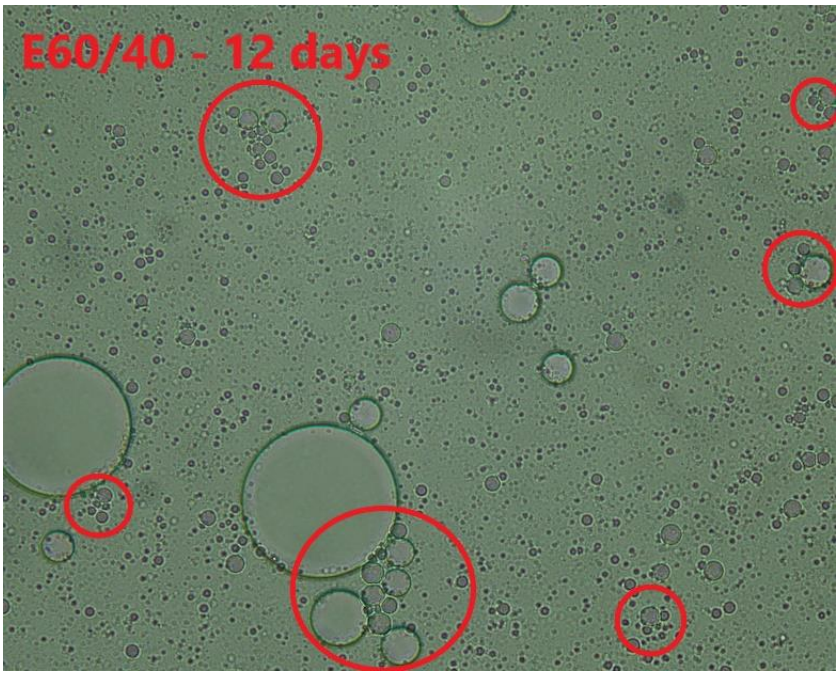

Fig. 4-8: Flocculation in E60/40 after 12 days

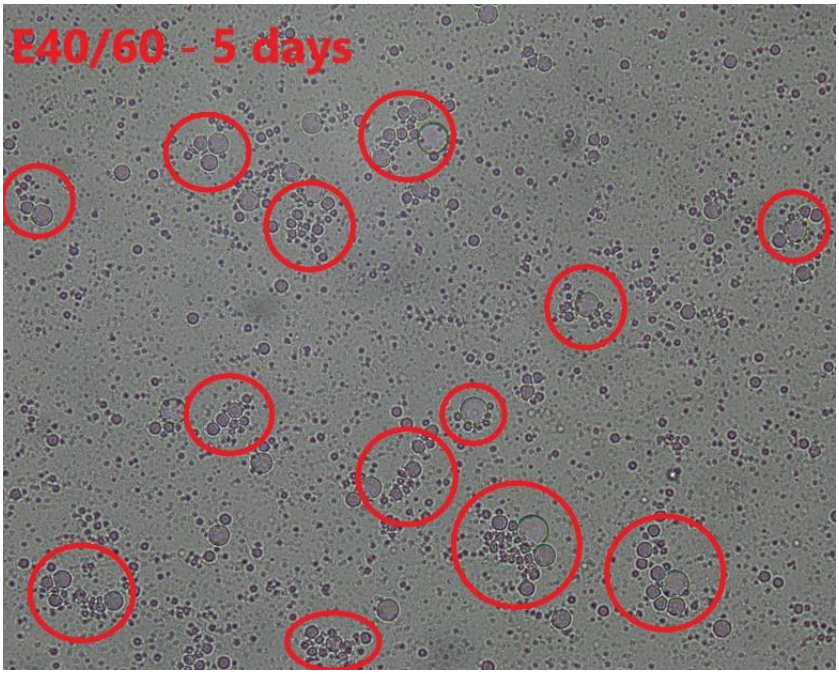

Fig. 4-9: Flocculation in E40/60 after 5 days

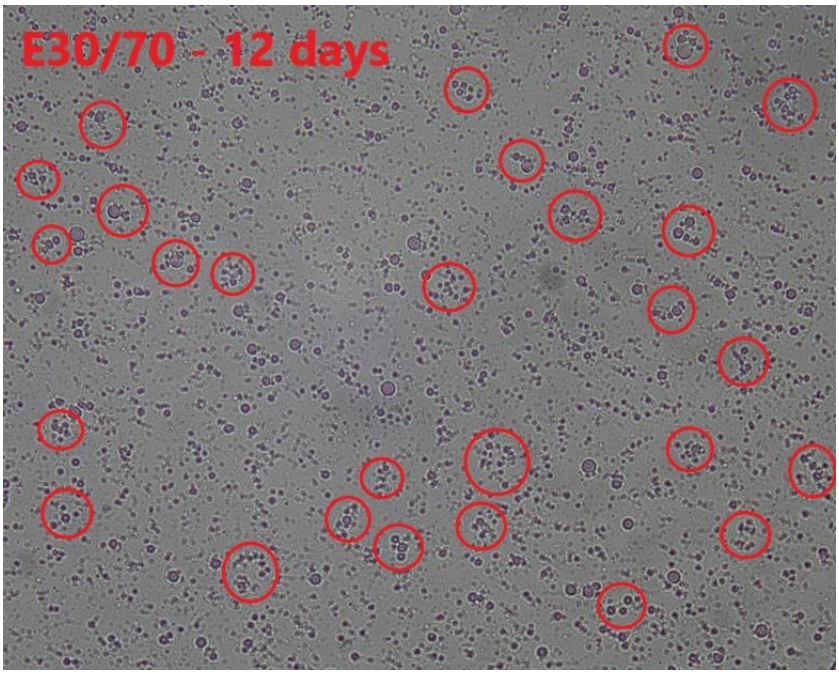

Fig. 4-10: Flocculation in E30/70 after 12 days

Note that some of the flocs circled in these pictures may not seem like flocs when the pictures are downscaled because some of the small droplets appear invisible and that not all flocs are circled.

Pal (1996) experienced that fine emulsions exhibit a greater tendency to flocculate. While the emulsions with a high water cut indicate some flocculation, the concentration of flocs is greater when the water content is lower. The flocs are naturally smaller, but they appear more often. The droplets in E30/70 are very small compared to the ones in E60/40, and it is clear that more water gives more coarse/heterogeneous emulsions when the mixing conditions are similar. Pal (1996) experienced that fine emulsions had higher apparent viscosity and stronger shear thinning effects than coarse emulsions when he compared fine and coarse emulsions of similar water contents. The results obtained here show that the coarse emulsions, hence the ones with more water, experience higher apparent viscosity and stronger shear thinning effects. This could mean that water cut is the dominating factor before polydispersity when it comes to determining the apparent viscosity of emulsions.

Two batches of E60/40 and E30/70 were made to observe the separation process. These two emulsions were selected for this visual separation project since they are the ones containing most water and oil respectively. The emulsions are stored in test tubes like the one seen in **Fig. 4-11**.

There were three different test tubes for each emulsion. One was placed in the fridge at 4°C, one was placed in the laboratory at room temperature (20°C) and the last one was placed in the oven at 60°C to resemble hot down-hole conditions.

The emulsion containing most oil experienced a rapid extraction of oil when exposed to high temperature (**Fig. 4-12**). When the emulsion contained most water, the extraction of oil happened much more slowly **(Fig. 4-13)**, but the temperature played a noticeable part of the separation process.

Fig. 4-11: Test tube for storing emulsions during temperature tests

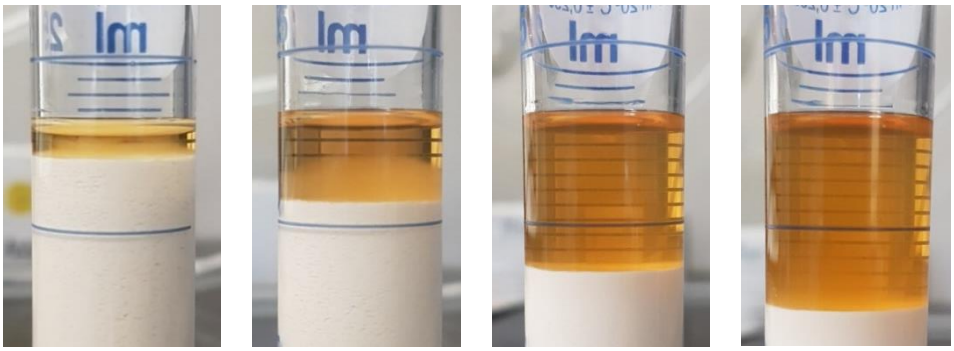

Fig. 4-12: E30/70 60°C

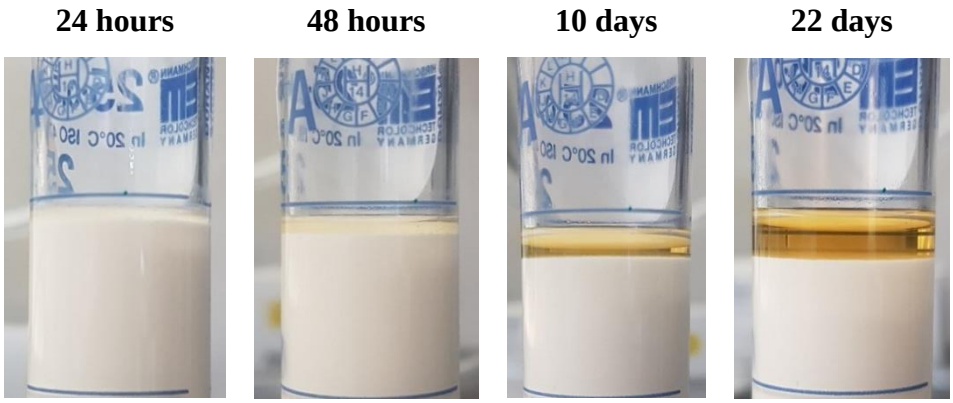

Fig. 4-13: E60/40 60°C

There were no signs of water coming out the emulsions at any time during the experiments. The reason why oil is the only fluid coming out is probably due to free oil in the emulsion, which is not in contact with any dispersed water. In addition to having less oil available, there are bigger water droplets in E60/40, which means that more oil is needed to enclose the droplets. But still, as seen in **Fig. 4-14** and **Fig. 4-15**, there is some free oil capable of coming out of the mixture. **Fig. 4-16** and **Fig. 4-17** show the impact temperature have on the rate of separation in the emulsions.

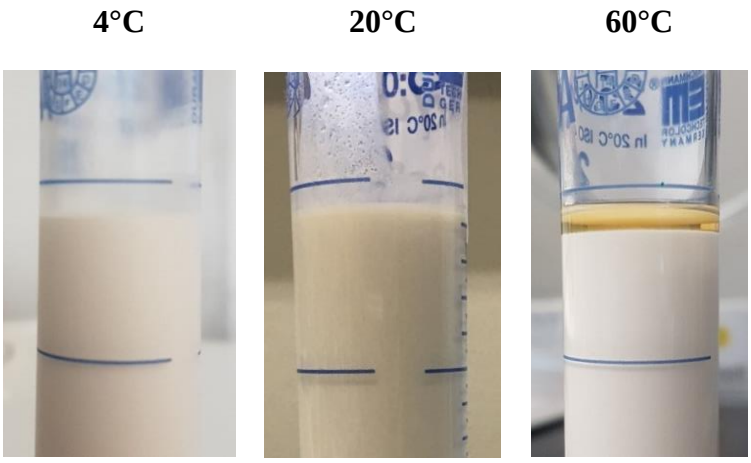

Fig. 4-14: E60/40 after 10 days

4°C 20°C 60°C

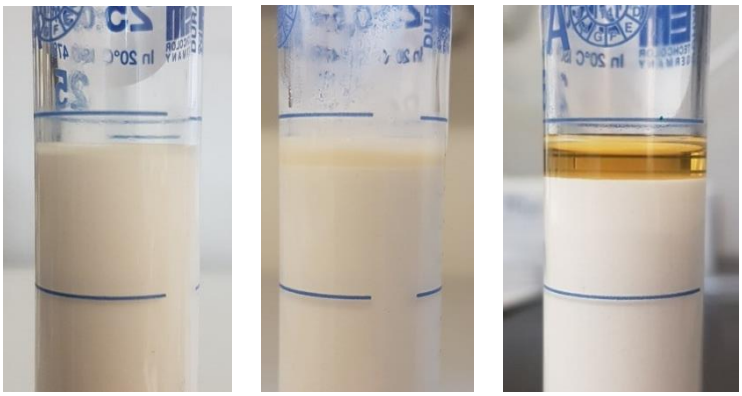

Fig. 4-15: E60/40 after 22 days

4°C 20°C 60°C

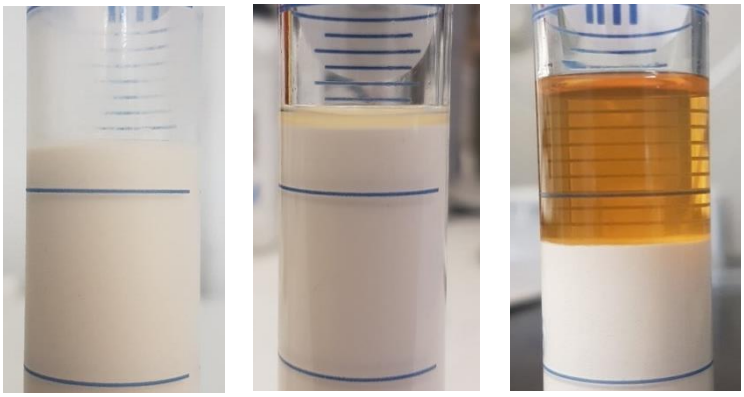

Fig. 4-16: E30/70 after 10 days

4°C 20°C 60°C

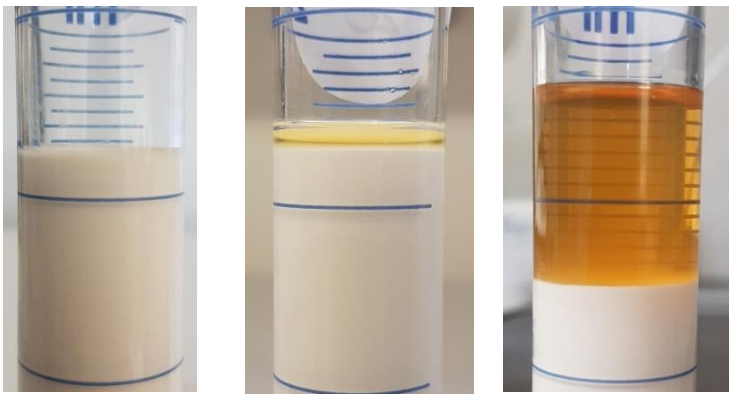

Fig. 4-17: E30/70 after 22 days

There were signs of extracted oil in both emulsions at 20°C after 22 days and the tests placed in the fridge at 4°C were still very stable. There were no signs of water in any of the emulsions after 22 days. This means that the water droplets must be fully enclosed in oil. As seen in Chapter 3.1.2 (page 25), the emulsion containing 70% water experienced a very rapid separation of water, which indicates that at a water volume fraction of 70% (at least), there are not enough emulsifying agents in the mineral oil to cover all the dispersed water droplets.

The results obtained using the Drop Shape Analyzer (Chapter 3.2.3) shows that the IFT between brine and the engine oil decreases when the temperature gets higher. That means that the two phases can separate more easily when exposed to heat since the forces that keep the surfaces stable are weaker. The visual observations done here shows that the emulsions separate much faster at high temperatures. During the IFT experiments in the Droplet Shape Analyzer, the droplet volumes were also measured. Due to higher IFT at lower temperature, the droplets measured at high temperatures were smaller.

The results presented in Chapter 3.3 Droplet Size Analysis, shows that there are no clear trends when it comes to droplet size due to aging using our method. While increasing droplet volumes were expected with aging, this could only be seen for the fresh, 4 hours – and 24 hours old emulsions. The droplet volumes after 5 – and 12 days, are irregular and often turned out to be smaller than when they were fresh. More clear and definite results could probably be obtained using another method or other fluids.

Table 8 includes the calculated average droplet volumes when the emulsions are fresh and 12 days old. The droplets in E40/60 and E30/70 increase in size during this period of time. However, the emulsions containing most water, experience a decrease in droplet size. The droplets were expected to grow with time, due to either coalescence or Ostwald ripening. The reason for the observed decrease in droplet size could be due to defects of the method employed. The emulsions were challenging to process in ImageJ, and this is decisive for the results. Another reason can be that since the emulsifying agents in the oil needed some time to spread out and surround all the dispersed water droplets in the emulsion, the water may have had time to split into smaller droplets before the spread of emulsifiers were completed.

In the study done by Pal (1996), fine emulsions were found to have higher apparent viscosity than the corresponding coarse emulsions with similar water concentration. Analyzing the droplet volumes (MATLAB code in Appendix F-1), shows that both E60/40 and E50/50 were more polydispersed when fresh, compared to after 12 days (**Fig. 4-18**). **Fig. 4-19** shows that the coarse emulsions had higher viscosities, which deviate from Pal's observations. However, the

emulsions Pal (1996) investigated were made at the same time, so there may be other factors influencing the apparent viscosity and both studies may show realistic and correct results.

Table 8: Average droplet volumes when fresh and 12 days old

Emulsion	Avg. Droplet Volume: Fresh [µm³]	Change	Avg. Droplet Volume: 12 days [µm³]
E60/40	548.29	Decrease	29.64
E50/50	1208.03	Decrease	143.56
E40/60	12.43	Increase	49.72
E30/70	2.70	Increase	10.25

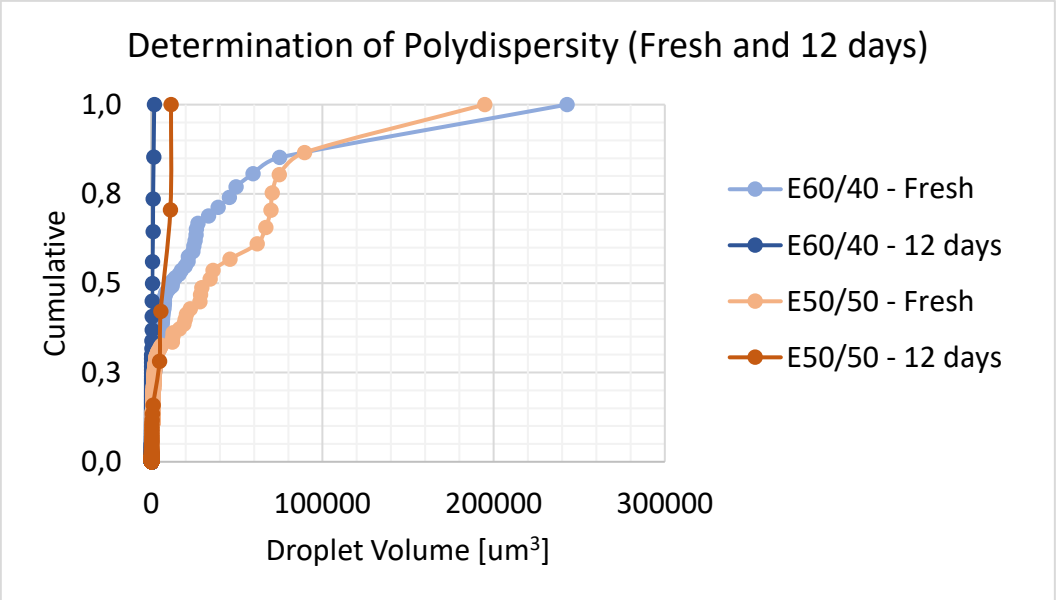

Fig. 4-18: Determination of Polydispersity of E60/40 and E50/50

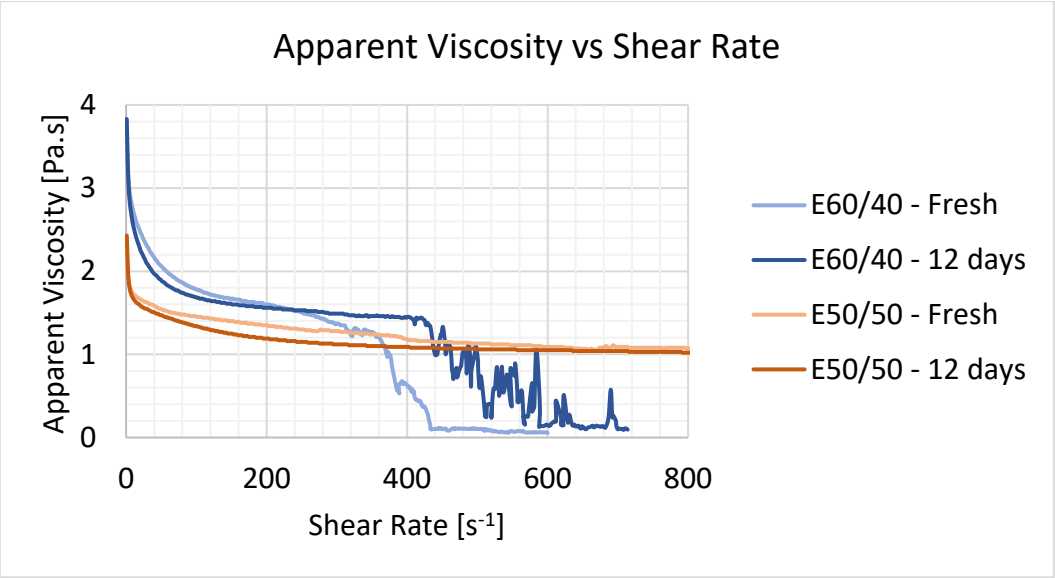

Fig. 4-19: Comparing Apparent Viscosity and Shear Thinning effects when fresh and 12 days old

4.3 Temperature

Fig. 4-20 and **Fig. 4-21** shows that the shear stress and apparent viscosity increase with lower temperatures. The reason is that as the temperature increases, the IFT decreases and reduces the apparent viscosity. Another observation is that the breaking of E60/40 gets delayed until higher shear rates are obtained when the temperature increases. This is incompatible to what is expected. As mentioned, heating is a common method when separating emulsions, because it will lead to earlier breaking. However, the observations done here shows that the emulsions break at lower shear rates when it is cold.

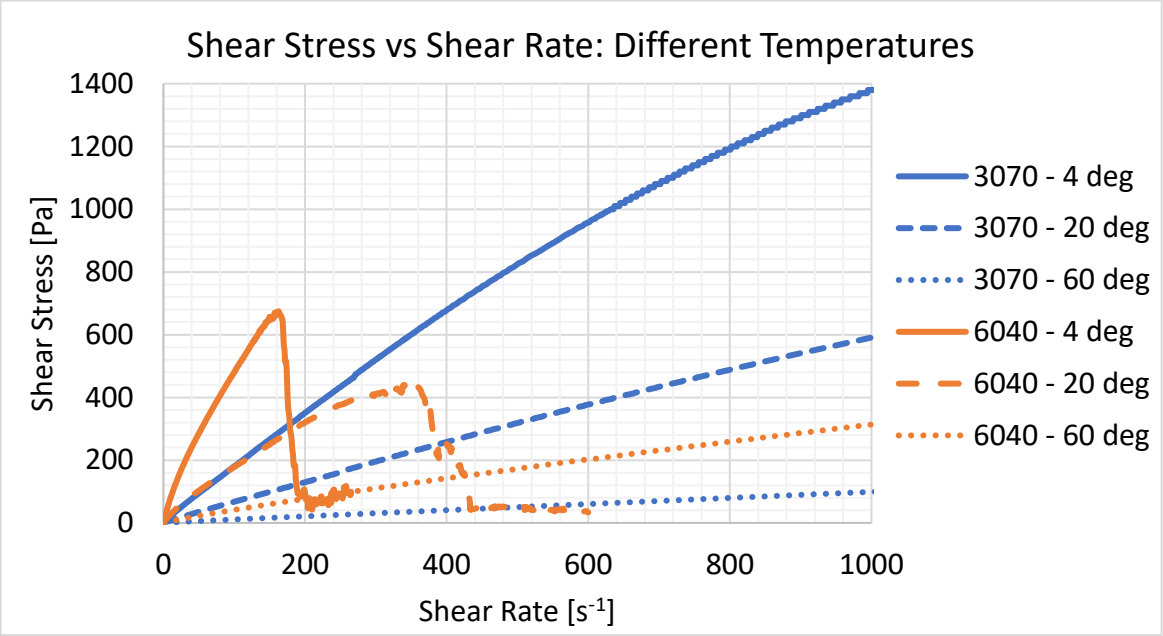

Fig. 4-20: Shear Stress vs Shear Rate: Different Temperatures

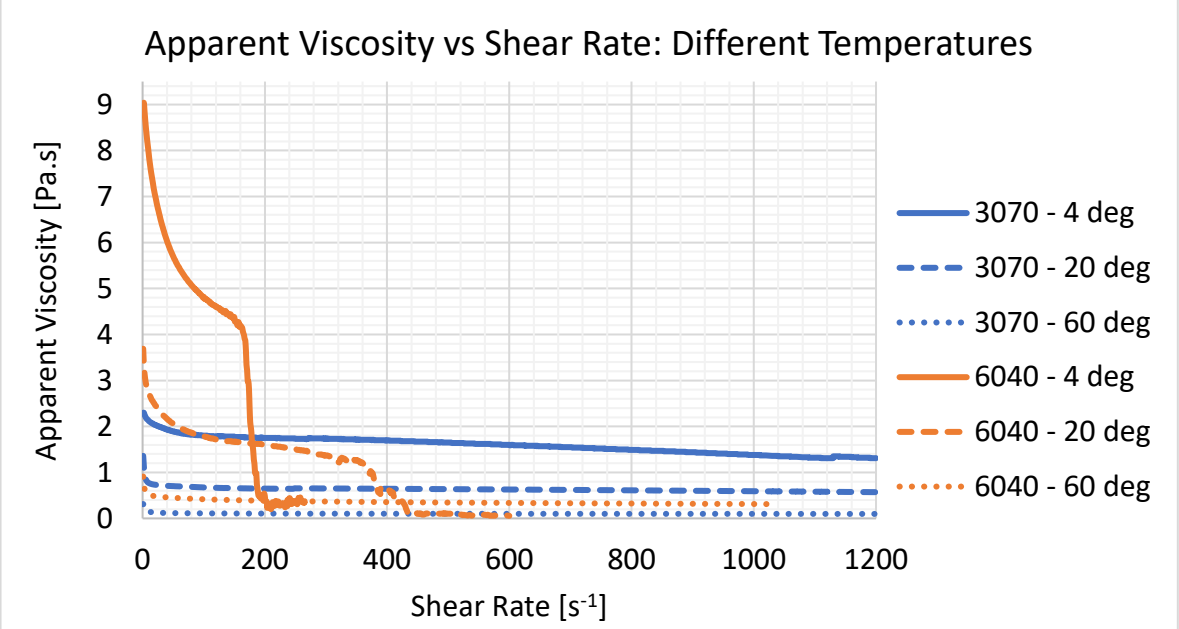

Fig. 4-21: Apparent Viscosity vs Shear Rate: Different Temperatures

E60/40 exhibits really strong shear thinning effects until breaking at 165 s^{-1} at 4°C. At 20°C, shear thinning occurs at shear rates below 100 s^{-1}. At 60°C, shear thinning is observed below 5 s^{-1}, even though there are minor signs of Bingham Plastic behavior until a shear rate of 1200 s^{-1} is reached. E30/70 shows clear shear thinning behavior below 5 s^{-1} at all temperatures and fits the Newtonian rheology model above 10 s^{-1} at 60°C with a R-squared value of 0.9998 based on a linear trendline. At 4°C and 20°C, E30/70 fits the Bingham Plastic rheology model, hence acts as a shear thinning fluid. The shear thinning effect is stronger at 4°C.

The ambient temperature at the seabed may be around 4°C and it is interesting to observe what happens when such low temperatures are attained. The apparent viscosity and shear stress increases drastically, and Chapter 4.2 shows that the low temperature also affects the degree of separation in the emulsion. Temperature is known to speed up all kinds of chemical reactions, and it is clear that it also speeds up the rate of separation in emulsions.

Fig. 4-22 shows the apparent viscosity of the emulsions at shear rates 1 s^{-1} and 100 s^{-1}. Water content and shear rate are bigger influencers of apparent viscosity at low temperatures. At high temperatures, the water content and shear rates are of less importance, since most emulsions and fluids will achieve a low viscosity when heated. Another observation is that even though both water content and temperature clearly have a strong impact on emulsion viscosity, it seems like water content is the dominating factor.

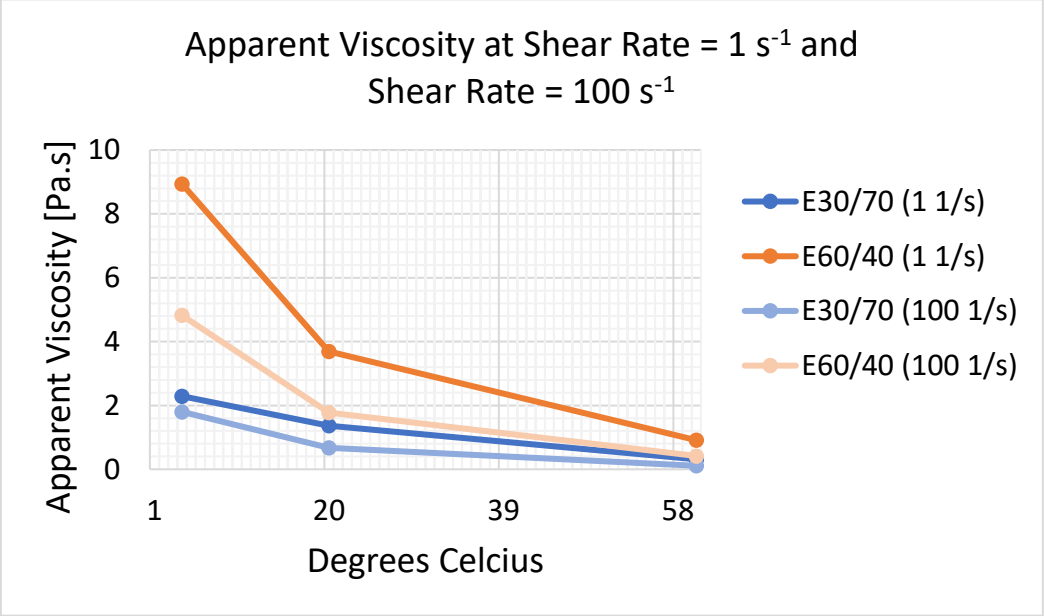

Fig. 4-22: Apparent Viscosity of E60/40 and E30/70 at different temperatures at shear rates 1 s^{-1} and 100 s^{-1}

4.4 Pipeline Flow Experiment

The pipeline flow results shows that the more visous engine oil emulsions flooded through the pipeline slower than the less viscous engine oil emulsions. This means that high water content in the engine oil emulsions made the emulsions flood through the pipe at a slower rate. The soybean oil emulsion flooded through the pipeline slower than the least viscous engine oil emulsion, even though the engine oil emulsion has a higher apparent viscosity. However, the soybean oil emulsion only has a lower apparent viscosity beyond a certain shear rate (here: 74 s^{-1}).

The flow of fluids and emulsions are dependent on so many different factors, but one of the reasons why the soybean oil flooded through the pipe slower than the more viscous, could be that when the emulsions are flooded through the pipe, they experience a shear rate. Since the soybean oil emulsion flooded through the pipe at a rate in between E40/60 and E30/70, the shear rate can be within the interval from 37 s^{-1} to 74 s^{-1} (**Fig. 4-23**). This interval indicates the shear rates where the apparent viscosity of the soybean oil emulsion first exceeds E40/60 and then E30/70. There are probably other factors with greater influence on the flow rate as opposed to the shear rate experienced in the pipe. Other possibilities can be that different emulsions experience different drag on the pipe wall, or that since the soybean oil emulsion suits the Herschel-Bulkley rheology model, the yield can influence the flow behavior, the latter being very likely.

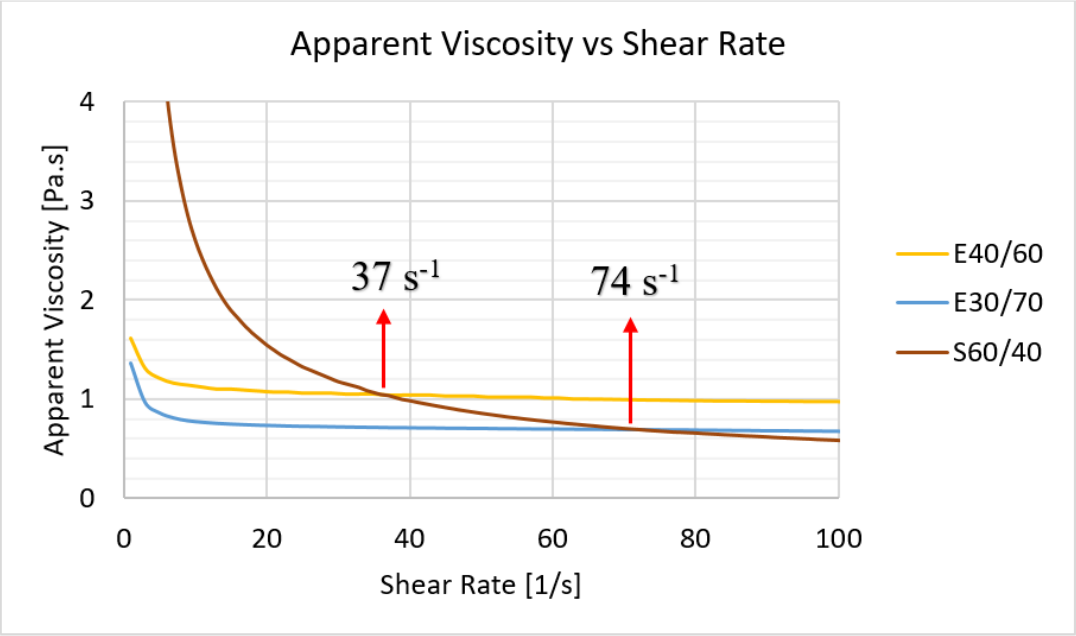

Fig. 4-23: Possible interval of shear rate experienced in pipeline

Table 9 and **Table 10** give the deviation in percentage between the calculated flow rates and the flow rates measured when flooding through the pipeline. Every emulsion gave a higher deviation between the two flow rates when the inappropriate rheology model was used, except E30/70 which shows lower deviation for both tests.

The percent deviation is calculated by using Eq. 13.

$$\frac{measured\ value - calculated\ value}{calculated\ value} \cdot 100\% \qquad \textbf{13}$$

Table 9: Percent Deviation between predicted and measured flow rate (Test 1)

Emulsion	Percent Deviation: Power-Law Model		Percent Deviation: Herschel-Bulkley Model
E60/40	- 31.4 %	<	- 38.3 %
E50/50	- 2.2 %	<	- 24.5 %
E40/60	- 12.5 %	<	- 13.0 %
E30/70	+ 17.4 %	>	+ 17.0 %
S60/40	- 39.2 %	>	- 28.2 %

Table 10: Percent Deviation between predicted and measured flow rate (Test 2)

Emulsion	Percent Deviation: Power-Law Model		Percent Deviation: Herschel-Bulkley Model
E60/40	- 35.4 %	<	- 41.9 %
E50/50	- 5.9 %	<	- 27.3 %
E40/60	- 14.1 %	<	- 14.6 %
E30/70	+ 10.3 %	>	+ 9.9 %
S60/40	- 40.7 %	>	- 30.0 %

Even though the appropriate rheology model shows lower deviation for all except E30/70, the results are not clear enough to safely say that the theoretical models demonstrate what actually happens. In the petroleum industry, there are pumps and turbines which contribute with pressure and therefore helps the fluid through the pipeline, whereas gravity and the weight of the fluid

column were the only forces acting on the emulsion in this scenario. However, the fluid column and gravity were the only factors considered in the MATLAB codes.

Even though the predicted flow rates had significant deviation from the measured flow rates, the models are a good place to start. The average deviation between measured and estimated flow rate using the Power-Law rheology model was 15.4%, whereas a deviation of 19.1% when the Herschel-Bulkley model was used for predicting the flow rate. These values include all the emulsions flooded through the pipe. Leaving out the soybean oil emulsion, that is the emulsion best fitted for the Herschel-Bulkley model, the Power-Law gives an average deviation of 9.2%, which is a good estimation.

4.5 Sources of Error

- A laboratory blender with a minimum speed of 18000 rpm was used when mixing the emulsions. The emulsions were mixed for 1.5 minutes, but the timing was done manually, which can lead to some differences from batch to batch. If the mixing time differs with 0.5 second this results in 150 rounds in the blender. This probably does not affect the rheological behavior of the emulsion too much, but better and more precise methods could be considered.
- ImageJ is not a valid or reliable tool when it is used on these kinds of pictures. Last year's experiments gave much clearer dispersed droplets compared to the ones made this year using engine oil. Since there were so many small and almost invisible droplets, it is difficult to make sure the right things are included/excluded.
- The valve at the bottom of the pipeline is opened manually, which means some error concerning time will be present.
- The weight of the emulsion being flooded through the pipeline and down on the scale were recorded using a simple slow-motion camera. The camera recorded the weight next to a stopwatch, which was started at the same time as the valve was opened. Other methods were attempted, for example Win Wedge, which should be able to record the weight on the scale versus a time stamp. The only problem with this program was that a pause on the scale was necessary for it to be recorded into Excel, and was therefore not useful for this experiment as the emulsion flooded through the pipeline continually. The slow-motion video was then used to write down the cumulative weight and the exact time on the stopwatch.
- When the emulsions were flooded through the pipeline, the pipe wall was covered with a thin film of the same emulsion being flooded. This was to avoid differences between

every time a new emulsion was flooded through, but this has not been included in the theoretical calculation of the flow rate. It is unsure how much this influenced the results, or if it did at all.

4.6 Recommendations for Further Work

- Emulsify heavy crude oil, to get an emulsion with lower viscosity than the initial oil. Do the same Anton Paar Rheometer tests, and the same tests regarding aging, water cut, and varying temperature.
- Do the visual observation tests in larger bottles and investigate how different substances affect the stability of the emulsions. Examples of such substances could be Zalo, table salt (NaCl) or proteins (for example gelatin). Take pH tests of the different bottles in order to compare the rate of separation with pH values.
- The Anton Paar Rheometer experiments should include higher shear rates. It would be interesting to see what happens to the emulsions containing less water when the shear rate exceeds 1200 s^{-1}.
- More rheometer test regarding aging could be done in order to obtain stronger and more clear trends.
- Do more investigation on the concept of mono- and polydispersity. The polydispersity could perhaps be controlled by combining several monodisperse emulsions with different droplet volumes.
- Try other and more reliable methods for finding droplet size. During these experiments, the emulsions were diluted in Exxsol D60. Using the same continuous phase as in the emulsions would probably be a better idea.
- If the shear rate interval in the Anton Paar Rheometer started at 0.1 s^{-1}, instead of 1 s^{-1}, maybe stronger shear thinning effects would be observed.

5. Conclusions

Based on the discussion, the following conclusions can be made:

1. Emulsions with higher water content showed stronger shear thinning effects, and experienced breaking at lower shear rates than emulsions with lower dispersed water fractions. All the engine oil emulsions behaved as Bingham Plastic fluids, but as the water content became smaller, the emulsions acted more and more as Newtonian fluids, hence the shear rate had less influence on the rheology.
2. Emulsions often become more stable with time. This may be explained due to the emulsifying agents becoming more spread in the emulsions, and surrounding all the dispersed droplets.
3. The apparent viscosity of the emulsions decrease with aging.
4. Shear thinning effects are stronger at low temperatures with a high dispersed water volume fraction.
5. The deviation between the measured flow rate and predicted flow rate was lower when the appropriate rheology model was used to predict the rate, with one exception. The average deviation was 9.2% when the Power-Law rheology model was used to predict the flow rates of the engine oil emulsions.

6. References

Armstrong, R. 2016. EOR: Thermal Methods. UNSW.

Becher, P. (2001) *Emulsions: Theory and Practice.* 3rd ed. edn. Washington: American Chemical Society.

Caenn, R., Darley, H. C. H. and Gray, G. R. (2011) *Equipment and Procedures for Evaluating Drilling Fluid Performance.* 6 edn.: Elsevier Inc.

Çengel, Y. A. and Cimbala, J. M. (2014) *Fluid Mechanics: Fundamentals and Applications.* 3rd ed. in SI units. edn. Boston: McGraw-Hill.

CES (2016) *Surfactants*: CES Silicones Europe. Available at: http://www.silicones.eu/science-research/adjuvants-and-auxiliaries/surfactants (Accessed: 20.11 2016).

Chen, Z. (2016) *Drilling Hydraulics and Cuttings Transportation. PTRL 4024/5024* Sydney, Australia.

Denney, D. (2000) 'Quantification of Factors Affecting Emulsion Stability'.

DowChemical (n.d) *Surfactant Basics - Definition of HLB, and How It Applies to Emulsions*. Dow Answer Center: The Dow Chemical Company. Available at: http://dowac.custhelp.com/app/answers/detail/a_id/3277/~/surfactant-basics---definition-of-hlb,-and-how-it-applies-to-emulsions (Accessed: 17.11 2016).

Education, T. F. S.-G. (2013) *What are emulsions?* [Video]. Available at: https://www.youtube.com/watch?v=bC_czAL24zY (Accessed: 20.10 2016).

Floury, J., Desrumaux, A. and Lardières, J. (2000) 'Effect of high-pressure homogenization on droplet size distributions and rheological properties of model oil-in-water emulsions', *Innovative Food Science and Emerging Technologies,* 1(2), pp. 127-134.

Garrett, R. L. (2016a) *Herschel-Bulkley fluid* Schlumberger Oilfield Glossary. Available at: http://www.glossary.oilfield.slb.com/Terms/h/herschel-bulkley_fluid.aspx (Accessed: 17.12 2016).

Garrett, R. L. (2016b) *Shear Rate*: Schlumberger Oilfield Glossary. Available at: http://www.glossary.oilfield.slb.com/Terms/s/shear_rate.aspx (Accessed: 26.11 2016).

Keleşoğlu, S., Pettersen, B. H. and Sjöblom, J. (2012) 'Flow properties of water-in-North Sea heavy crude oil emulsions', *Journal of Petroleum Science and Engineering*.

Kokal, S. L. (2005) 'Crude Oil Emulsions: A State-Of-The-Art Review'.

Krishnan, J. M., Sunil, K. P. B., Deshpande, A. P., Murali, K. J. and SpringerLink (2010) *Rheology of Complex Fluids.* Springer New York : Imprint: Springer.

KRÜSS (2017) *Drop Shape Analyzer – DSA100*. Hamburg, Germany: KRÜSS GmbH (Accessed: 08.06 2017).

Martínez-Palou, R., Mosqueira, M. d. L., Zapata-Rendón, B., Mar-Juárez, E., Bernal-Huicochea, C., de La Cruz Clavel-López, J. and Aburto, J. (2011) 'Transportation of heavy and extra-heavy crude oil by pipeline: A review', *Journal of Petroleum Science and Engineering,* 75(3), pp. 274-282.

Mezger, T. G. (2014) *The Rheology Handbook: For users of rotational and oscillatory rheometers. European coatings tech files* 4th rev. ed. edn. Hannover: Vincentz Network.

Oliveira, R. C. G. and Gonçalves, M. A. L. 'Emulsion Rheology - Theory vs. Field Observation', 2005/1/1/. OTC: Offshore Technology Conference.

Pal, R. (1996) 'Effect of droplet size on the rheology of emulsions', *AIChE Journal*, 42(11).

Pilehvari, A., Saadevandi, B., Halvaci, M. and Clark, P. E. 'Oil/Water Emulsions for Pipeline Transport of Viscous Crude Oils', *Annual Technical Conference and Exhibition of the Society of Petroleum Engineers*, Houston, TX, 1988/1/1/. SPE: Society of Petroleum Engineers.

Schramm, L. L. (2005) *Emulsions, Foams and Suspensions: Fundamentals and Applications.* Weinheim: Wiley-VCH.

Skalle, P. 12.05 2017. *RE: Explaining how emulsions in drilling fluid can solve gumbo shale related problems.*

Wagner, T. (2015) *Shape Filter*: ImageJ. Available at: http://imagej.net/Shape_Filter (Accessed: 16.12 2016).

Zang, L. (2016) *Lecture 9: Particle Coarsening: Ostwald Ripening*. University of Utah: Deparment of Materials Science & Engineering (Accessed: 20.12 2016).

Zhang, J., Tian, D., Lin, M., Yang, Z. and Dong, Z. (2016) 'Effect of resins, waxes and asphaltenes on water-oil interfacial properties and emulsion stability', *Colloids and Surfaces A: Physicochemical and Engineering Aspects*, 507, pp. 1-6.

A. List of Symbols and Abbreviations

A	Area of plates (two-plates model), m^2
$\dot{\gamma}$	Shear rate, s^{-1}
cP	centi Poise, $1\ cP = 0.001\ kg/m \cdot s$
C	Consistency parameter, $Pa \cdot s^n$
ΔP	Hydraulic potential, $k/m \cdot s^2$, Pa
d_d	Droplet diameter, m
D	Hydraulic diameter of pipe, m
ε	Energy dissipation, m^2/s^3, W/kg
F	Force applied to upper plate (two-plates model), N
g	Acceleration of gravity, m/s^2
h	Average between h_{bottom} and h_{top}, m
h_{bottom}	Fluid height when the fluid has flooded through the pipe (pipeline facility), m
h_{top}	Fluid height before valve is opened (pipeline facility), m
κ	Consistency index, $Pa \cdot s^n$
L_{pipe}	Length of pipe (pipeline facility), m
L	Length of pipe, m
μ	Dynamic viscosity, $kg/m \cdot s$
μ_p	Plastic viscosity, $(N \cdot s)/m^2$, $Pa \cdot s$
n	Flow behavior index, dimensionless
N_{Re}	Reynolds Number, dimensionless

ρ	Density of fluid, kg/m^3
ρ_d	Density of dispersed droplet, kg/m^3
ρ_f	Density of surrounding liquid, kg/m^3
Q	Flow rate, m^3/s
r	Distance between plates (two-plates model), m
r_0	Boundary radius (Herschel-Bulkley), m
r_w	Radius as wall (Herschel-Bulkley), m
R	Inner radius of pipe, m
τ	Shear stress, $N/m^2,\ Pa$
τ_0	Shear stress at boundary radius, Pa
τ_y	Yield strength, $N/m^2,\ Pa$
v	Velocity of upper plate (two-plates model), m/s
v_0	Velocity at boundary radius, m/s
v_s	Rate of sedimentation, m/s
V_{avg}	Mean velocity of the fluid, m/s

Abbreviations

API	American Petroleum Institute
CCD	Charged Coupled Device
HLB	Hydrophile-Lipophile Balance
IFT	Interfacial Tension
O/W	Oil-in-water
PPD	Pour Point Depressant
SAGD	Steam-Assisted Gravity Drainage
W/O	Water-in-oil
W/O/W	Water-in-oil-in-water
W/O/W/O	Water-in-oil-in-water-in-oil
w/v	Weight/Volume

B. Anton Paar Measurements

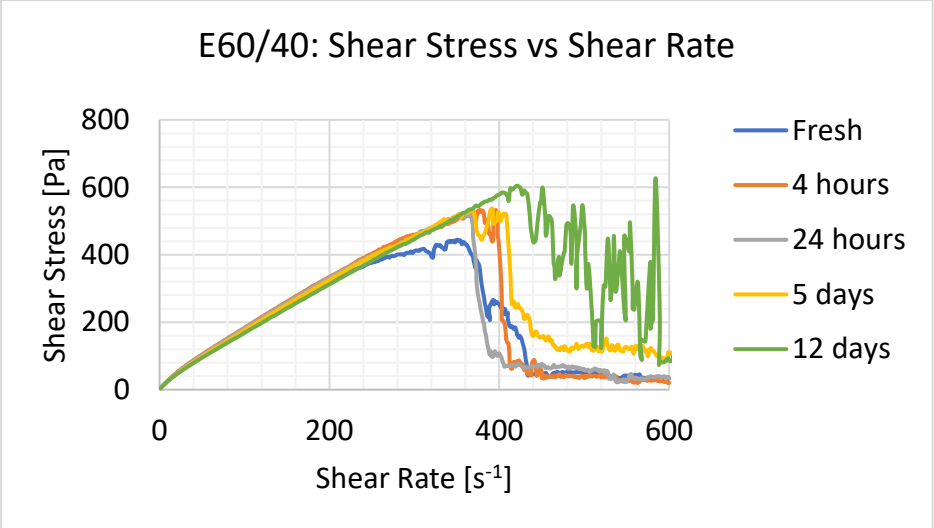

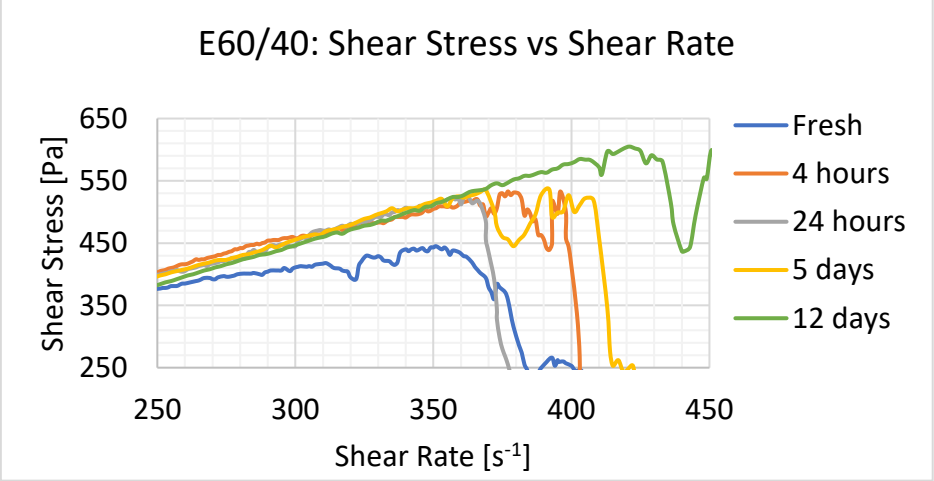

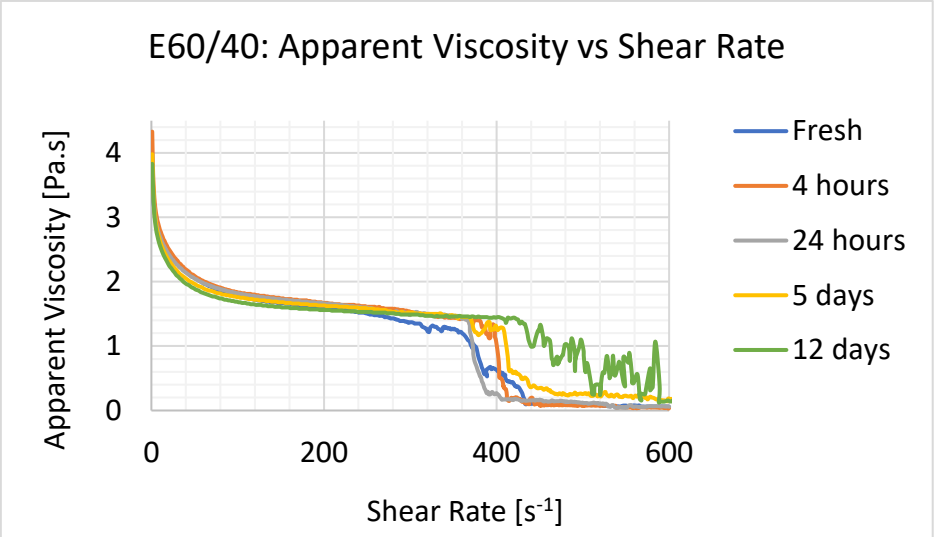

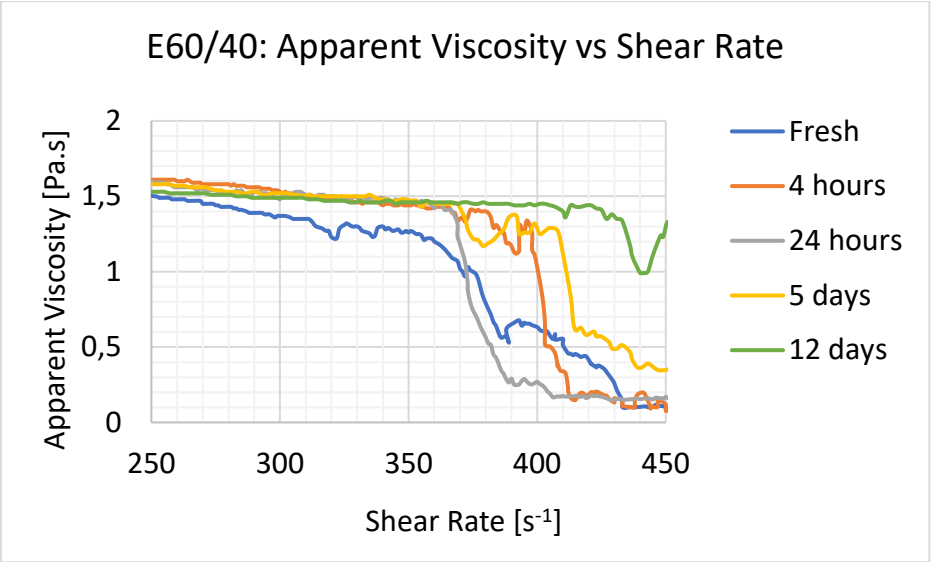
E60/40: Apparent Viscosity vs Shear Rate
Apparent Viscosity [Pa.s]
2
1,5
1
0,5
0
250
300
350
400
450
Shear Rate [s-1]
Fresh
4 hours
24 hours
5 days
12 days

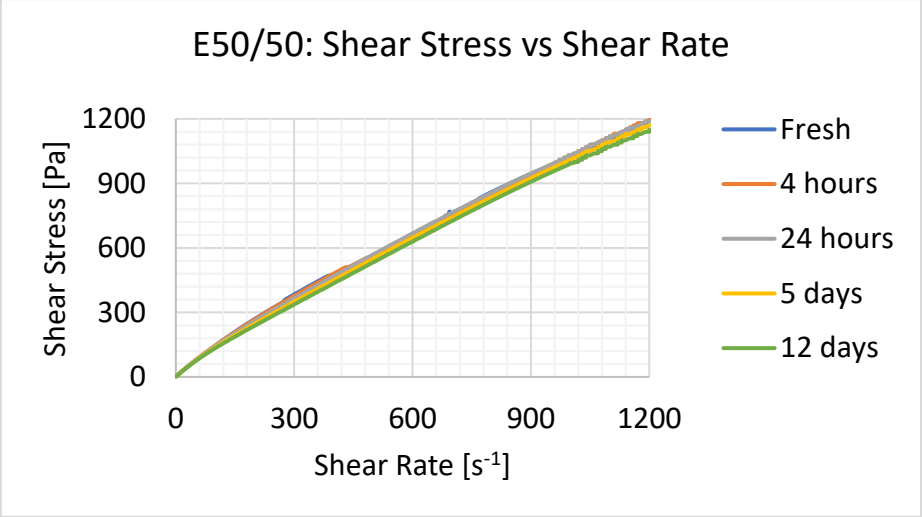
E50/50: Shear Stress vs Shear Rate
Shear Stress [Pa]
1200
900
600
300
0
0
300
600
900
1200
Shear Rate [s-1]
Fresh
4 hours
24 hours
5 days
12 days

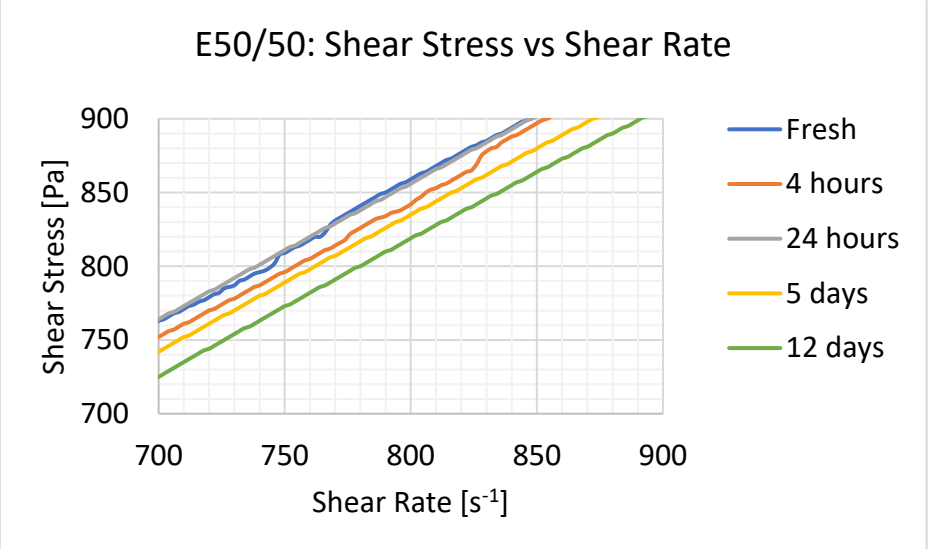
E50/50: Shear Stress vs Shear Rate
Shear Stress [Pa]
900
850
800
750
700
700
750
800
850
900
Shear Rate [s-1]
Fresh
4 hours
24 hours
5 days
12 days

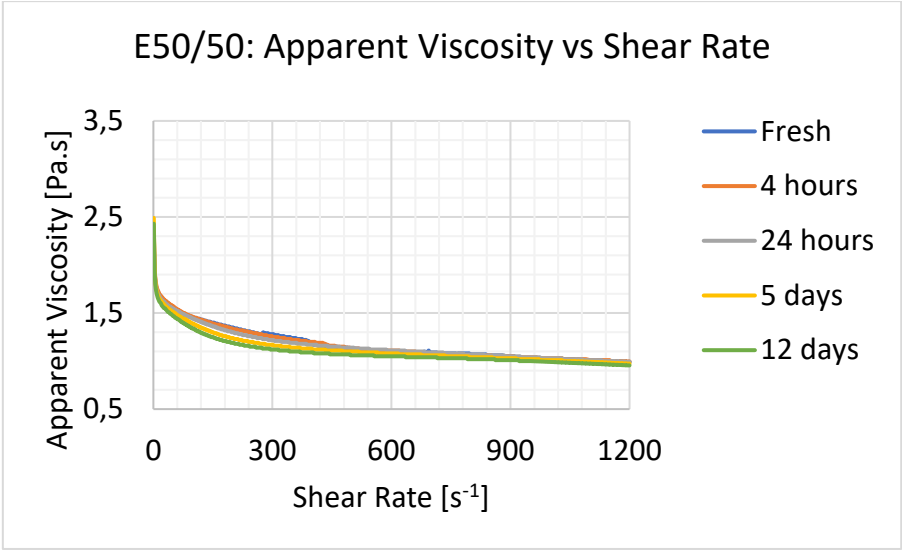
E50/50: Apparent Viscosity vs Shear Rate
Apparent Viscosity [Pa.s]
3,5
2,5
1,5
0,5
0
300
600
900
1200
Shear Rate [s-1]
Fresh
4 hours
24 hours
5 days
12 days

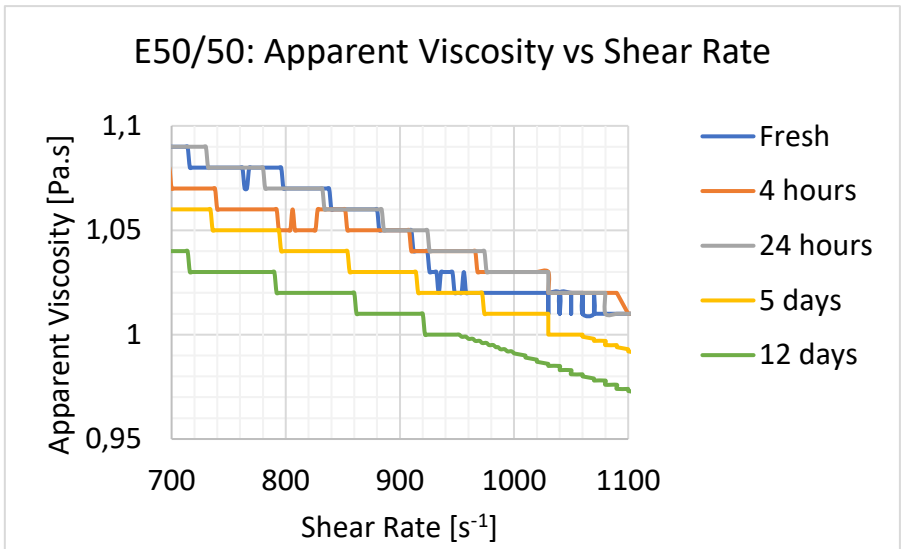
E50/50: Apparent Viscosity vs Shear Rate
Apparent Viscosity [Pa.s]
1,1
1,05
1
0,95
700
800
900
1000
1100
Shear Rate [s-1]
Fresh
4 hours
24 hours
5 days
12 days

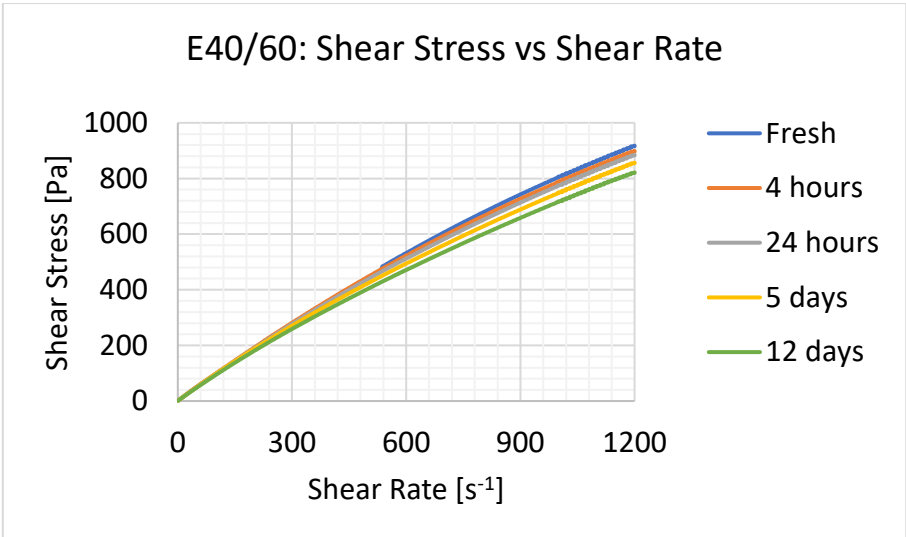
E40/60: Shear Stress vs Shear Rate
Shear Stress [Pa]
1000
800
600
400
200
0
0
300
600
900
1200
Shear Rate [s-1]
Fresh
4 hours
24 hours
5 days
12 days

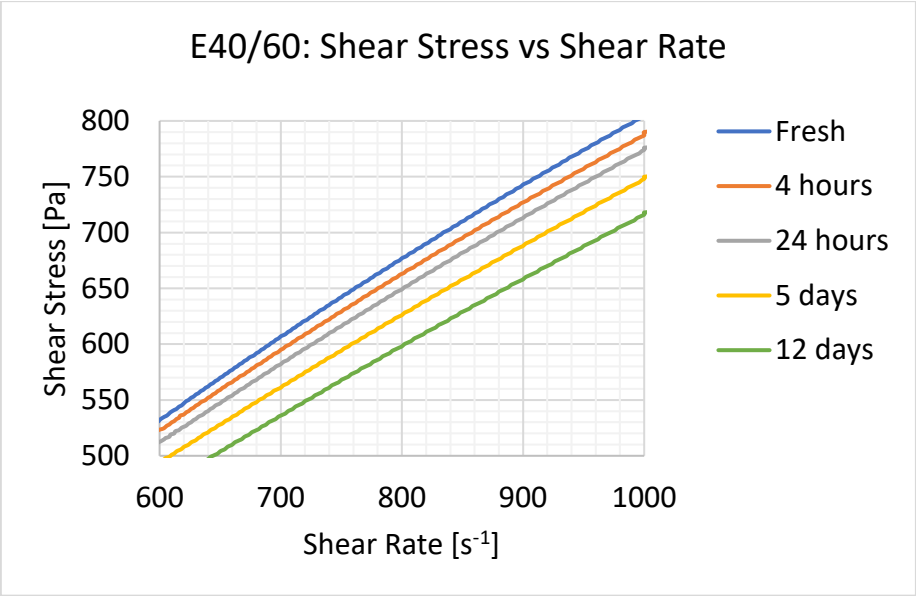
E40/60: Shear Stress vs Shear Rate
Shear Stress [Pa]
800
750
700
650
600
550
500
600
700
800
900
1000
Shear Rate [s-1]
Fresh
4 hours
24 hours
5 days
12 days

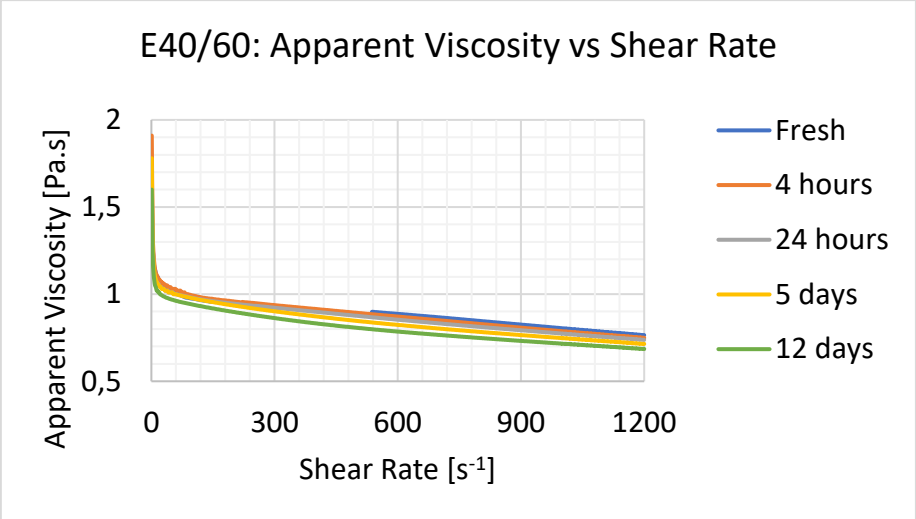
E40/60: Apparent Viscosity vs Shear Rate
Apparent Viscosity [Pa.s]
2
1,5
1
0,5
0
300
600
900
1200
Shear Rate [s-1]
Fresh
4 hours
24 hours
5 days
12 days

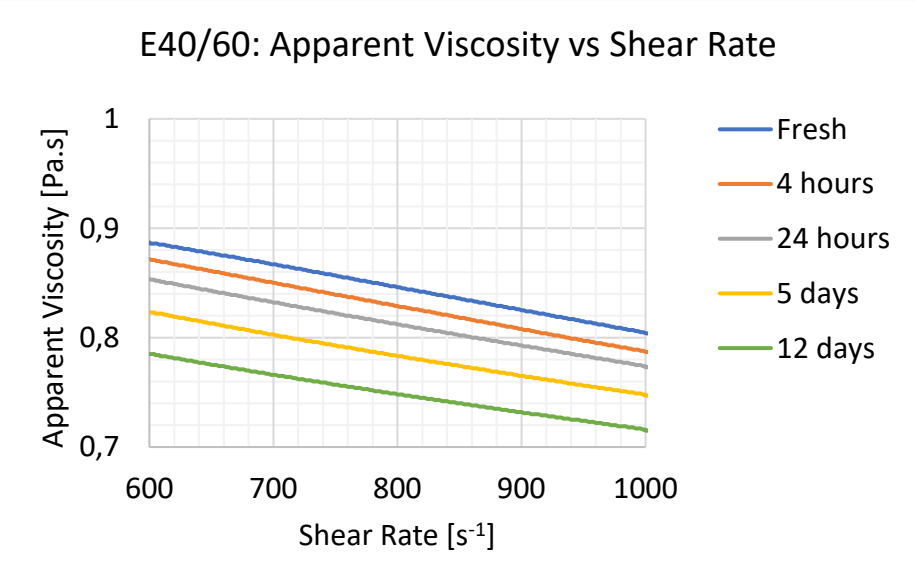
E40/60: Apparent Viscosity vs Shear Rate
Apparent Viscosity [Pa.s]
1
0,9
0,8
0,7
600
700
800
900
1000
Shear Rate [s-1]
Fresh
4 hours
24 hours
5 days
12 days

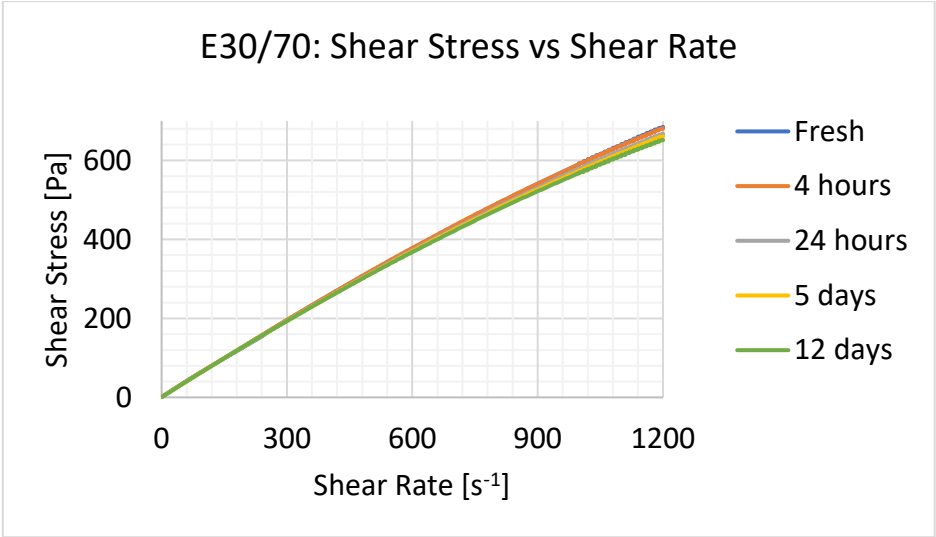
E30/70: Shear Stress vs Shear Rate
Shear Stress [Pa]
600
400
200
0
0
300
600
900
1200
Shear Rate [s-1]
Fresh
4 hours
24 hours
5 days
12 days

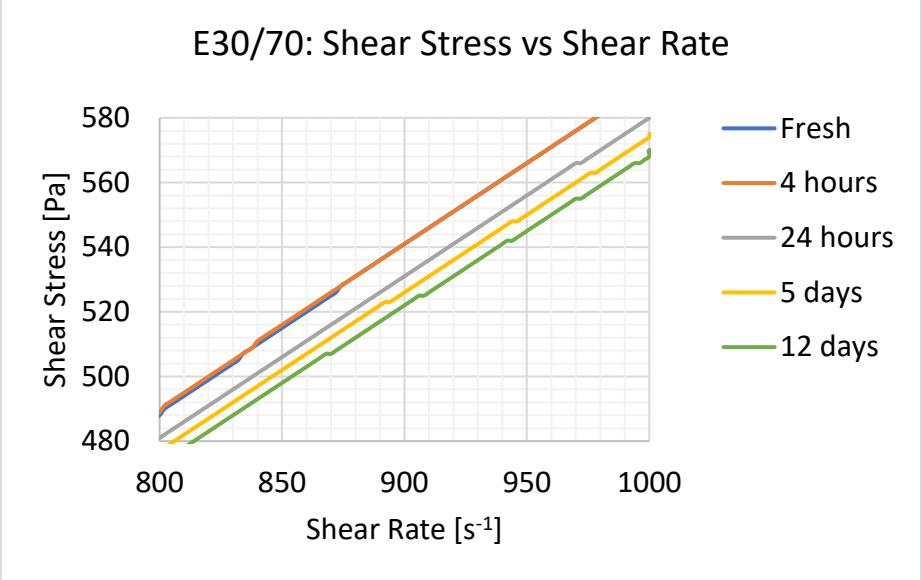
E30/70: Shear Stress vs Shear Rate
Shear Stress [Pa]
580
560
540
520
500
480
800
850
900
950
1000
Shear Rate [s-1]
Fresh
4 hours
24 hours
5 days
12 days

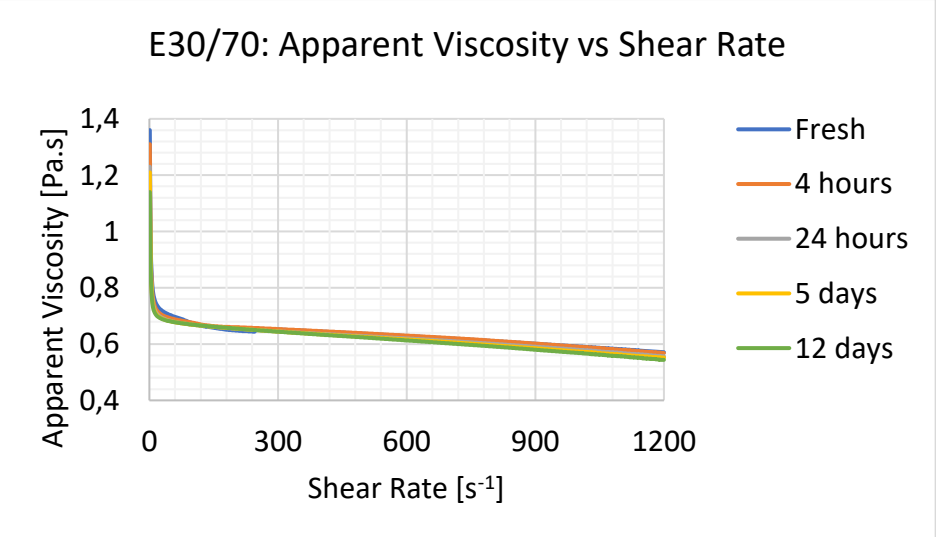
E30/70: Apparent Viscosity vs Shear Rate
Apparent Viscosity [Pa.s]
1,4
1,2
1
0,8
0,6
0,4
0
300
600
900
1200
Shear Rate [s-1]
Fresh
4 hours
24 hours
5 days
12 days

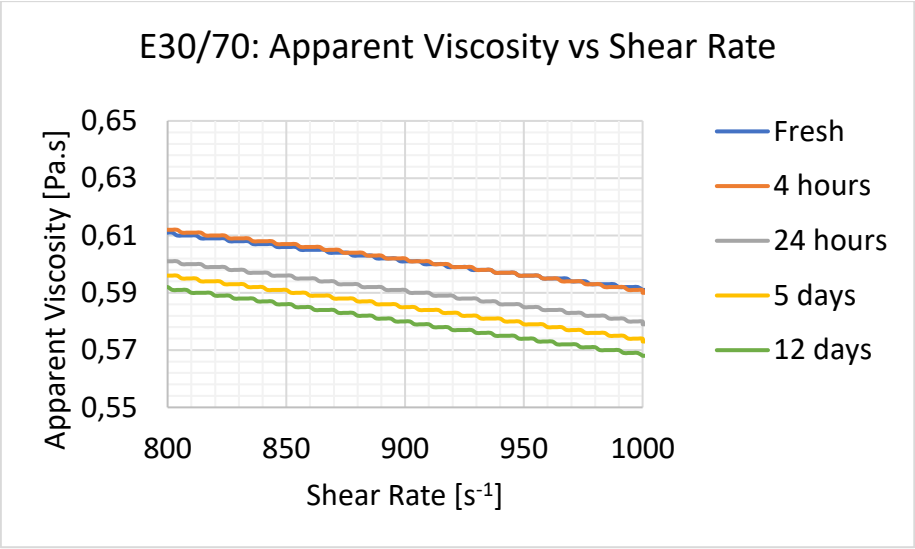
E30/70: Apparent Viscosity vs Shear Rate
Apparent Viscosity [Pa.s]
0,65
0,63
0,61
0,59
0,57
0,55
800
850
900
950
1000
Shear Rate [s-1]
Fresh
4 hours
24 hours
5 days
12 days

C. Flow Rate – Power-Law Rheology Model

$$A = \pi r^2$$

$$S = 2\pi r$$

$$Q = uA$$

$$P = \frac{F}{A} \rightarrow F = PA$$

Force balance:

$$\Delta PA = \tau SL$$

$$\Delta P \pi r^2 = \tau 2\pi r L$$

$$\Delta P\, r = \tau 2L$$

$$\frac{\Delta P}{L} = \frac{2\tau}{r}$$

Since both ΔP and L are independent of r,

that means that $\frac{2\tau}{r}$ are too.

$$\tau = Cr$$

$$@\ r = 0 \rightarrow\ \tau = 0$$

$$@\ r = \frac{D}{2}\ (at\ the\ pipe\ wall) \rightarrow\ \tau = \tau_w$$

$$\rightarrow \tau_w = C\frac{D}{2} \rightarrow C = \frac{2\tau_w}{D}$$

$$\rightarrow\ \tau = \frac{2\tau_w}{D} r = \frac{r}{R}\tau_w$$

$$where: \tau_w = \frac{\Delta P R}{2L}$$

Power-Law Fluid:

$$\tau = C\dot{\gamma}^n$$

$$\dot{\gamma} = -\frac{du}{dr}$$

$$\tau = -C\left(\frac{du}{dr}\right)^n$$

This gives

$$\tau = \frac{r}{R}\tau_w = -C\left(\frac{du}{dr}\right)^n$$

$$\frac{r}{R}\frac{\Delta P\, R}{2L} = -C\left(\frac{du}{dr}\right)^n$$

$$\frac{\Delta P\, r}{2L} = -C\left(\frac{du}{dr}\right)^n$$

$$\left(\frac{\Delta P\, r}{2CL}\right)^{\frac{1}{n}} = -\frac{du}{dr}$$

$$\int du = -\left(\frac{\Delta P}{2CL}\right)^{\frac{1}{n}} \cdot \int r^{\frac{1}{n}} dr$$

$$u = -\left(\frac{\Delta P}{2CL}\right)^{\frac{1}{n}} \cdot \frac{n\, r^{\frac{1}{n}+1}}{n+1} + C_1$$

$$@\ wall: r = \frac{D}{2} = R$$

$$u = 0$$

$$0 = -\left(\frac{\Delta P}{2CL}\right)^{\frac{1}{n}} \cdot \frac{n\, R^{\frac{1}{n}+1}}{n+1} + C_1$$

$$C_1 = \left(\frac{\Delta P}{2CL}\right)^{\frac{1}{n}} \cdot \frac{n\, R^{\frac{1}{n}+1}}{n+1}$$

$$u = -\left(\frac{\Delta P}{2CL}\right)^{\frac{1}{n}} \cdot \frac{n\, r^{\frac{1}{n}+1}}{n+1} + \left(\frac{\Delta P}{2CL}\right)^{\frac{1}{n}} \cdot \frac{n\, R^{\frac{1}{n}+1}}{n+1}$$

$$u = \frac{n}{n+1}\left(\frac{\Delta P}{2CL}\right)^{\frac{1}{n}}\left(R^{\frac{1}{n}+1} - r^{\frac{1}{n}+1}\right)$$

$$Flowrate: Q = uA$$

$$Q = \int u\, dA = \int_{r=0}^{r=R} u(r) 2\pi r \cdot dr$$

$$= \frac{2\pi n}{n+1}\left(\frac{\Delta P}{2CL}\right)^{\frac{1}{n}} \int_{r=0}^{r=R} r\left(R^{\frac{1}{n}+1} - r^{\frac{1}{n}+1}\right) dr$$

$$= \cdots \int_{r=0}^{r=R} \left(rR^{\frac{1}{n}+1} - r^{\frac{1}{n}+2}\right) dr$$

$$= \cdots \left[\frac{r^2}{2} R^{\frac{1}{n}+1} - \frac{r^{\frac{1}{n}+2+1}}{\frac{1}{n}+2+1}\right]_0^R$$

$$= \cdots \left[\frac{r^2}{2} R^{\frac{1}{n}+1} - \frac{r^{\frac{1}{n}+3}}{\frac{1}{n}+3}\right]_0^R$$

$$= \cdots \left[\frac{r^2}{2} R^{\frac{1}{n}+1} - \frac{n\, r^{\frac{1}{n}+3}}{3n+1}\right]_0^R$$

$$= \cdots \left[\frac{R^2}{2} R^{\frac{1}{n}+1} - \frac{n\, R^{\frac{1}{n}+3}}{3n+1} - 0 + 0\right]$$

$$= \cdots \left[\frac{R^{\frac{1}{n}+3}}{2} - \frac{n\, R^{\frac{1}{n}+3}}{3n+1}\right]$$

$$= \cdots \left[\frac{(n+1)R^{\frac{1}{n}+3}}{2(3n+1)}\right]$$

$$Q = \frac{2\pi n}{(n+1)}\left(\frac{\Delta P}{2CL}\right)^{\frac{1}{n}} \cdot \frac{(n+1)R^{\frac{1}{n}+3}}{2(3n+1)}$$

$$Q = \frac{n\pi R^3}{3n+1}\left(\frac{\Delta PR}{2CL}\right)^{\frac{1}{n}}$$

$$Q = \frac{\pi R^3}{\frac{1}{n}+3}\left(\frac{\Delta PR}{2CL}\right)^{\frac{1}{n}}$$

D. Flow Rate – Herschel-Bulkley Rheology Model

This method for finding the Herschel-Bulkley flow rate is developed by Harald A. Asheim.

1. General Force Balance:

   From the force balance along a pipe:

$$\tau_w = \frac{\Delta p \cdot r_w}{2L} \tag{1}$$

   The potential drop has to be the same for every radial position:

$$\tau(r) = \frac{\Delta p}{2L} r = \frac{r}{r_w} \tau_W \tag{2}$$

2. Herschel-Bulkley

   This assumes that the relation between shear stress and shear rate can be illustrated as

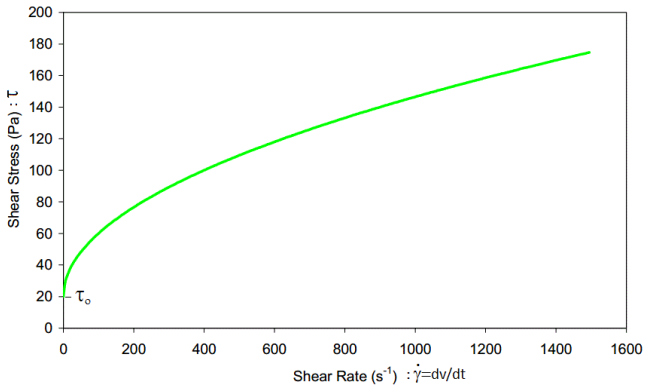

Figure 1

   And can be expressed as Power-Law once the yield is exceeded

$$\tau = \tau_0 + C \left(\frac{dv}{dr}\right)^n \tag{3}$$

   For the fluid to flow, the shear stress must overcome the initial gel strength: $\tau(r) \geq \tau_0$.

   From (2): At stationary flow, the following boundary is reached at radius:

$$r_0 = \tau_0 \frac{2L}{\Delta p} \tag{4}$$

   Within this radius, the fluid will flow as a firm plug; and outside this radius as a Power-Law fluid with shear stress relation (3). Velocity and shear stress is illustrated in figure 2 below.

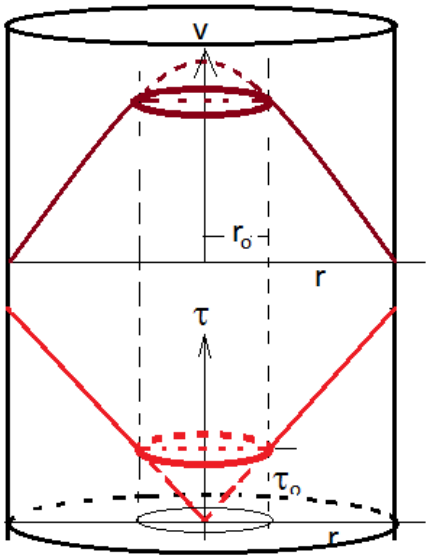

Figure 2

3. Velocity Profile

Combination of (2), (3) and (4) gives

$$\tau(r) = \frac{\Delta p}{2L} r = \frac{\Delta p}{2L} r_0 + C \left(\frac{dv}{dr}\right)^n$$

This gives the following velocity relation for: r > r_0.

$$\frac{dv}{dr} = C_1 \hat{r}^{\frac{1}{n}}$$

Where $C_1 = \left(\frac{\Delta p}{2CL}\right)^{\frac{1}{n}}$ and $\hat{r} = r - r_0$

Integrated velocity relation:

$$v(\hat{r}) = C_1 \frac{n}{n+1} \hat{r}^{\frac{n+1}{n}} + C_0$$

By the wall: $\hat{r}_w = r_w - r_0$, the velocity will be zero. Inserted in the integrated velocity relation this gives us the integrational constant C_0

$$C_0 = -\left(\frac{\Delta p}{2CL}\right)^{\frac{1}{n}} \frac{n}{n+1} (r_w - r_0)^{\frac{n+1}{n}}$$

The velocity profile then becomes (at $r = r_0$):

$$v_0 = -\left(\frac{\Delta p}{2CL}\right)^{\frac{1}{n}} \frac{n}{n+1} (r_w - r_0)^{\frac{n+1}{n}} \quad (5)$$

Between the plug and the pipe wall ($r_0 < r < r_w$):

$$v(r - r_0) = -\left(\frac{\Delta p}{2CL}\right)^{\frac{1}{n}} \frac{n}{n+1} (r_w - r_0)^{\frac{n+1}{n}} \left(1 - \left(\frac{r - r_0}{r_w - r_0}\right)^{\frac{n+1}{n}}\right) = v_o \left(1 - \left(\frac{r - r_0}{r_w - r_0}\right)^{\frac{n+1}{n}}\right)$$

Or, more compact:

$$v(\hat{r}) = v_0\left(1 - \left(\frac{\hat{r}}{\hat{r}_w}\right)^{\frac{n+1}{n}}\right) \tag{6}$$

Where $\hat{r}_w = r_w - r_0$

4. Flow rate

The flow rate can now be found by integrating the velocity profile over the pipe cross-section; that is for a plug flow to r_0 and non-newtonian further out to r_w.

$$Q = \int_0^{r_w} v(r)2\pi r\, dr = v_0\pi r_0^2 + 2\pi\int_0^{\hat{r}_w} v(\hat{r})(\hat{r} + r_0)d\hat{r} \tag{7}$$

The velocity in (6) is inserted into (7):

$$2\pi\int_0^{\hat{r}_w} v(\hat{r})(\hat{r} + r_0)d\hat{r}$$

$$= 2\pi v_0\int_0^{\hat{r}_w}\left(1 - \left(\frac{\hat{r}}{\hat{r}_w}\right)^{\frac{n+1}{n}}\right)(\hat{r} + r_0)d\hat{r}$$

$$= 2\pi v_0\int_0^{\hat{r}_w}\left(r_0 + \hat{r} - \hat{r}_w^{-\frac{n+1}{n}}\cdot\hat{r}^{\frac{2n+1}{n}} - r_0\hat{r}_w^{-\frac{n+1}{n}}\cdot\hat{r}^{\frac{n+1}{n}}\right)d\hat{r}$$

Integrated, this becomes:

$$= 2\pi v_0\left[r_0\hat{r} + \frac{1}{2}\hat{r}^2 - \hat{r}_w^{\frac{n+1}{n}}\frac{n}{3n+1}\hat{r}^{\frac{2n+1}{n}+1} - r_0\hat{r}_w^{-\frac{n+1}{n}}\frac{n}{2n+1}\hat{r}^{\frac{n+1}{n}+1}\right]_0^{\hat{r}_w}$$

Boundaries inserted:

$$= 2\pi v_0\left(r_0\hat{r}_w + \frac{1}{2}\hat{r}_w^2 - \frac{n}{3n+1}\hat{r}_w^{-\frac{n+1}{n}}\cdot\hat{r}_w^{\frac{n+1}{n}+2} - \frac{n}{2n+1}r_0\hat{r}_w^{-\frac{n+1}{n}}\cdot\hat{r}_w^{\frac{n+1}{n}+1}\right)$$

$$= 2\pi v_0\left(r_0\hat{r}_w + \frac{1}{2}\hat{r}_w^2 - \frac{n}{3n+1}\hat{r}_w^2 - \frac{n}{2n+1}r_0\hat{r}_w\right)$$

$$= \pi v_0\left(\frac{n+1}{3n+1}\hat{r}_w^2 + \frac{2n+2}{2n+1}r_0\hat{r}_w\right)$$

Inserted in (7), flow rate is given:

$$Q = v_0\pi\left(r_0^2 + \frac{2n+2}{2n+1}r_0(r_w - r_0) + \frac{n+1}{3n+1}(r_w - r_0)^2\right) \tag{8}$$

Where $r_0 = \tau_0\frac{2L}{\Delta p}$ and $v_0 = -\left(\frac{\Delta p}{2CL}\right)^{\frac{1}{n}}\frac{n}{n+1}(r_w - r_0)^{\frac{n+1}{n}}$

E. ImageJ – Image Processing Procedure

Download ImageJ for free from: https://imagej.nih.gov/ij/download.html

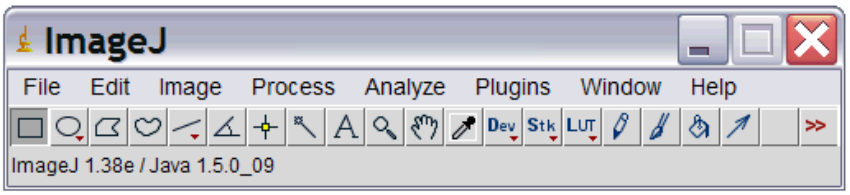

1. Upload picture (File – Open)
2. Set scale (Draw a straight line over known distance - Analyze - Set scale)
3. Make the picture smaller (Rectangular – Draw – Image – Duplicate) (a good idea is to make two duplicates and only use one further on – that makes it easier to compare the pictures to each other)
4. Diminish the background (Process – Subtract Background) (Press Preview, and explore with the rolling ball radius)
5. Make the picture 8-bit (Image – Type – 8 bit)
6. Contrast (Image – Adjust – Brightness/Contrast)
7. B/W (Image – Adjust – Threshold)
8. Make the picture binary (only two colors) (Process – Binary – Make Binary)
9. Remove noise (use Oval or the Paintbrush Tool to draw unclear circles and remove things that are not droplets) (use the other duplicate to compare)
10. Fill the holes (Process – Binary – Fill Holes)
11. Mask (Process – Binary – Convert to Mask)
12. Separate droplets that are close together (Process – Binary – Watershed)
13. Select desired data (Analyze – Set Measurements) (here: Area and Feret's Diameter)
14. Get the results (Analyze – Analyze Particles) (here: exclude on edges and display results)

F. MATLAB Codes

1. Graphical Representation of the Droplets

This code is made by Harald Arne Asheim

```
%% LogNormal dropletdistribution
clear all
clf
clc
load aging3070_24hr.txt
data=aging3070_24hr;
ant=size(data);
n=ant(1);               % number of measuringpoints, 1st column
Excel file

   A=data(1:n,2);       % areal calculated by ImageJ, 2nd
column Excel file
   dmax=data(1:n,3);    % Feret diameter, 3rd column Excel file
    dmin=data(1:n,4);   %Minimum Feret diameter, 4th column
Excel file

%% Volume, assumed rotational ellipsoids
pf=1.6075;
for i=1:n
V(i)=4/3*pi*(dmin(i)/2)*(dmax(i)/2)^2;% volume, rotational
ellipsoid
Sf(i)=pi*( (dmax(i)^(2*pf) +
2*dmax(i)^pf*dmin(i)^pf)/3)^(1/pf);  % surface, rotation
ellipsoide
end
%% Empirical distribution
   Vs=sort(V);          % sort dropletvolume in ascending order
   Vsum(1)=Vs(1);
   for i=2:n
   Vsum(i)=Vsum(i-1)+Vs(i);
   end
   Vtot=Vsum(n);
   Fe=Vsum/Vtot;        % Fe(Vs) = empirical cummulative
distribution
%% Surface area
    for i=1:n
   S(i)=(6*pi^(1/2)*Vs(i))^(2/3);    % surfaces, sorted
   end
   osp=40e-3; %surface tension
   Stot=sum(S);
   Srel=Stot/Vtot;
   Sfrel=sum(Sf)/Vtot;
%% Block diagram showing empirical probability density
```

```
nf=10;  % Number of discretization points
Vint=linspace(0,Vs(length(Vs))*1.001,nf); % dividing into
intervals
for j=1:nf-1
   % finding volume increase in each interval
   Vf(j)=0;
   for i=1:length(Vs)
       if Vs(i)>Vint(j)& Vs(i)<Vint(j+1)
   Vf(j)=Vf(j)+Vs(i);
       end
   end
   Vip(j)=(Vint(j)+Vint(j+1))/2;      % interval midpoint
   fV(j)=(Vf(j)/(Vint(j+1)-Vint(j)))/Vtot;  %  empirical
probability density
end

 %% Mean value and variance of measured data
 Em=0;
for i=2:n
Em=Em+Vs(i)^2/Vtot;
end
var=0;
 for i=2:n
     var=var+Vs(i)^3/Vtot;
 end
 sm=var^0.5;

%% Expected estimates of location parameter: my and scale
parameter: s2
 my=log(Em)-0.5*log(1+var/Em^2);
 s2=log(1+var/Em^2);

 %% Deviation
 f=0;
 for i=1:n
Fi=0.5*erfc(-(log(Vs(i))-my)/(2*s2)^0.5);
f=f+(Fi-Fe(i))^2;
 end
 f=f/n; %average deviation
 errm=100*f^0.5;

%% Calculation of LogN-distribution before optimization
x=linspace(0.001,Vs(n));
for i=1:length(x)
fv(i)=(1/(2*s2*pi)^0.5)/x(i)*exp(-(log(x(i))-my)^2/(2*s2));
Fv(i)=0.5*erfc(-(log(x(i))-my)/(2*s2)^0.5);
end


 %-----------------  optimize ------------------------------
-
```

```
global Feg xg
Feg=Fe;            % empirical cummulative distribution
xg=Vs;             % x-axis
pa0= [my s2 ];    % initial parameter estimate
[pa,fval]=fminunc(@optfun,pa0);

 % optimized estimate of location paramete: my and scale
parameter: s2
 myopt=pa(1);
 s2opt=pa(2);
 % writing out
 disp([ '....LogNormal distribution, adjusted to measured
droplet volumes.'])
 disp(['.................  From starting data --------- '])
disp(['Standard deviation of measured data :
',num2str(sm,'%5.3e\n')])
disp(['Total droplet volume           :
',num2str(Vtot,'%5.3e\n'),' mm^3'])
disp(['Surface area/droplet volume    :
',num2str(Srel,'%5.3e\n')])
disp(['Surface area/droplet volume rotational ellipsoid    :
',num2str(Sfrel,'%5.3e\n')])
% surface
 C=(6*sqrt(pi))^(2/3);
  Sf(1)=0;
 for i=2:length(x)
 Sf(i)=Sf(i-1)+ C*fv(i)/x(i)^(1/3)*(x(i)-x(i-1));
 end

Sfmax=Sf(length(x));
Sf2=C*exp((1/18*(-6*my+s2)));          % analytical

disp(['.................  Direct fitting --------- '])
disp(['Mean value                   : ',num2str(Em,'%5.3e\n')])
disp(['Standard deviation                :
',num2str(sm,'%5.3e\n')])
disp(['Surface area/droplet volume
:',num2str(Sf2,'%5.3e\n'),'  (1/mm )'])
disp(['Error while fitting            :
',num2str(errm,'%5.3e\n'),'  %'])


%  LogN-distribution based on optimized parameters
 z=linspace(0.0001,2*Vs(n), 300);
for i=1:length(z)
fao(i)=(1/(2*s2opt*pi)^0.5)/z(i)*exp(-(log(z(i))-
myopt)^2/(2*s2opt));
Fao(i)=0.5*erfc(-(log(z(i))-myopt)/(2*s2opt)^0.5);
end
```

```
   m=exp(myopt+s2opt/2)% mean value, 1. moment of distribution
sd=((exp(s2opt)-1)*exp(2*myopt+s2opt))^0.5; %standard
deviation
 sdi2=0;
 for i=2:length(z)
     sdi2=sdi2+(z(i)-m)^2*fao(i)*(z(i)-z(i-1));
 end

 sdi=sdi2^0.5;  %Standard deviation with numerical integration

 err=100*fval^0.5;
 dfsd=(1+(sd/m^2)^0.5);
disp(['.................  Optimized fitting --------- '])
disp(['Mean value                        ',num2str(m,'%5.3e\n')])
disp(['Standard deviation
',num2str(sd,'%5.3e\n')])
disp(['Error while fitting
',num2str(err,'%5.3e\n'),'  %'])

  %
  xmax=1.1*Vs(n);
   subplot(2,1,1)
 hold on
 plot(Vs,Fe,'.')
 plot(x,Fv,'k')
  plot(z,Fao,'r--')
  plot([Em Em],[0 1],'r')
   % plot([Em+sm Em+sm],[0 1],'m-')
 hold off
 xlabel('\bf Droplet volume: V_d (\mum^3)')
 ylabel('\bfCummulative: F  (-)')
 grid
 %legend('Measured ','_Distribution: F_N(m,s)','Optimzed
distribution','Mean value: m','m + Measured standard
deviation')
 legend('Measured data','Logarithmic distribution:
F_N(m,s)','Optimized distribution','Mean value: m')
 legend('Location','SouthEast')
axis([0 xmax 0 1 ])

 % density
 maxf=1.2*max([max(fv),max(fao)]);
subplot(2,1,2)
hold on
%bar(Vip,fV)
 plot(x,fv,'k')
plot(z,fao,'r--')
 %plot([Em Em],[0 1],'r-.')
    %plot([Em+sm Em+sm],[0 1],'m-')
% plot([E E],[0, max(f)],'b-.')
hold off
```

```
xlabel('\bf Droplet volume: V_d  (\mum^3)')
 ylabel('\bf Distribution density: f_v')
 %legend('Distribution density: f_v(m,s)','Optimized
distribution density','  Målt middelverdi','m + Målt
standardavvik')
    legend('Direct estimate','Optimized estimate')
   grid
    axis([0 xmax 0 maxf ])
   % legend('Grouped measurements','Adjusted to logN')
```

2. Finding Power-Law Constants

Constants_powerlaw.m

```
%% Taking values from Anton-Paar
load flow_fresh6040.txt
data = flow_fresh6040;
ant=size(data);
n=ant;              %Number of measuring points

rate=data(1:n,1);   %1st column
stress=data(1:n,2); %2nd column



%% Plotting and fitting line to get C and n
plot(rate,stress)
hold on
f = fit(rate, stress, 'power1')
plot(f,rate,stress)
title('Plot')
xlabel('Shear rate')
ylabel('Shear stress')
```

3. Using Power-Law Constants to Calculate Fluid Flow

powerlaw.m

```
%% Input from Anton-Paar:
C = 2.802;              % (a) Consistency parameter [Pa*s^n]
n = 0.6573;             % (b) Flow behavior index n [dim.less]


%% Input based on seperate measurements
rho = 950;                %Density [kg/m^3]

%% Loading data
load flow_fresh6040.txt
data = flow_fresh6040;
```

```
ant=size(data);
no=ant;                         %Number of measuring points
mu =data(1:no,3);               %Viscosity [Pa*s]

%% Designing Pipe by guessing R and L:
R = 0.0125;                     %Inner radius R [m]
D = 2*R;                        %Diameter D [m]
L = 1.8;                        %Length of pipe [m]
h = 1.8636;                     %Total fluid height [m]


%% Flow Equation for Power Law:
g = 9.81;                      %Gravity [m/s^2]
Hp = rho*g*h;                  %Hydraulic potential [Pa]

Q = ((pi*R^3)/(3+1/n))*((Hp*R)/(2*C*L))^(1/n); %[m^3/s]
Q_l = Q/0.001                  %Flowrate [l/s]

A = pi*R^2;                    %Area [m^2]
v = Q/A                        %Velocity [m/s]
v_cm = v*10^2;                 %Velocity [cm/s]

%% Checking the Flow Regime and Entry Length

for i = 1:length(mu)
    Re(i) = (rho*v*D)/mu(i);       %Reynolds number
    f(i) = 64/Re(i);        %Friction factor in a circular pipe
end

if Re <= 2300
  disp('Laminar flow')
  L_entry_lam = 0.05*Re*D;    %Entry length laminar flow
elseif Re >= 4000
  disp('Turbulent flow')
  L_entry_turb = 1.359*Re^(1/4)*D;%Entry length turbulent flow
else
    disp('Transitional flow')


end
```

4. Finding Herschel-Bulkley Constants

Constants_herschelbulkley.m

```
%% Taking values from Anton-Paar
load flow_fresh_S6040.txt
data = flow_fresh_S6040;
ant=size(data);
n=ant;                    %Number of measuring points

rate=data(1:n,1);         %1st column
stress=data(1:n,2);       %2nd column


%% Plotting and fitting line to get C and n
plot(rate,stress)
hold on
f = fit(rate, stress, 'power2')
plot(f,rate,stress)
title('Plot')
xlabel('Shear rate')
ylabel('Shear stress')
```

5. Using Herschel-Bulkley Constants to Calculate Fluid Flow

```
%% Input from Anton-Paar:

C    = 1.078;                                  % (a) Consistency
parameter [Pa*s^n]
n    = 0.791;                                 % (b) Flow
behavior index n [dim.less]
t_0 = 18.64;                                  % (c)

%% Input based on seperate measurements
rho = 950;                                  %Density [kg/m^3]

%% Loading data
load flow_fresh_S6040.txt
data = flow_fresh_S6040;
ant=size(data);
no=ant;                                %Number of measuring points
mu =data(1:no,3);                          %Viscosity [Pa*s]
t = data(1:no,3);                          % Shear Stress [Pa]

%% Capillary viscometer parameters
R = 0.0125;                                 %Inner radius R [m]
D = 2*R;                                    %Diameter D [m]
L = 1.8;                                    %Length of pipe [m]
h = 1.8636;                               %Total fluid height [m]
```

```
%% Flow Equation for Herschel-Bulkley:
g = 9.81;                                %Gravity [m/s^2]
Hp = rho*g*h;                            %Hydraulic potential [Pa]
r_0 = (t_0*2*L)/Hp;
v_0 = ((Hp/(2*C*L))^(1/n))*(n/(n+1))*(R-r_0)^((n+1)/n);

Q = v_0*pi*(r_0^2+((2*n+2)/(2*n+1))*r_0*(R-
r_0)+((n+1)/(3*n+1))*(R-r_0)^2);        %Flowrate [m^3/s]

Q_l = Q/0.001                             %Flowrate [l/s]
A = pi*R^2;                               %Area [m^2]
v = Q/A                                   %Veloity [m/s]
v_cm = v*10^2;                            %Veloity [cm/s]


%% Checking the Flow Regime and Entry Length
for i = 1:length(mu)
    Re(i) = (rho*v*D)/mu(i);            %Reynolds number
    f(i) = 64/Re(i);       %Friction factor in a circularpipe
end

if Re <= 2300
    disp('Laminar flow')
    L_entry_lam = 0.05*Re*D;         %Entry length laminar flow
elseif Re >= 4000
    disp('Turbulent flow')
L_entry_turb = 1.359*Re^(1/4)*D; %Entry length turbulent flow
else
disp('Transitional flow')

end
```

G. Recipe for making emulsions

Preparation of water-in-soybean oil emulsions

Edible oils will be the base oils for the preparations. However, the same procedure can be used with petroleum as base oil, usually without adding emulsifiers.

1. Prepare the necessary amount of artificial sea water and oil. Artificial seawater is prepared by dissolving 34 g/l of sodium chloride (NaCl) in tap water. If 300 ml emulsion with for example water content of 70 volume % is going to be made, the following amounts of oil and water are needed:

Ingredient	volume %	Amount [ml]	Comments
Base oil	30	90	For example edible oil
Seawater	70	210	Artificial 3,4 % NaCl
Total	**100**	**300**	

2. For making edible oil emulsion we generally use approximately 1 volume %, based on oil volume, of Palsgaard emulsifier, 0.5 % of DGM 0298 and 0.5 % DGPR 4175. DGM 0298 is a solid and waxy material. The oil has to be heated to approximately 40 ^{o}C to easily dissolve DGM 0298. Heat a part (20-30 ml) or all of the edible oil and dissolve the emulsifiers in the oil using a hand stirrer ending with a clear (not "milky") solution. Eventually mix the total oil volumes together.

3. Start making w/o-emulsion by stirring the oily phase at slow speed, 100-200 rpm. A cheap hand held kitchen mixer running at low speed is handy for this purpose. Slowly pour the artificial seawater in batches of about 10-30 ml into the oily phase, carefully looking after that there are no visible water droplets in the emulsion before pouring in a new batch. The emulsion will be whiter and whiter as the water content is increasing. This is shown in Fig. 1.

Figur 1.
70 vol % sjøvann-i-soyaolje emulsjon ved 10 ^{o}C og tilsynelatende viskositet ca 15000 cP (mPas) ved et skjær på 10 sek^{-1}.

4. Continue adding water until the wanted amount is reached. It is wise now and then to check that the product is water-in oil type of emulsion and isn't inverted to the oil-in water type. This can happen if too much mixing energy is introduced. The type of emulsion is checked by placing a droplet of the mix on a clear water surface. If the emulsion is dissolving into the water creating a milky cloud, the emulsion has inverted and one has to start all over again using new ingredients and lower the mixing speed or interval and rate of pouring water into the oily phase.

Trondheim, February 3, 2014.
Knut Gåseidnes
Cellular: +47 922 94 440
Email: mlab@multinet.no

H. Risk Assessment

Detailed Risk Report

ID	20268	**Status**	**Date**
Risk Area	Risikovurdering: Helse, miljø og sikkerhet (HMS)	Created	01.06.2017
Created by	Marthe Bodahl Lunde	Assessment started	01.06.2017
Responsible	Harald Arne Asheim	Actions decided	01.06.2017
		Closed	01.06.2017

Risk Assessment:

Risk Assessment - Master Thesis Spring 2017

Valid from-to date:
1/11/2017 - 6/11/2020

Location:
Petroleumsteknisk Senter

Goal / purpose
We want to conduct a risk assessment in order to be aware of the possible nonconformities that might occur, and how to handle it in the right way.

Background
By doing this risk assessment we want to address the possible risks of doing laboratory work related to the master thesis.

Description and limitations
Units that might be affected by the subject of this risk assessment are ourselves and co-workers in the lab. There are no previous risk assessments used as reference. This risk assessment is only applicable for work in the mud lab at PTS, and for the spring semester 2016.

Prerequesites, assumptions and simplifications
Similar measurements were done in the laboratory last semester.

Attachments
[Ingen registreringer]

References
[Ingen registreringer]

Summary, result and final evaluation

The summary presents an overview of hazards and incidents, in addtition to risk result for each consequence area.

Hazard: **Contact with skin over time**

Incident:

Not to be analyzes.

Hazard: **Inhalation**

Incident:

Not to be analyzes.

Hazard: **Swollowing**

Incident:

Not to be analyzes.

Hazard: **Waste**

Incident: **Waste Handling**

Consequence area: Materielle verdier Risk before actions: Risiko after actions:

Planned action	Responsible	Registered	Deadline	Status
Waste Handling	Marthe Bodahl Lunde	01.06.2017	01.06.2017	Evaluated

Hazard: **Spilling**

Incident:

Not to be analyzes.

Final evaluation

It is important to inform new lab - visitors about the waste bucket measure. If they are working with very viscous fluids, they should use the black waste bucket with the big inlet, instead of the waste bucket in the fume hood with the pipe inlet.

Organizational units and people involved

A risk assessment may apply to one or more organizational units, and involve several people. These are lsited below.

Organizational units which this risk assessment applies to

- Institutt for geovitenskap og petroleum

Participants

Ann-Othilie H. Væhle
Marthe Bodahl Lunde

Readers

[Ingen registreringer]

Others involved/stakeholders

[Ingen registreringer]

The following accept criteria have been decided for the risk area Risikovurdering: Helse, miljø og sikkerhet (HMS):

Helse	Materielle verdier	Omdømme	Ytre miljø

Overview of existing relevant measures which have been taken into account

The table below presents existing measures which have been take into account when assessing the likelihood and consequence of relevant incidents.

Hazard	Incident	Measures taken into account
Waste	Waste Handling	Fume hood and waste bucket

Existing relevant measures with descriptions:

Personal protective equipment

Safety boots, goggles, labcoat and gloves for different tasks

Fume hood and waste bucket

When pouring the oil into beakers, the fume hood will be used to prevent inhaling the oil mist.
A waste bucket will be used when throwing the oil away.

Lab tour

Introductory tour to get to know the lab and get some guidance.

HSE Introductory Course

Online Course

Risk analysis with evaluation of likelihood and consequence

This part of the report presents detailed documentation of hazards, incidents and causes which have been evaluated. A summary of hazards and associated incidents is listed at the beginning.

The following hazards and incidents has been evaluated in this risk assessment:

- **Waste**
  - Waste Handling

Detailed view of hazards and incidents:

Hazard: Waste

Incident: Waste Handling

The viscous emulsion clogged the waste bucket inlet.

Cause: Cause of incident

Description:

Too much emulsion were poured in the waste bucket inlet, so it was difficult to notice the clogged pipe.

Likelihood of the incident (common to all consequence areas): **Likely (3)**

Kommentar:

[Ingen registreringer]

Consequence area: Materielle verdier ***Risk:***

Assessed consequence: **Small (1)**

Comment: The pipe is only temporarily clogged, and the only concequence is that people have to wait in line to use the waste bucket. There are other available waste buckets in the laboratory.

Overview of risk mitiating actions which have been decided:

Below is an overview of risk mitigating actions, which are intended to contribute towards minimizing the likelihood and/or consequence of incidents:

- Waste Handling

Overview of risk mitigating actions which have been decided, with description:

Waste Handling

Empty the emulsion in mud waste bucket instead of in the waste collectors in fume hoods.

Action decided by:	Marthe Bodahl Lunde
Responsible for execution:	Marthe Bodahl Lunde
Deadline for execution:	6/1/2017

Detailed view of assessed risk for each hazard/incident before and after mitigating actions

Hazard: Waste

Incident: Waste Handling

Likelihood assessment (common to all consequence areas)

Initial likelihood: Likely (3)

Reason:

Likelihood after actions: Unlikely (1)

Reason:

Consequence assessments:

Consequence area: Materielle verdier ***Risk:***

Initial consequence: Small (1)

Reason: The pipe is only temporarily clogged, and the only concequence is that people have to wait in line to use the waste bucket. There are other available waste buckets in the laboratory.

Consequence after actions: Small (1)

Reason: When the waste bucket inlet pipe gets clogged, it needs time to drain into the bucket. Maybe other people have to wait in line to use the waste bucket, but there are other buckets available in the laboratory.